Drill-Core And Geophysical Investigation Of The Western Part Of The Crystalline Rim Of Wetumpka Impact Structure, Alabama

by

Pascual Tabares Rodenas

A thesis submitted to the Graduate Faculty of
Auburn University
in partial fulfillment of the
requirements for the Degree of
Master of Science in Geology

Auburn, Alabama
August 4, 2012

Keywords: Wetumpka, impact, crater, crystalline rim,
LiDAR, DEM.

Copyright 2012 by Pascual Tabares Rodenas

Approved by

David T. King Jr. (Co-Advisor), Professor, Department of Geology and Geography
Jens Örmo (Co-Advisor), Doctor, Centro de Astrobiología
Lorraine W. Wolf, Professor, Department of Geology and Geography

ABSTRACT

The present research project on Wetumpka impact structure, Elmore County, Alabama, is focused on understanding the effects of hypervelocity impact upon sedimentary target rocks and underlying crystalline bedrock in the impact of a modest-sized asteroid. In particular, this study focuses on the development of the crystalline rim at Wetumpka. This study will improve our knowledge about how a liquid layer (here marine water) as part of the target materials affects the cratering process not only on our planet, but on other celestial bodies such as Mars.

The Wetumpka impact structure is a complex crater located in Elmore County, central Alabama (N32˚31'; W86˚ 10'). It was first was proposed as an impact feature in 1976 by Thornton L. Neathery, Robert D. Bentley, and Gregory C. Lines. The size of the Wetumpka apparent crater (about 5 km in diameter) indicates that it most likely has a buried central uplift (the central uplift is not evident topographically). The diameter of this structure is based on field mapping of the outer reaches of impact deformation and has been shown to be a marine-target impact.

This study is aimed at attaining a better understanding of the behavior of the crystalline rocks in this kind of explosive event, specifically what are the mechanisms that relate to the deformation of the border rim and the emplacement of the crystalline border crater rim.

The present study includes: a complete descriptive analysis of drill core #09-01, which penetrates through the crystalline crater rim; a 3D resistivity survey on the western part of the

rim, near the drill site, which reveals crystalline rim rock fractures in a detailed way; and maps and cross-sections derived from Light Detection And Ranging (LiDAR) for the a very accurate construction of maps and cross-sections used for interpretation of the surface and shallow subsurface geology of the impact structure. LiDAR data with approximately two-meter resolution allows for construction of Digital Elevation Models (DEMs) and others derivative images, which have helped the present study greatly.

ACKNOWLEDGMENTS

This work was supported in part by a NASA grant "Shallow exploratory core drilling at Wetumpka impact structure, a marine target impact crater in Alabama, USA" *(#*NNX09AD90G awarded to King and Ormö). Also, this work was supported in part by a Gulf Coast Association of Geological Societies (GCAGS) student grant "Drill-core and geophysical investigation of the western crystalline rim of Wetumpka impact structure, Alabama." The author thanks the landowners of the western rim area for allowing access to their properties for research, and Chris Carter at Coosa River Adventures for an unforgettable boat trip through the rumbling waters searching for crystalline outcrops to measure along the river. Thanks to Dr. Lorraine Wolf and the Advanced Geophysics class, (Mike Natter, Jeff Keevan, Yang Peng, and James Taylor) for their help with setting up the electrodes of the 3D resistivity survey. Thanks to Steven Jaret for sharing with me a bit of his vast knowledge about mineralogy and optical microscopy. Also thanks to Michael Smith and Jake Gunn for assistance in the lab and field. Thanks to Dr. Jens Ormö, for his assistance and collaboration on this thesis with new ideas for research topics, but more importantly to show me this opportunity overseas. I could never thank enough my advisor Dr. David T. King Jr., for his counsel, guidance, and unlimited support through these years in United States; and to his wife Lucille, for making me feel like not that far from home. Finally special thanks to my family, my Dad, my Mom my brother Claudio, and Eva, for all their love and encouragement on this adventure.

Table of Contents

ABSTRACT ..... **II**

ACKNOWLEDGMENTS ..... **IV**

LIST OF FIGURES ..... **VIII**

LIST OF TABLES ..... **XII**

INTRODUCTION **1**

BACKGROUND AND GEOLOGICAL SETTINGS **3**

PREVIOUS WORK **6**

OBJECTIVES **10**

METHODOLOGY **12**

1. DRILL-CORE ANALYSIS 12

a) Cleaning and alignment *14*

b) Core logging *14*

c) Photography *15*

d) Data format and data base *16*

e) Quantitative Mineral Analysis Method *18*

f) Thin Sections *22*

2. LIGHT DETECTION AND RANGING (LIDAR) 24

LIDAR acquisition methods *24*

Elmore County DEM Analysis *27*

a) Slopes Analysis *27*

b) Aspect Analysis (Dipping Surfaces) *28*

3. 3D RESISTIVITY IMAGING 32

4. FIELD METHODS 37

RESULTS **39**

1. DRILL CORE 39
a) Photographs *39*
b) RQD over Depth *43*
c) Schistosity and fractures families. *45*
d) Mineralogy *50*
e) Thin sections *54*
2. FRACTURE INVENTORY OF THE STUDY AREA. 56
3. 3D RESISTIVITY 58
4. LIDAR & GIS 60
a) Wetumpka DEM (Digital Elevation Model) *60*
b) Detailed Cross-sections *62*
c) 3D map *64*
d) Slopes Map *64*
e) Aspect map *66*
f) Geologic map *68*

INTERPRETATIONS **69**

1. DRILL CORE 69
2. FRACTURE PATTERN IN THE AREA OF STUDY 70
3. 3D RESISTIVITY 79
4. LIDAR AND DEMS 81

CONCLUSIONS **86**

DRILL CORE 86
FRACTURE PATTERN OF THE INVESTIGATED WESTERN SECTION OF THE WETUMPKA CRATER RIM 87
3D RESISTIVITY 87
LIDAR 88
FUTURE WORK 88

REFERENCES **89**

APPENDICES.....93

A) DRILL CORE.....93

B) THIN SECTIONS 122

C) DIGITAL GEOLOGICAL MAP 134

LIST OF FIGURES

Figure 1. Residual gravity profile W-E direction (from Wolf et al., 1997). The gravity profile is one of the early lines of evidence that pointed to the feature at Wetumpka as an impact structure..... 7

Figure 2. Drill-core box picture example. The reading direction of the core sections is marked by arrows from "Top" to "Bottom." Also shown are the standard color reference scheme and scale in cm and inches..... 13

Figure 3. DCB 03 with an example of mineral classification using unsupervised classification. In this picture we can see the different zones subjected to unsupervised classification. This method discerns well the differences in color tones between quartz, feldspar, muscovite, and biotite. Once the pixels are classified we can calculate mineral percentage..... 21

Figure 4. Aerial picture showing the area for LiDAR survey (Elmore County, Alabama). The north-south “columns” show the flight lines. 26

Figure 5. Slope in degrees versus percent. Image taken from ArcGIS 10..... 31

Figure 6. Diagram showing an input elevation dataset and the output aspect raster. Also is shown the aspect directions. Image taken from ArcGIS 10..... 31

Figure 7. Example of surface window for calculation..... 31

Figure 8. Area chosen for 3D resistivity survey (rectangle). Note location of Gardner well (#09-01) relative to survey (blue dot).33Figure 9. Sketch of the most common arrays set up used in resistivity(from Burger, 1992), where P = potential electrode and C = current electrodes. This style of array was chosen due to its capacity to map vertical structures. 35

Figure 10. Map view of electrodes geometry for 3D resistivity survey. The dots show the location of electrodes. The distances are in meters. The cable layout is shown by red and blue lines, which end in arrows pointing to the connection with SuperSting R1 meter. .. 36

Figure 11. Time-lapse image showing the process of inversion. An *a priori* model is updated by comparing data calculations with the data observation. Each iteration reduces the error. 36

Figure 12. Example of the instruments used during fieldwork. From left to right: field notebook, geologic compass, GPS. Rock outcrop is on the southeastern rim area of Wetumpka impact structure. 38

Figure 13. An example of a drill-core box (DCB) photograph print format. It includes the same features listed in the methodology part for photographs and also, it has been accompanied by other useful information about the core. This information includes image name, site and "GPS" location, depth range (in meters and feet), elevation of the drill site, and RQD%. 41

Figure 14. RQD percentage with depth. The segmented lines represent the length of every drill-core box. 44

Figure 15. Normal frequency distribution of the schistosity dip angle measured throughout the core. 46

Figure 16. Weighted average and mean of the fractures dip angle calculated in each box. The tendency lines show a reduction in schistosity angle from the upper boxes to the lower ones. 47

Figure 17. Stereographic projection from GEOrient, showing main dip planes of fractures logged within the #09-01 core. In this stereograph, schistosity is not taken into account in the data. 49

Figure 18. Biotite, muscovite, feldspar, and quartz percentage plotted versus depth. The segmented lines represent the length of each drill-core box. 51

Figure 19. Mineral percentage versus RQD. In this case muscovite and biotite % has been combined to obtain the percentage of micas through the core. The relation between micas

% and RQD can be seen here. Increasing percent of micas also increases the RQD, and vice versa. 53

Figure 20. Presence of very small garnets ("micro garnets") in drill core #09-01 at 61.2 ft. (18.7m) depth. The occurrence of garnets decreases with depth, being practically nonexistent below 150 ft. (45.7m). 55

Figure 21. DEM of Wetumpka's rim area showing the inventory of fractures (red symbols) and schistosity (black symbols). This inventory has been separated into three zones; Zone 1 is the main area of study and covers the western rim; Zone 2 covers Coosa River; and Zone 3 cover the south eastern rim. In this DEM, higher areas correspond with bright colors while blue and more pale colors are the lower elevations. Research wells are plotted also in this figure. 57

Figure 22. 3D resistivity rendered volume. The higher resistivity values (ohm-m) correspond with reddish-orange colors and the lower with green to blue colors. As an example, at right, one of the transverse planes has been taken out of the volume..... 59

Figure 23. Differences in resolution between older DEM of Wetumpka (based on old US Geological Survey 7.5 minute quadrangles, (above) and the new DEM generated from 2010 LiDAR data that have a spatial resolution of 2 m (below). 61

Figure 24. Two example elevation profiles of Wetumpka impact crater. At the top is a digital elevation model of the crater area where the lines of cross-sections AA' (NW-SE) and BB' (NE-SW) are marked. Below the map is AA' and BB' profile. 63

Figure 25. Image showing an aerial photograph of Wetumpka crater area (top), the slope map of the same area (center), and the combination of both images (bottom). High slopes areas are represented in red while low slopes or flat surfaces are in blue. 65

Figure 26. Aspect map of Elmore County. Some lineation (dashed lines) can be seen thanks to this derivative of the Elmore County DEM. The shape of Wetumpka crater (box) is also very well highlighted using this method. 67

Figure 27. Detailed map showing the measures of dip and strike taken along the Coosa River and the western rim area. Fractures in the area are represented as red symbols and schistosity measures as black symbols. 71

Figure 28. Stereographic projection of the measurements taken on the western rim area (Figure 19). This projection shows a strong directionality of the foliation towards NW (N327°/37°). The fold axis direction has been calculated also, which bears northeast (N037°). 73

Figure 29. Sketch and cross-section illustrating the disposition of the schistosity and the suggested interpretation as a fold axis of the overturned flap at the investigated western section of the rim of Wetumpka. The upper right layered model represent the area content in the red box on the map (colors of the model do not represent geology) and is created using the online application from www.visiblegeology.com (Rowan, 2011). 74

Figure 30. Stereographic projection of the measurements taken along the Coosa River section (just south of the Bibb Graves Bridge to north of Moccasin Gap in the Coosa River). In this figure, the foliation is no longer the dominant bedding plane that derives into two orientations. 76

Figure 31. Stereographic projection of the measurements taken at the southeastern part of the rim. The picture shows a dominant foliation direction concordant with the bedding planes similarly as on the western rim. The measurements show a strong directionality toward the north east (N067°). 78

Figure 32. Aerial photograph of an area on the western rim with the local resistivity map superimposed. The resistivity map shows the resistivity surface at 4 m depth. 80

Figure 33. Digital elevation model of Wetumpka at a scale which shows the fluvial patterns mentioned in the text (antecedent and trellis versus consequent). 82

Figure 34. Map showing the 1976 geologic map units and the relative value of the slopes (see value scale) obtained from the Wetumpka LiDAR-based DEM, which is plotted on a high resolution orthophoto of the Wetumpka area. Geologic map was digitized from Neathery et al. (1976). 84

LIST OF TABLES

Table 1. Thin sections are shown in this table along with the depth in the drill core #09-01, type of texture, and general grain size. For more information, see thin sections in the Appendix. 23

Table 2. Settings used during the aerial LiDAR survey 25

INTRODUCTION

The ongoing investigation of the Wetumpka Impact Crater focuses on understanding the effects of a hypervelocity impact of an asteroid into a target made up of seawater, poorly consolidated sedimentary rock and a crystalline basement.

Presently, our knowledge of impact cratering is based not only on theoretical and experimental studies of shock waves, experimental production of small craters, and remote sensing of craters in extraterrestrial locations such as the Moon, but also on analysis and research of previously known impact craters in different parts of the world. As ~ 70% of the Earth´s surface is covered by water, most impacts will have occurred at sea. One of best places to study a marine-target crater structure is at Wetumpka, Alabama, the site of a ~5 km marine-target crater. This study improves our knowledge about how marine water has affected the target materials and cratering processes not only on our planet, but also on other celestial bodies in the solar system where water or other liquids may have been included in the target. At Wetumpka, the target mainly consisted of a crystalline basement covered by several tens of meters of a thick sequence of poorly consolidated sediments and a few tens of meters of seawater.

The impact excavated deep into the basement generating an elevated crater rim of mainly crystalline rock and a thick crater infill.

This study is aimed at understanding the mechanisms involved in the formation of the crystalline rim of Wetumpka impact crater. The analysis utilizes a new drill core that penetrates through the crystalline crater rim, a field inventory of fractures near the drill site and a 3D resistivity study of these fractures, as well as processed Light Detection and Ranging (LiDAR) data and DEMs (Digital Elevation Models) generated from this data.

BACKGROUND AND GEOLOGICAL SETTINGS

The Wetumpka impact structure is a complex marine-target crater located in Elmore County, central Alabama (N32˚31'; W86˚ 10'), which first was proposed as an impact feature by Neathery et al. (1976).

For some time, Wetumpka has been known to have formed during Late Cretaceous; at that time, Wetumpka area was located just offshore from a barrier-island shoreline and specifically the impact target area was submerged continental shelf of the sea that was to form the Gulf of Mexico. Based on facies analyses of the target formation (Mooreville Chalk) found within the crater and regional paleogeographic reconstruction, it is reasoned that the target water layer of this sea at the Wetumpka impact site was between 30 and 100 m deep (King et al., 2002; 2003; King and Ormö, 2011).

Wetumpka structure has a recognizable crystalline rim that forms a horseshoe shape (Nelson, 2000; King et al., 2002; King and Ormö, 2011), specifically the apparent crater diameter based on this horseshoe shape is about 5 km (King et al., 2006). This size indicates that it falls just above the boundary between simple and complex terrestrial craters in crystalline rock. This is important to note because complex craters of this size

have central uplifts, so the apparent absence of a topographic expression of a central uplift suggests that Wetumpka has a buried central uplift. Like the Chesapeake Bay Impact Structure in Virginia, another well-studied and documented marine-target impact crater (e.g. Horton et al., 2005), the Wetumpka crater displays a deep inner bowl shape and a collapsed zone outside the basement crater rim (i.e., the extra-crater terrain; King et al, 2003). The failure of collapsed segment of the crystalline rim on the south side of the crater could be in part due to significantly decrease of the rim structural strength caused by a smaller amount of uplifted crystalline basement materialized into a resistant rim due to a southward dip of the basement, a thickening of the sedimentary target sequence towards the south, and the deeper target water on the southern, ocean-facing side of the crater (King et al. 2006). This weak configuration of the southern rim is thought to have aided the extensive post-impact slumping and possible oceanic resurge (King et al., 2002; 2004; 2006; King and Ormö 2007; 2011).

The sedimentary target sequence of the Wetumpka impact consisted of:

Upper Cretaceous sedimentary section comprising the following units (from top to bottom) -- Mooreville Chalk, which is a poorly consolidated sediment composed of chalky ooze (<30 m), Eutaw formation, characterized by paralic marine sand (~30 m), and Tuscaloosa Group (~60 m) which is composed by terrestrial clayey sand and gravels.

Below the Upper Cretaceous sequence follows a crystalline basement peneplain that dips 10 to 20 m/km to south-southwest. This crystalline basement includes Piedmont metamorphic units such as Emuckfaw Group and Kowaliga Gneiss (Neathery et al., 1976; King et al., 2002; 2003). Emuckfaw group in Wetumpka is a medium to fine grained quartz-muscovite-biotite-

feldspar schist. Kowaliga Gneiss in Wetumpka area is made out of several meta–igneous bodies that intrude into the metasedimentary Emuckfaw group (Nelson, 2000).

PREVIOUS WORK

Modern mapping studies at Wetumpka were made by Thornton L. Neathery, Robert D. Bentley and Gregory L. Lines in 1968-1970, as part of an effort to create a new detailed state geological map for the Geological Survey of Alabama. After several years, in 1976, Thornton L. Neathery and other members of the mapping team published an article in the *Bulletin of the Geological Society of America* referring to Wetumpka as a "cryptoexplosion structure" and as an "astrobleme" (Neathery et al., 1976; Neathery, 1997).

Building on the results of geologic mapping, Wolf et al. (1997) conducted a gravity survey that showed residual gravity values typical of impact structures. This gravity survey bisected Wetumpka impact structure along a right-of-way path through the entire crater from east to west (Figure 1).

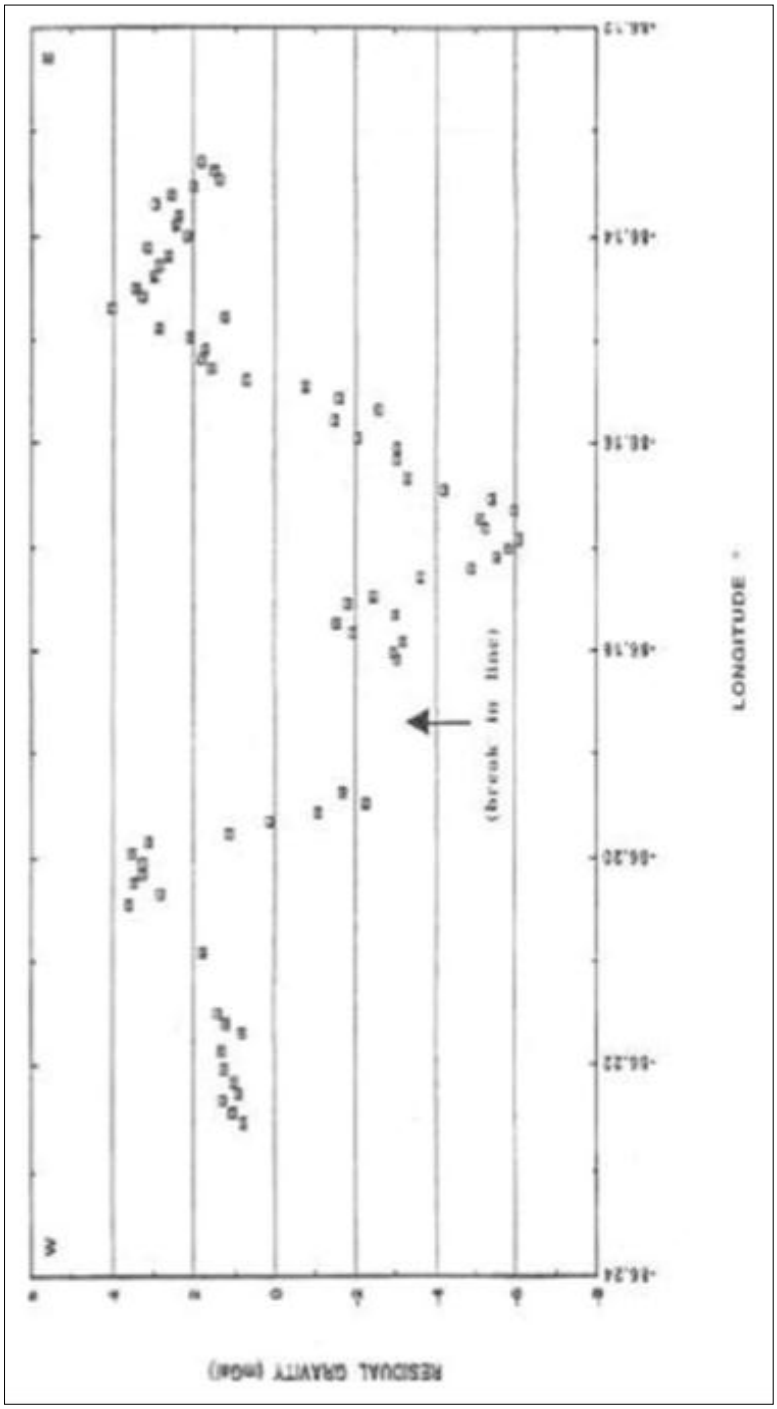

Figure 1. Residual gravity profile W-E direction (from Wolf et al., 1997). The gravity profile is one of the early lines of evidence that pointed to the feature at Wetumpka as an impact structure.

In 1998, two research drill cores (Schroeder well #98-01 and Reeves well #98-02) were brought up from the center of the Wetumpka structure to help clarify the origin of Wetumpka as an impact crater. The investigation of the drill cores from these two scientific wells revealed not previously known impact breccias, shock-metamorphic features, and elevated iridium, nickel, and cobalt concentrations. All these characteristics provided confirmation of Wetumpka structure as an impact crater (King et al., 2002; 2003).

Johnson (2007) studied the Wetumpka stratigraphy of crater-filling materials drilled at the crater center (Schroeder and Reeves wells). He concluded that according to the stratigraphy observed Wetumpka is a perfect candidate for an impact crater due the presence of a central peak, and a filled inner basin and disturbed slumped mega-blocks. He documented that there is a 100-m layer of slump and potential resurge deposits consisting entirely of sedimentary megablocks, which is underlain by a 100-m unit containing impact breccias, crystalline megablocks, and sedimentary megablocks.

In 2009, NASA funded further Wetumpka research in the form of a grant awarded Dr. David King (Auburn University) and Dr. Jens Ormö (Centro de Astrobiología, Madrid). Thanks to this grant, it was possible to retrieve four new research drill cores from different areas of the crater, including drill core #09-01(Gardner well) that is described in this study. Unlike the two wells drilled at the crater center in 1998, the new 2009 NASA-funded well drilling between the central area and the impact structure's rim revealed thick sequences of slumped and debris-flow-like sediments. Preliminary interpretations of these drill cores (King et al. 2011; Ormö et al. 2007; 2010; Markin, in preparation) suggest Wetumpka as a shallow-marine impact structure strongly affected by collapse and slumping of parts of the sedimentary target sequence as well as by a marine resurge process.

OBJECTIVES

The primary objectives for the present research project are as follows:

- To provide a comprehensive drill-core description in narrative and digital format for drill core #09-01;

- To conduct structural, 3D resistivity survey in the vicinity of the Gardner well, where drill core #09-01 was extracted, to assist in a better understanding of the field relationships between the crystalline basement unit and its fracture system as observed in the drill cores. Specifically, field work will be aimed at understanding the inter-relationships of the crystalline rim flap, basal breccias and breccias dikes, and underlying bedrock in the northwestern quadrant of the crystalline rim;

- To synthesize the drill-core data and field-based descriptions with previous work on the impact structure and thus enhance our understanding of the processes of the emplacement of the crystalline rim flap during the cratering process; and

- To apply new remote-sensing techniques, such as Light Detection and Ranging (LiDAR) and HD aerial pictures to gain better topography information of the

crater and the surrounding areas.

This project offers the opportunity to better understand the emplacement of crystalline basement rocks during a cratering process strongly influenced by a shallow marine target water layer (in this instance, water between 30m and 100m depth).

METHODOLOGY

1. Drill-Core Analysis

The analysis of drill core #09-01 is one of the main objectives of the present project. For this reason, it is important to create a good data base on the drill core (i.e., a detailed drill-core log). Having this database can help further investigations not only for Wetumpka impact but also, for the understanding of any other crater formed in anisotropic rock basement.

Drill core #09-01, has a total of 78 m (256 ft) divided up in standard core boxes (a total of 29) that can hold up to 3 m (10 ft) per box. Every 10-ft box has been marked with the drill core number (in this case, #09-01), the box number, and the top and bottom depth of the core segment (in feet) that is contained in that box. To orient the drill core in each box, labels were written on the top right corner (TOP) and bottom left corner (BOTTOM). These numbers were written on the boxes in the field during drilling operations. These marks are useful to understand the position of the core in the box, having the shallower depth in the upper right corner and the deeper part in the bottom left corner as we can see in Figure 2.

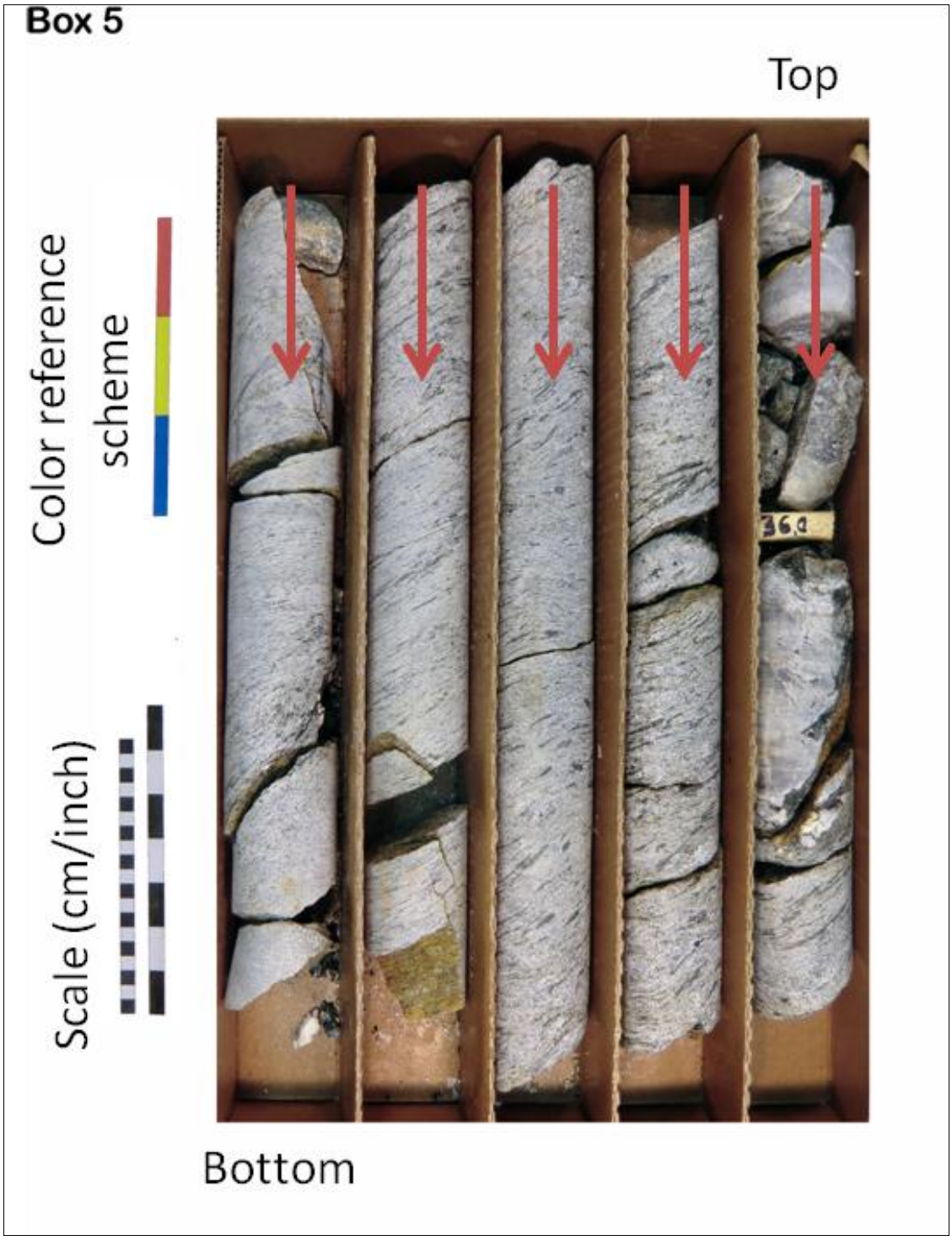

Figure 2. Drill-core box picture example. The reading direction of the core sections is marked by arrows from "Top" to "Bottom." Also shown are the standard color reference scheme and scale in cm and inches.

The procedure for the analysis of this drill core is as follows:

a) Cleaning and alignment

The cleaning process and alignment was made at the same step. Taking sets of 5 boxes, each box was opened and placed close to the next one in order to see if they keep continuity and the fractures match from one box to the next. Carefully the core is turned pointing the dip of foliation planes towards the left side of the box. This dip direction was made consistent with the *in-situ* dip measurement on foliation taken on outcrop at the exact drill site.

Once the set of five core boxes is fully oriented, each box is cleaned from dust and placed back in the standard core box with protective foam in the open spaces. At this point, it is ready to be measured and photographed.

b) Core logging

This core is made up of crystalline rock, so the way to log differs in some ways from core logging of sedimentary cores. In drill core #09-01, the main purpose of the log was to make a detailed inventory of the fractures within the core, as well as the measure of the orientation of these fractures. It was also very important to log the number of fractures and also calculate the Total Core Run (TCR), Solid Core Run (SCR) and Rock Quality designation Index (RQD) of the boxes that compose the drill core (Deere, 1964; 1984).

In order to keep track of the fractures and core pieces, a hand-drawn sketch was made of every core box, so each fracture was noted and every core piece numbered.

The core pieces length were measured one by one, using an SI (international system of units) tape measure set to the total length of every section to reduce errors. Then, the location of every fracture was measured with the intention of knowing at what depth is the fracture position.

The next step was to measure dip direction and dip angle of fractures. In this case, the fracture direction was uncertain due to that no *in-situ* borehole fracture detection technique was applied during drilling operations. At first look, the drill core showed predominant fractures along schistosity planes, so a study of dip direction of schistosity in outcrop around the drill site was done in order to obtain an average dip direction of schistosity planes, and use this "reference orientation" to orient the fractures along the core.

Dip angle was measured using a Brunton "base transparent" geologic compass described later on the surface fracture. The compass was aligned along the center of the core piece with the aid of a laser line that crossed from top to bottom through the middle of the investigated section. In this way the compass was aligned with the vertical axis of the core if the laser crossed the compass 270 and 180 degrees marks simultaneously. The angle of dip was then measured by moving the north arrow to align it to the maximum angle of dipping obtaining this way the real dip direction of the fracture.

c) Photography

Digital pictures were taken using a High Definition photo-camera (CASIO EXILIM EX-HX15, 14.1 megapixels).

A special structure was used as photography workspace. This structure is composed of: (1) stand table with white flat surface, where the drill core boxes are placed to be photographed; (2) railed tower, which controls the vertical distance between Camera and the drill core box

(DCB); (3) camera arm, which is attached to the railed tower, where the camera is plugged (this arm also controls the roll axis of the camera); and (4) light supports, which are two structures located at each side of the stand board that allow extra support to place the illumination lights.

Every box was placed on the stand table, illuminated by 4 halogen lights (130V 100W). A spatial (cm-inch scale bar) and spectral (red-yellow-blue stripe) reference was placed along with the box.

Two pictures of each box were taken, one dry and another one with a thin, sprayed water coat. The reason for water coat is because the mineralogy is better differentiated with this water coat covering the core pieces; on the other hand, most fractures are better seen without the water coat.

d) Data format and data base

All the information gathered at the laboratory about the drill core was transferred to an Excel data sheet. This data base contains:

- Site investigation information included Country, State, County, City, GPS location, Research well name, and elevation (m) of the drill site.
- Drill-core description information included borehole orientation, box number, drill core diameter, depth range of the box in meters and feet, box section of core pieces, core piece number, core piece length, rock type, weathering condition, color, and main mineralogy (% quartz, % feldspar, % muscovite, and % biotite). The latter was estimated using the quantitative mineral analysis described next. In this section, TCR, SCR and RQD values are added as well.

Total Core Run (TCR) is the difference in depth of the first piece in the box and the last, and also, the total length of the pieces measured in a specific box. Both numbers are correct nevertheless in some boxes this number deviates from 1 because the rock is so highly fractured that it is possible to have lost material during drilling.

$$TCR(m) = Initial\ Depth(m) - Final\ Depth(m)$$

$$or$$

$$TCR(m) = \Sigma\ lenght\ of\ core\ pices\ (m)$$

Solid Core Run (%) measure how much of the core is solid rock.

$$SCR(\%) = \frac{\Sigma \text{ solid } core\ pieces\ length(m)}{TCR(m)}\ x\ 100$$

Rock Quality Designation Index (%) measures of the degree of fracture in the drill core. It is expressed in %, and it takes into account only the core pieces larger than 10 cm. High-quality rocks have an RQD of more than 75%; low quality less than 50%.

$$RQD(\%) = \frac{\Sigma \text{ solid } core\ pieces\ length > 10\ cm}{TCR(cm)}\ x\ 100$$

- Drill-core discontinuities included box section, discontinuity reference name dip direction, distance until fracture, and comments. Here is also given the dip angle of the schistosity measured at 10 to 15 cm intervals along the core.
- Grain size and layering description includes the kind of grain and foliation for every section of the box.
- Two detailed drill core box pictures (wet and dry core) were made for each.

e) Quantitative Mineral Analysis Method

Once the pictures have been taken, they are subject to an unsupervised classification process in ERDAS 2010 to differentiate between quartz, muscovite, feldspar and biotite (Figure 3).

ERDAS IMAGINE uses the ISODATA algorithm to perform an unsupervised classification. The meaning for ISODATA is "Iterative Self-Organizing Data Analysis Technique." It is “iterative” because it repeatedly performs an entire classification (thematic raster layer) and recalculates statistics and "Self-organizing" due that it structures the clusters that are characteristic in the dataset (ERDAS 2010).

The ISODATA clustering method uses the same principle from above but the classification of data clusters is calculated through the minimum spectral distance formula. It begins with either arbitrary cluster means or means of an existing signature set, and each time the clustering repeats, the means of these clusters are shifted. The new cluster means are used for the next iteration.

The ISODATA utility repeats the clustering of the image until either:

• Maximum number of iterations has been performed, or

• Maximum percentage of unchanged pixels has been reached between two iterations.

The output file after the unsupervised classification has a grayscale color scheme if the initial cluster means are arbitrary (ERDAS 2010). The steps followed for this classification are as follows.

Subset the drill-core images into the areas we want to classify by creating a set of shape files (.aoi). Those areas are constrained to several quality parameters such as:

1. Exposure levels. The areas chosen for the classification must not be areas with high or low brightness in order to avoid alteration of the minimum spectral distance.

2. Materia. The areas chosen for the classification were restricted to rock exposures (avoiding card board, foam, cracks, or any other elements in the picture that can produce any alteration during the classification).

3. General areas. The areas chosen were consistent with the core direction in most of the cases; this is done by creating thin rectangular stripes along the vertical axis of the core.

Once the image is subset, and this new subset image is saved, it is time to classify it following the next steps:

- Classifier > Unsupervised Classification
- Input raster file: "*Drill core box subset.img*"
- Output Cluster Layer: "*Drill core box # unsupervised.img*"
- Output Signature Set: "*Drill core box # signature. sig*"
- Number of classes : 12 classes

When the image has been classified into these new 12 classes, we need to recode them into 5 new classes including unclassified, muscovite, biotite, feldspar and quartz. This is done by differentiating between values obtained in the classification. In order to do that, I used the attribute table of "*Drill core box # unsupervised.img*" and then I classified the 12 classes into 'unclassified,' biotite, muscovite, feldspar and quartz depending of the numerical value of every pixel and geologic interpretation of the "*visu"* drill core. It is needed to save the changes on the

attribute table of "*Drill core box # unsupervised.img*" once we are finished doing the new classification in order to jump to the next step.

The recoding process is as follows:

- Interpreter > GIS Analysis > Recode
- Input File: "*Drill core box # unsupervised.img*"
- Setup recode: It is assigned a new value for each new class recoded (e.g. 0 = 0; 1,2,3 = 1 (biotite); 4,5,6 = 2 (muscovite);7,8,9 = 3 (feldspar); 10,11,12 = 4 (quartz).)
- Output File: "*Drill core box # recode.img*"

"*Drill core box # recode.img*" is created and in the attribute table of the image you can see that it has been classified into 5 new classes (unsupervised = 0, biotite = 1, muscovite = 2, feldspar = 3, and quartz = 4) and they have assigned a total number of pixels for each class.

The number of pixels obtained from the recode is run in EXCELL 2010 in order to obtain the % of minerals for each box.

The process was repeated for the 29 boxes that composed the drill core #09-01 that was the subject for this study.

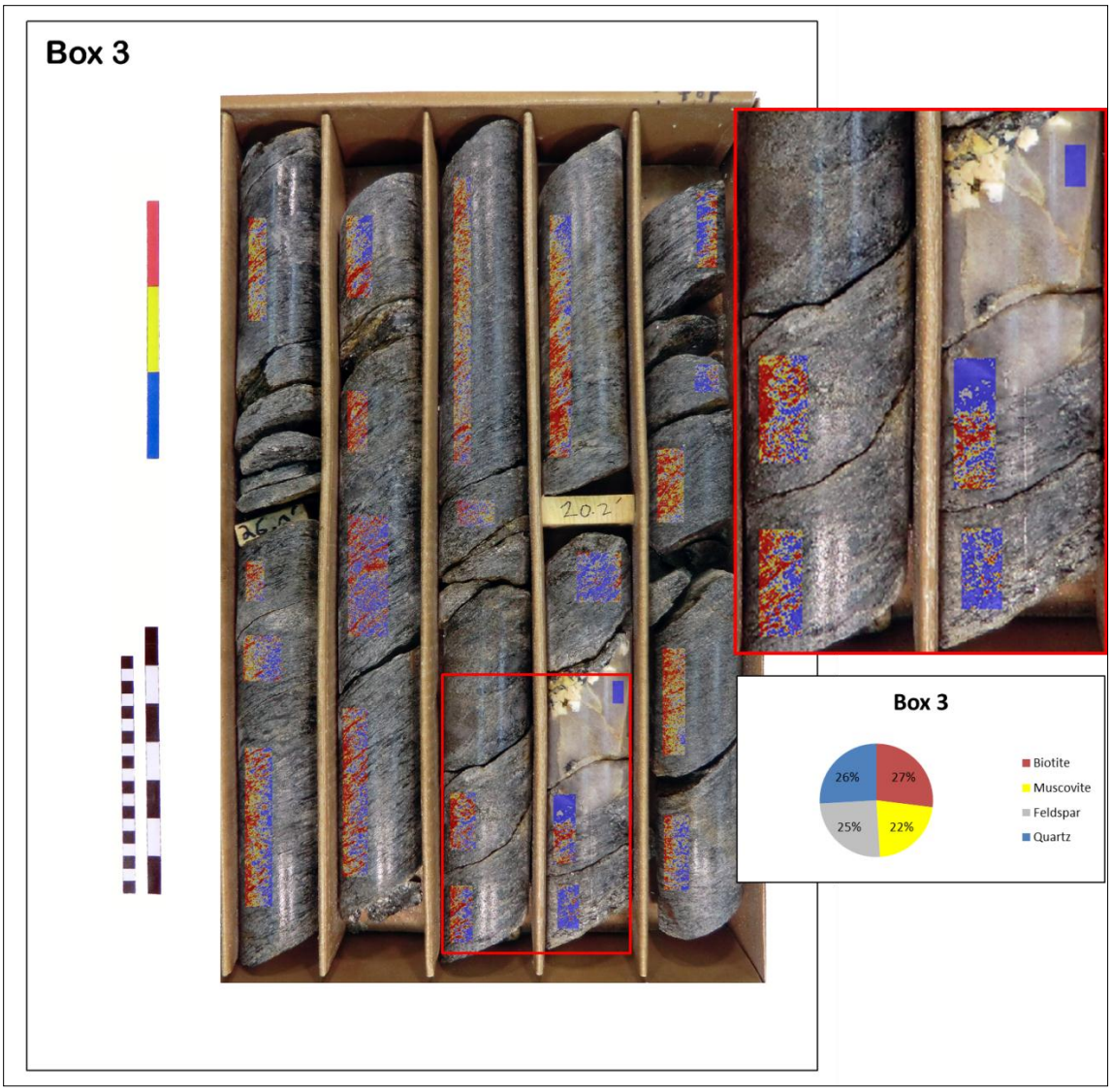

Figure 3. DCB 03 with an example of mineral classification using unsupervised classification. In this picture we can see the different zones subjected to unsupervised classification. This method discerns well the differences in color tones between quartz, feldspar, muscovite, and biotite. Once the pixels are classified we can calculate mineral percentage.

f) Thin Sections

A total of 11 thin sections were made at different depths in the core. In the table below gives the depth of every thin section and an overall picture of it (Table 1).

The thin sections were photographed with a Nikon Eclipse 50i Pol. microscope housed in Petrie Hall, Auburn University. The NIS-Elements D 2.30 software was used to measure grains on thin sections, and capture the photographs.

A database was created with photographs and information such as thin section number, general texture, primary and secondary minerals, mineral percentages, grain size (maximum, minimum, and average), mineral formula, color, habits. The database provide easy access to data for further investigations and to complete the detailed description of the drill core #09-01 (for more on the thin sections, see the Appendix).

Thin Section :#09-01 (61.2) Depth: 61.2 Ft Rock Name: Mica Schist Grain Size : <1mm Texture: Foliated	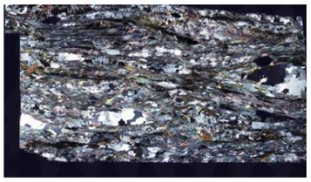	Thin Section :#09-01 (174.7) Depth: 174.7 Ft Rock Name: Mica Schist Grain Size : <1mm Texture: Foliated/ granoblastic quartz bands	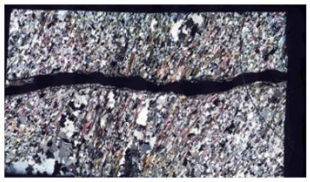
Thin Section :#09-01 (65.2) Depth: 65.2 Ft Rock Name: Mica Schist Grain Size : <1mm Texture: Crenulated	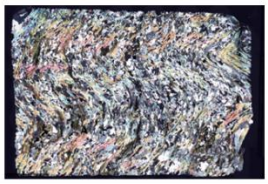	Thin Section :#09-01 (216) Depth: 216 Ft Rock Name: Mica Schist Grain Size : <2mm to 4mm> Texture: Highly strained grains.	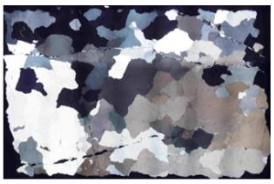
Thin Section :#09-01 (98) Depth: 98 Ft Rock Name: Mica Schist Grain Size : >2mm Texture: Highly strained grains.		Thin Section :#09-01 (222.8) Depth: 222.8 Ft Rock Name: Mica Schist Grain Size : <1mm to 3mm> Texture: Foliated	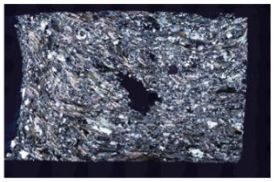
Thin Section :#09-01 (111.8) Depth: 111.8 Ft Rock Name: Mica Schist Grain Size : <1mm to >2mm Texture: Foliated	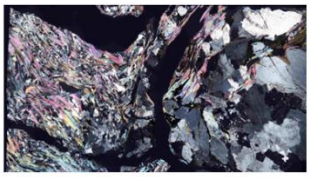	Thin Section :#09-01 (255) Depth: 255 Ft Rock Name: Mica Schist Grain Size : <1mm Texture: Foliated	
Thin Section :#09-01 (135.8) Depth: 135.8 Ft Rock Name: Mica Schist Grain Size : <1mm Texture: Foliated	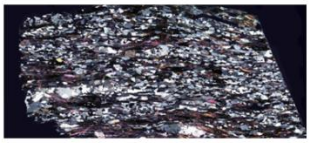	Thin Section :#09-01 (Breccia zone) Depth: 210 to 222.8 Ft Rock Name: Mica Schist Grain Size : <1mm Texture: Brecciated/sand	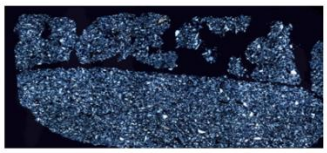
Thin Section :#09-01 (141) Depth: 141 Ft Rock Name: Mica Schist Grain Size : <1mm to 3mm> Texture: Foliated / Granoblastic bands	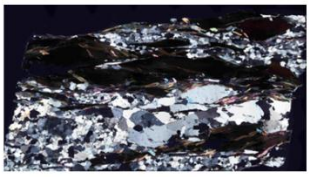		

Table 1. Thin sections are shown in this table along with the depth in the drill core #09-01, type of texture, and general grain size. For more information, see thin sections in the Appendix.

2. Light Detection and Ranging (LiDAR)

LiDAR is been used for multiple purposes in recent years, mainly geology and geography. There are many examples of the use of this powerful tool. NASA has been using it to track satellites, and in aspects of planetary exploration (Bellian et al., 2005).

Briefly, LiDAR method uses pulses of light to measure distance. This light pulse travels from the device in a straight line until it hits the target surface and the travels back again to the receptor. The distance is calculate and stored, in an instant, as a cloud points file (.LAS). This file has the XYZ coordinates for every point measured. The processing of this .LAS file will result into a Digital Elevation Model image.

LIDAR acquisition methods

The data for Elmore County were provided to us by the Elmore County Revenue Commissioner's office in Wetumpka, Alabama. The contractor company in charge of the project was The Atlantic Group LLC (http://www.theatlgrp.com/), which executed the LiDAR survey in 2010.

For data collection a Cessna 310, tail number N69622 (The Atlantic Group LLC property) was used. The aircraft was installed with an Optech ALTM Gemini LiDAR system (The Atlantic Group LLC, 2010).

In order to cover successfully the total surface of the Elmore County, Alabama, which is approximately 1950 km^2, it was necessary to design a total of 97 flight lines including the control line (The Atlantic Group LLC, 2010; Figure 4). The lines were flown using the settings in Table 2.

Altitude	1175m
Overlap	30%
Speed	140 kts. (260Km/h)
System PRF	100 kHz
Scan Frequency	46 Hz
Scan Half Angle	20°

Table 2. Settings used during the aerial LiDAR survey

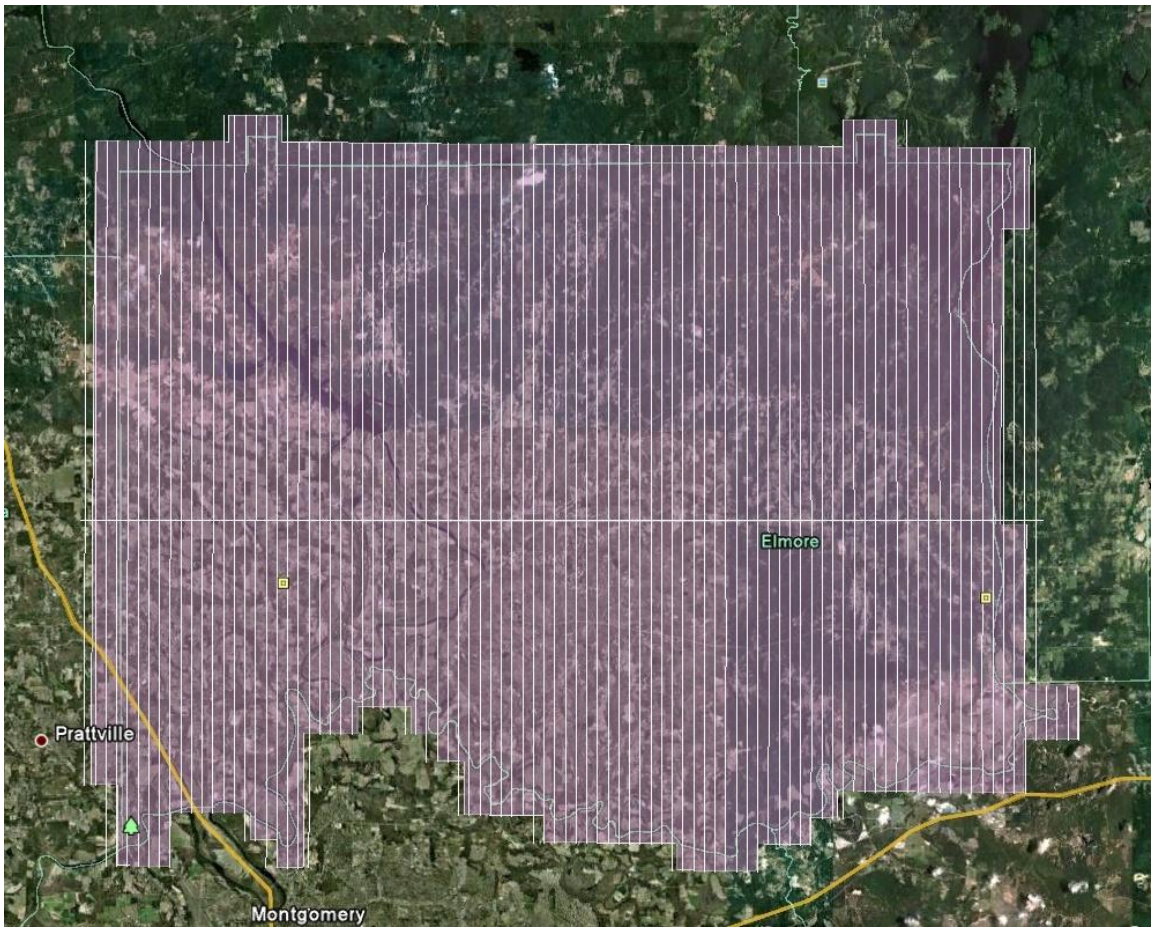

Figure 4. Aerial picture showing the area for LiDAR survey (Elmore County, Alabama). The north-south “columns” show the flight lines.

Elmore County DEM Analysis

Once we have accesses to the DEM file, the next step for this project is to create a slopes map over the crater area and along the crater proximities. Using ERDAS 2010, the image is loaded and processed through the following stages:

1. Start > All Programs > Erdas 2010 > Erdas Imagine 2010 > Erdas Imagine classic Interface.

2. In Viewer #1 > File > Open > Raster layer > Elmore_County.tiff.

a) Slopes Analysis

Once the image is loaded in our viewer, we follow the next actions in ERDAS 2010 to obtain the slopes map:

Interpreter > Topographic Analysis > Slope.

A window will appear, and we need to fill some of the required spaces.

Input DEM File => Elmore_County.tiff

Output File => Elmore slopes. Tiff

This process identifies the slope (gradient, or rate of maximum change in z-value) from each pixel of a raster surface (ArcGIS 10, 2010).

For each cell, the Slope tool calculates the maximum rate of change in value from that cell to its neighbors, which in essence is the maximum change in elevation over the distance between neighbor cells (ArcGIS 10, 2010).

This tool creates a plane that has a slope value calculated using the average maximum technique of every 3x3 cell (Burrough & McDonell, 1998). The direction the plane faces is the aspect for the processing cell. The general rule is the lower the slope value, the flatter the terrain; and the higher the slope value, the steeper the terrain (ArcGIS 10, 2010).

In case there is a No Data z-value in one of the cell locations, the z-value of the center cell will be assigned to the location. At the edge of the raster, at least three cells (outside the raster's extent) will contain No Data as their z-values. These cells will be assigned the center cell's z-value. The motive to do so is to flatten the 3 x 3 plane fitted to these edge cells, and lead it to a reduction in the slope (ArcGIS 10, 2010).

The output raster (slope map) can be calculated either in degrees or percent units (percent raise). The percent is known as the rise divided by the run, multiplied by 100. In the figure below (Figure 5), we can find an example. If we consider the triangle *B, w*hen the angle is 45 degrees, the rise is equal to the run, and the percent rise is 100 percent. As the slope angle approaches vertical (90 degrees), as in triangle *C*, the percent rise begins to approach infinity (ArcGIS 10, 2010).

b) Aspect Analysis (Dipping Surfaces)

Another derivative applied to our digital elevation model is the Aspect tool. This derivative is used by most of the remote sensing software nowadays and uses the same code. In our case study I have used both ArcGIS 10 and ERDAS Imagine 2010. Nevertheless, the software capabilities of ArcGIS versus ERDAS make ArcGIS the chosen tool for this study.

Aspect identifies the downslope direction of the maximum rate of change in value from each cell to its neighbors. It can be thought of as the slope direction. The values of each cell in

the output raster indicate the cardinal direction that the surface faces at that location or in that particular cell. It is measured clockwise in degrees from 0 (due north) to 360 (again due north), creating a full circle. A value of -1 is given to flat areas due to that they have no variation in downslope direction (Burrough et al. 1998)

Burrough et al. (1998) noted that the value of each cell in an aspect dataset indicates the direction the cell's slope faces. This can be seen in Figure 6.

The Aspect algorithm

It is created through a moving 3 x 3 cell window that moves around the raster image stopping at each cell, and then an aspect value is calculated for each cell in the center of the window, using the values of the cell's eight neighbors. As an example (Figure 7), the cells are identified as letters *a* to *i*, with *e* representing the cell for which the aspect is being calculated (Burrough et al. 1998).

The rate of change in X direction for cell *e* is calculated with the following algorithm:

$$\frac{\partial z}{\partial x} = \frac{((c + 2f + i) - (a + 2d + g))}{8}$$

The rate of change in Y direction for cell *e* is calculated with the following algorithm:

$$\frac{\partial z}{\partial y} = \frac{((g + 2h + i) - (a + 2b + \mathrm{c}))}{8}$$

Taking the rate of change in both X and Y direction for cell *e*, aspect is calculated using:

$$Aspect = 57.29578 \times \tan^{-1} 2\left(\left[\frac{\partial z}{\partial y}\right], -\left[\frac{\partial z}{\partial x}\right]\right)$$

The aspect value is then converted to compass direction values (0-360 degrees), according to the following rule:

If *aspect* < 0

Cell = 90.0 - *aspect*

Else if *aspect* > 90.0

Cell = 360.0 - *aspect* + 90.0

Else

Cell = 90.0 - *aspect*

The Steps to obtain the Aspect map of Elmore County were the following:

- Open “Elmore County DEM” in ArcMap 10.
- In Arc toolbox window > Spatial Analysis tools > Surface > Aspect
- A window will pop up asking for:
- Input raster file > Elmore_County.tiff
- Output name file > Elmore_County_Aspect.tiff

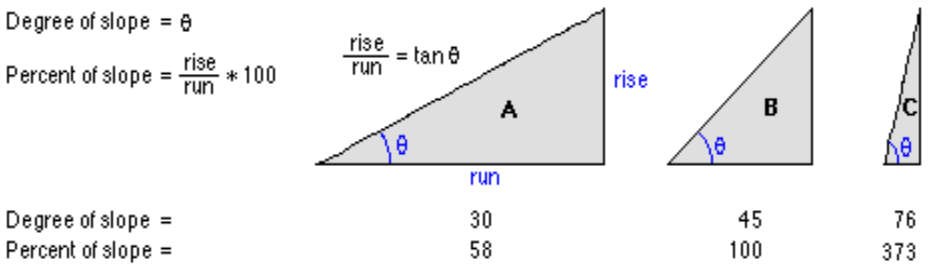

Figure 5. Slope in degrees versus percent. Image taken from ArcGIS 10.

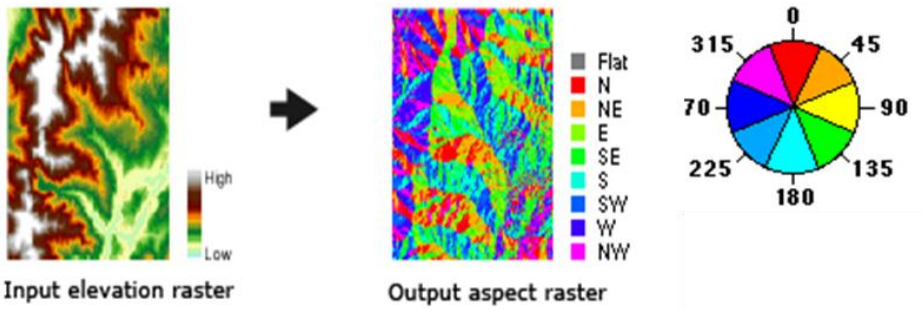

Figure 6. Diagram showing an input elevation dataset and the output aspect raster. Also is shown the aspect directions. Image taken from ArcGIS 10.

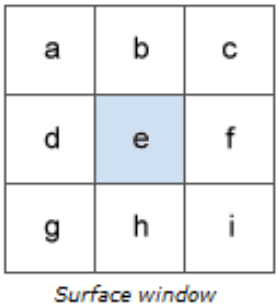

Figure 7. Example of surface window for calculation.

3. 3D Resistivity Imaging

An electrical resistivity survey was conducted to explore the continuity and development of fractures on the rim near the drill site 70m to SE from the Gardner scientific core hole #09-01 (Figure 8).

The study area is located at the top of a hill, on a rather flat bedrock surface sporadically covered by 20 to 50 cm of soil (saprolite) with some scattered areas of ~1m^2 of exposed fractured mica schist. The survey was performed during October, 2011. The weather conditions recorded for that day were clear skies with a mean temperature of 75°F.

Figure 8. Area chosen for 3D resistivity survey (rectangle). Note location of Gardner well (#09-01) relative to survey (blue dot).

For the resistivity survey, an Advanced Geosciences Inc. SuperSting R1 was used. The survey utilized a mixed dipole-dipole array, with 48 electrodes and automated switching (Figure 9). This type of array was chosen because it is sensitive to horizontal changes in resistivity which means that it is good for mapping fracture directions at specified depth interval. The survey grid used was a 10m wide and 28m long (Figure 10). The chosen spacing of the electrodes was 2 m, which yielded an imaging depth of about 6 m; this is enough depth for defining a fracture pattern under the saprolite while still maintaining high resolution.

Once the survey was finished all the data gathered from the SuperSting R1 were processed and interpreted using EarthImager 3D™. In Figure 11 we can see the process of inversion used in the software.

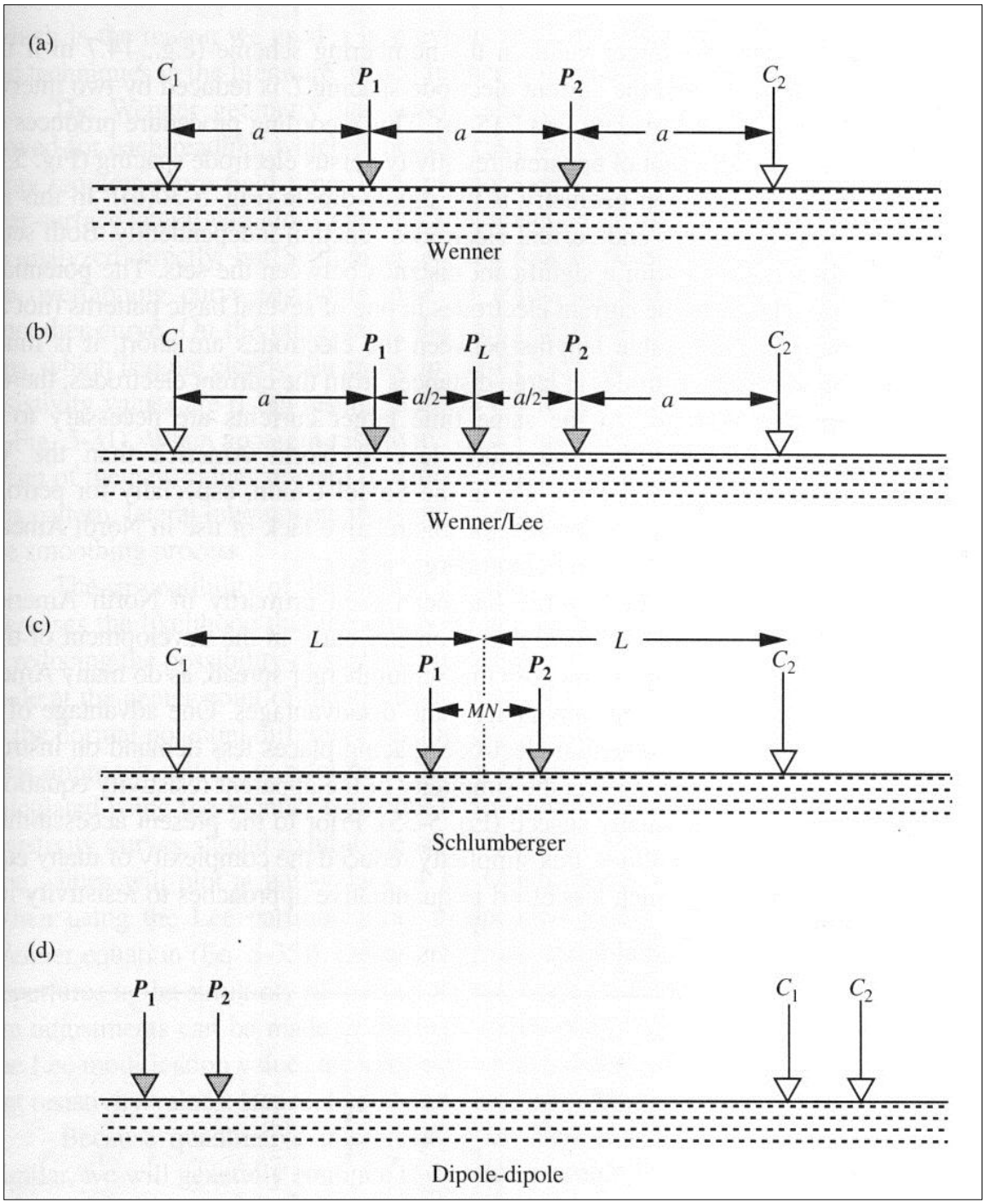

Figure 9. Sketch of the most common arrays set up used in resistivity(from Burger, 1992), where P = potential electrode and C = current electrodes. This style of array was chosen due to its capacity to map vertical structures.

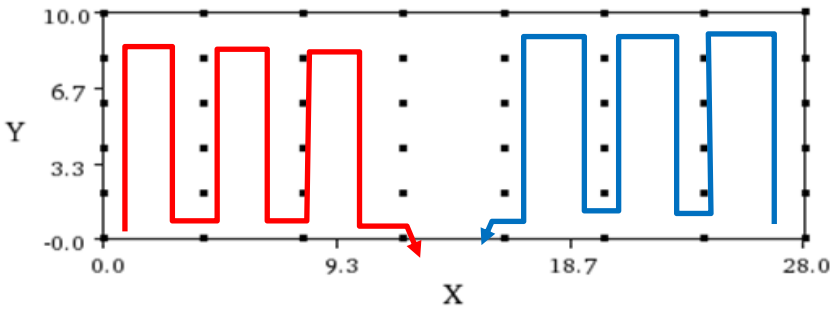

Figure 10. Map view of electrodes geometry for 3D resistivity survey. The dots show the location of electrodes. The distances are in meters. The cable layout is shown by red and blue lines, which end in arrows pointing to the connection with SuperSting R1 meter.

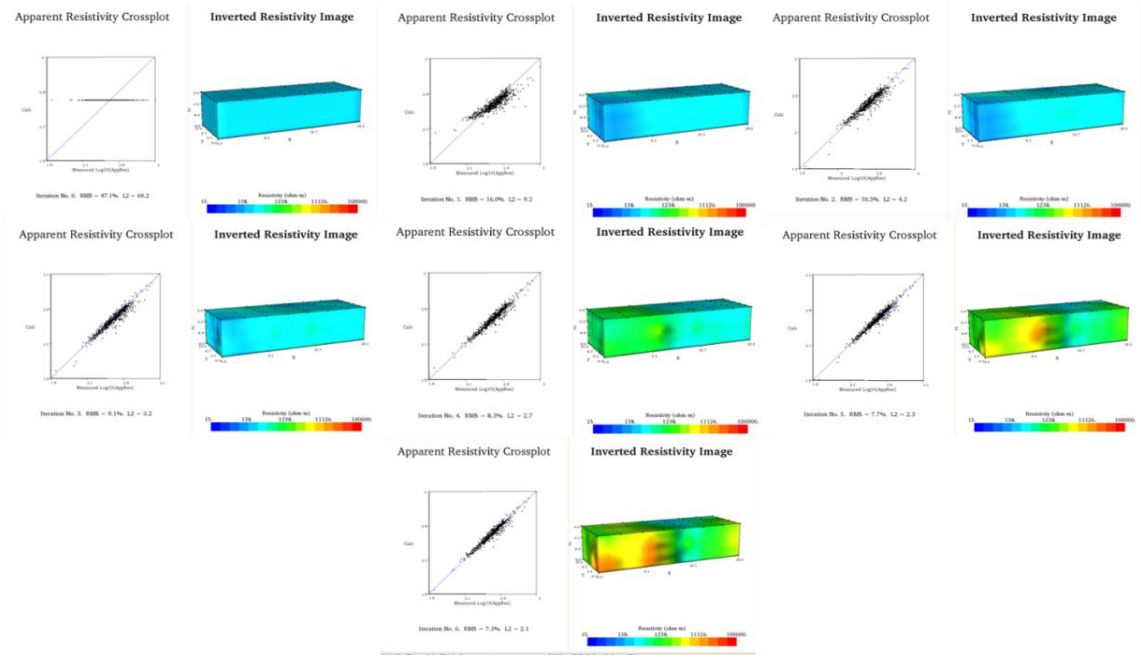

Figure 11. Time-lapse image showing the process of inversion. An *a priori* model is updated by comparing data calculations with the data observation. Each iteration reduces the error.

4. Field Methods

The inventoried areas are a part of the western sector of the basement crater rim of Wetumpka, a section along the Coosa River beginning near the rim and going upstream from the rim, and an outcrop on the southeastern part of the rim. These areas provide access to the best places where relatively unweathered rocks of the rim are exposed. In these areas, the survey was performed as follows. Every key-point of every outcrop was measured using a geologic compass along with the GPS location and a digital picture was made (Figure 12).

I kept track of this inventory, first in a personal field book, and later all the information was transferred to an ArcGIS database. Fractures and schistosity planes were measured using dip direction and dip angle, instead of strike and dip.

Figure 12. Example of the instruments used during fieldwork. From left to right: field notebook, geologic compass, GPS. Rock outcrop is on the southeastern rim area of Wetumpka impact structure.

RESULTS

This chapter summarizes the results obtained from the analyses conducted. First, the results achieved by drill-core logging and photographs are presented as RQD (Rock Quality Designation Index). Then, the fracture-families analysis showing the diverse fracture families in the drill core #09-01 are presented. After that, the mineralogy results obtained to compute an unsupervised classification in ERDAS 2010 software and thin sections are presented. Later, the fracture inventory is shown, providing dip direction and dip angle of the main features, around Wetumpka impact crater rim. And, finally the results gathered from the 3D resistivity survey are given before presenting the results from the LiDAR and GIS analysis.

1. Drill core

a) Photographs

A total of 58 photographs have been made, thus every drill-core box has a pair of pictures, and one in dry conditions and the other with a fine water coat to bring out all the mineral colors (see Photographs folder on the DVD that accompanies this thesis).

The print format used to present the resulting drill core photographs is shown on the example picture below (Figure 13). In these prints, a few spaces with information related to the core such as image name have been added at the end, including site and "GPS" location, depth range (in meters and feet), elevation of the drill site, and RQD%.

The resulting set of photographs is a compound of high-quality pictures of the drill core and main drill-core data, organized by depth, which offers an entire graphic record of the drill core #09-01. Another advantage of this set of photographs is the possibility to obtain a fast overview not only of the drill core but also the fracture families, dip-direction and angle, and the fracture system's degree of development along the core.

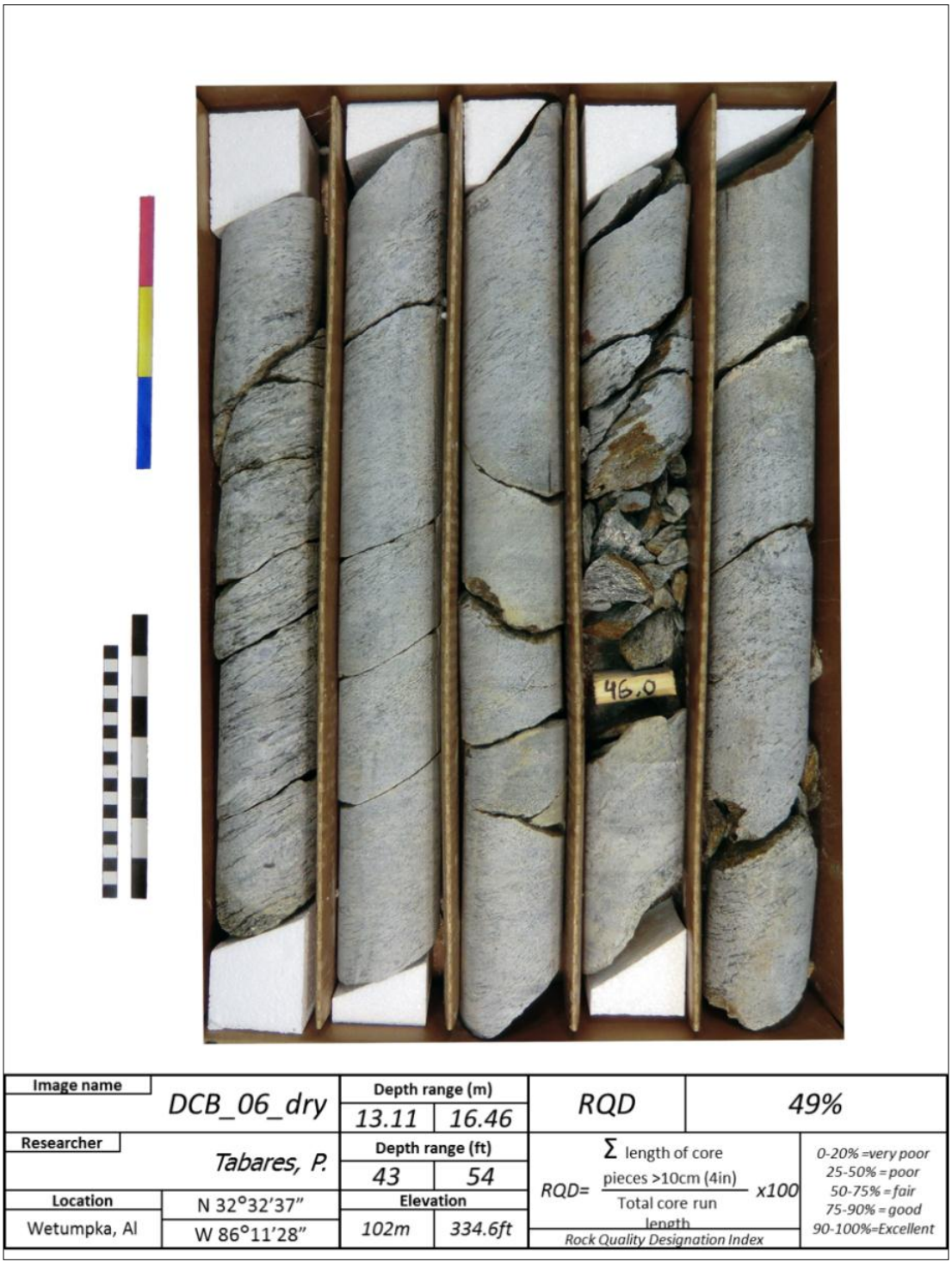

Figure 13. An example of a drill-core box (DCB) photograph print format. It includes the same features listed in the methodology part for photographs and also, it has been accompanied by

other useful information about the core. This information includes image name, site and “GPS” location, depth range (in meters and feet), elevation of the drill site, and RQD%.

b) RQD over Depth

Some of the most relevant data about the fractures in a rock mass is the RQD. In this project, the concept of RQD has been adapted to the studied drill core, in order to get a representative percentage of the fractures along the core.

Once all the fracture information was collected and the RQD calculated for each box, it was possible to reproduce the fracture percentage virtually; the result is a chart where it can be seen how this RQD varies over depth (Figure 14).

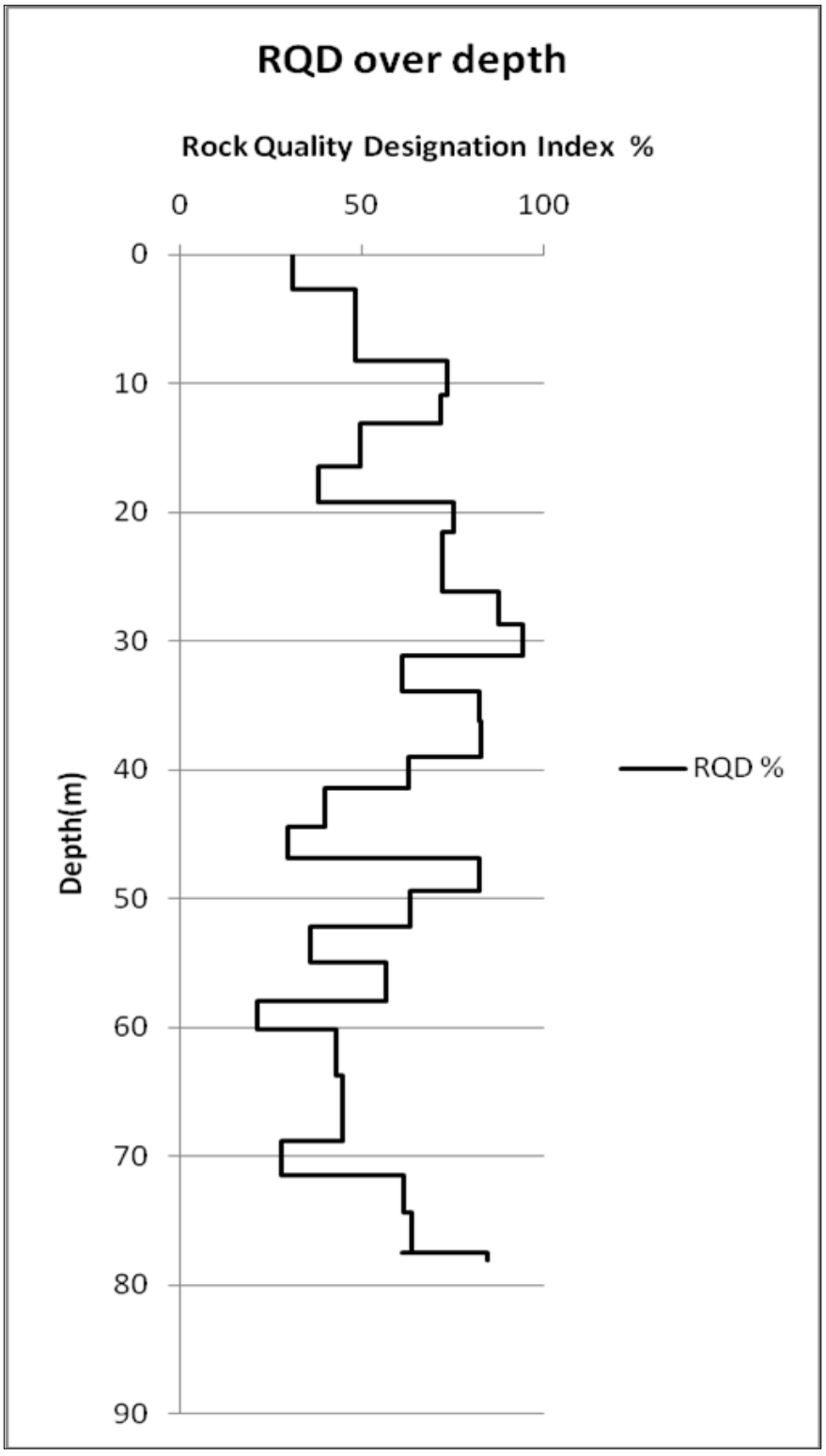

Figure 14. RQD percentage with depth. The segmented lines represent the length of every drill-core box.

c) Schistosity and fractures families.

Schistosity Analysis

The main fracture pattern along the core is dominated by the fractures that follow the schistosity planes. These planes have been oriented according to the schistosity orientation on surface, as described in the methodology part of the present project. The orientation of these planes is referenced as N350°.

During the drill-core logging, the reduction in the dip angle of the schistosity planes was noted, which allows a statistical treatment of the data with respect to normal frequency distribution of the schistosity dip angle along the full length of drill core #09-01 (Figure 15).

The analysis gave that over a population of 528 measurements, the most frequent schistosity dip angle is 30°.

A second statistical analysis was done measuring the dip angle of the fractures of every drill-core box (Figure 16). The pattern of fracture dip angles displays high variations; nevertheless a linear trend confirmed a decreasing tendency of the schistosity plunge with depth.

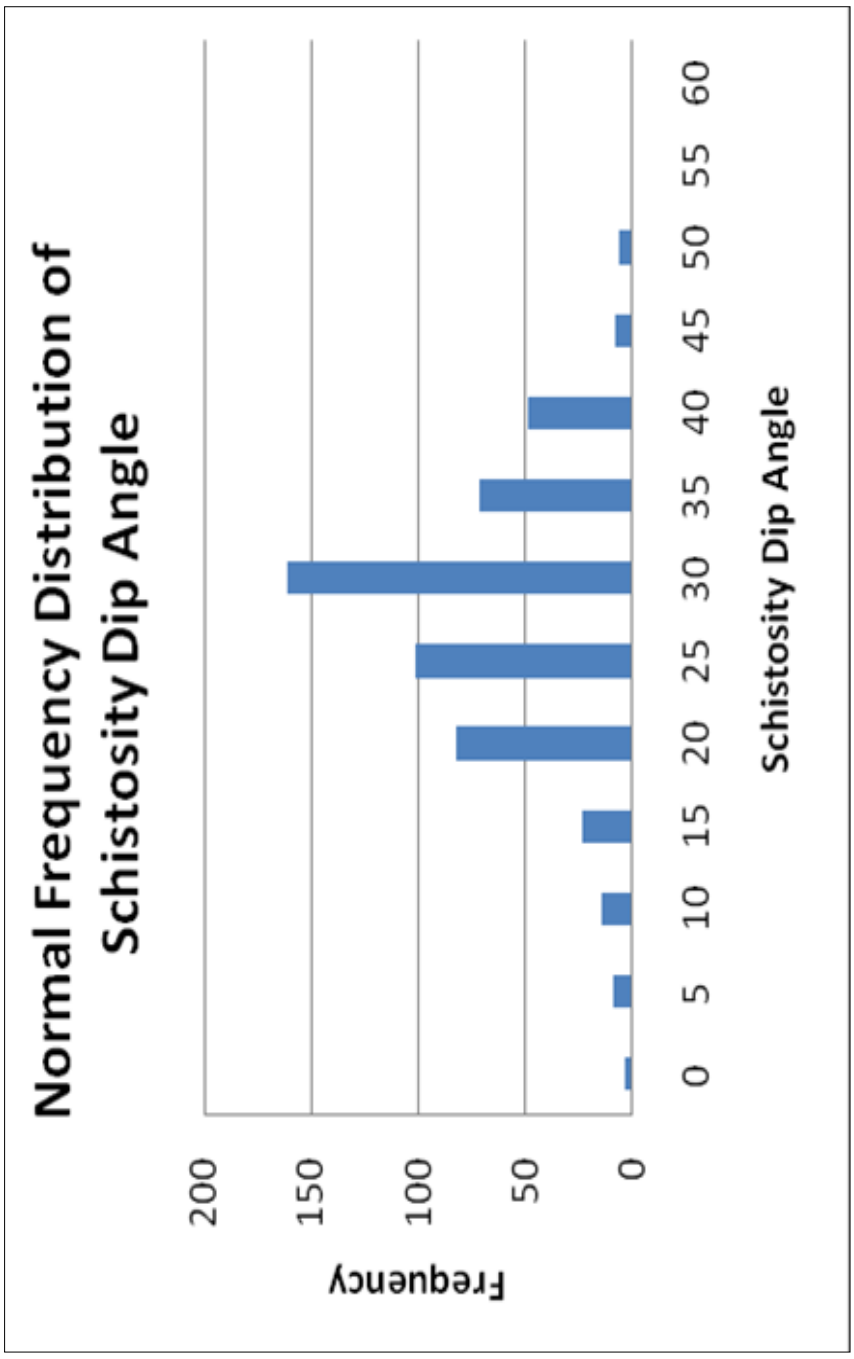

Figure 15. Normal frequency distribution of the schistosity dip angle measured throughout the core.

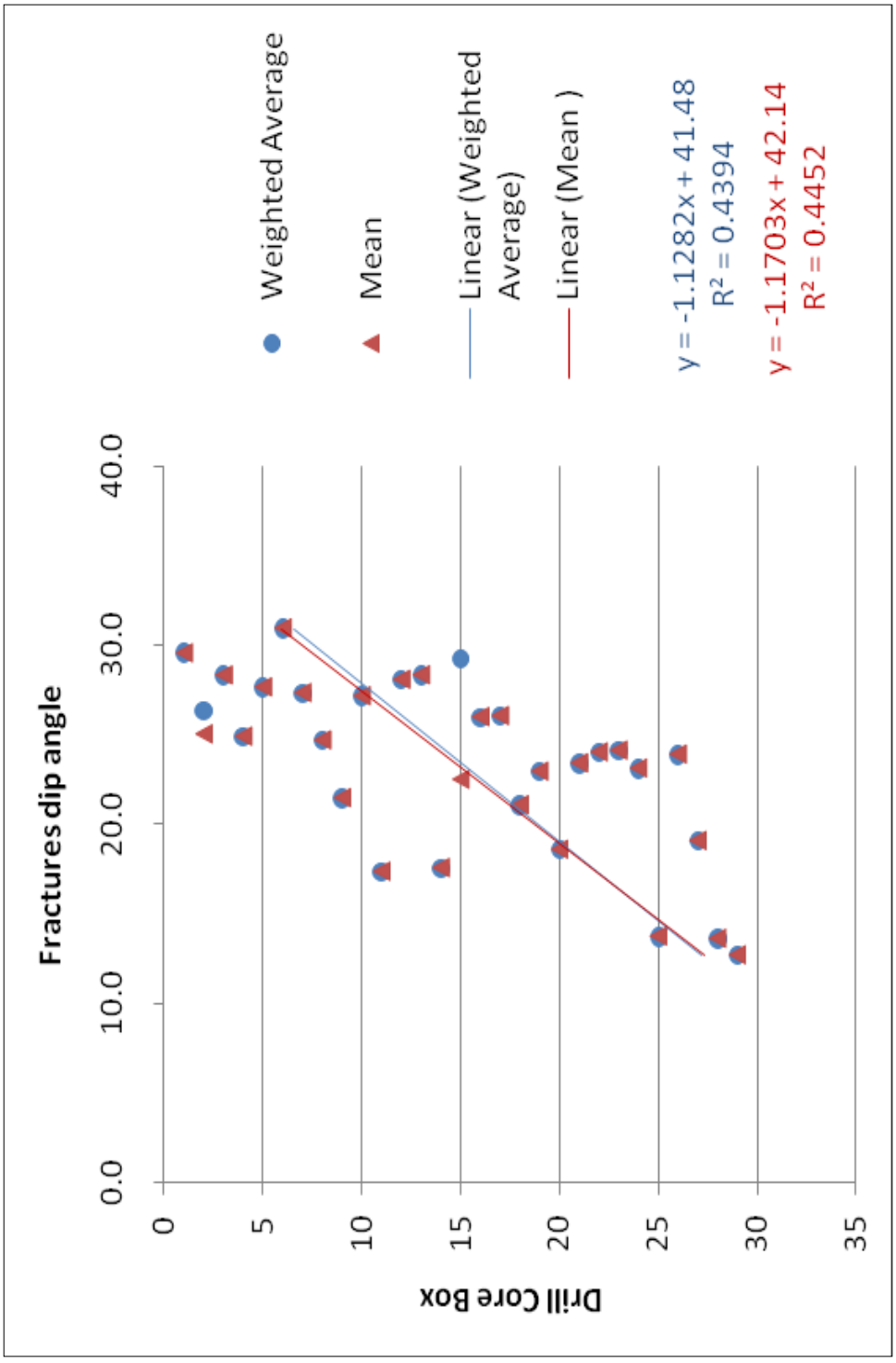

Figure 16. Weighted average and mean of the fractures dip angle calculated in each box. The tendency lines show a reduction in schistosity angle from the upper boxes to the lower ones.

Other fracture families.

Even though the statistical analysis of the fractures shows a highly fractured pattern following the schistosity planes, other secondary or less abundant fracture families do also occur.

The fracture families found along the core are presented on the stereograph in Figure 17. These have been classified into three different families, which, as noted before, do not follow the schistosity planes. In order of decreasing population density, the first family (F1) has approximately N180° of dipping direction and an average dip angle of 35°; the second family (F2) has a dip direction of N130° and approximately 55° in dip angle; and finally the third family (F3) of fractures has N245° dip direction and about 45° in dip angle (Figure 17).

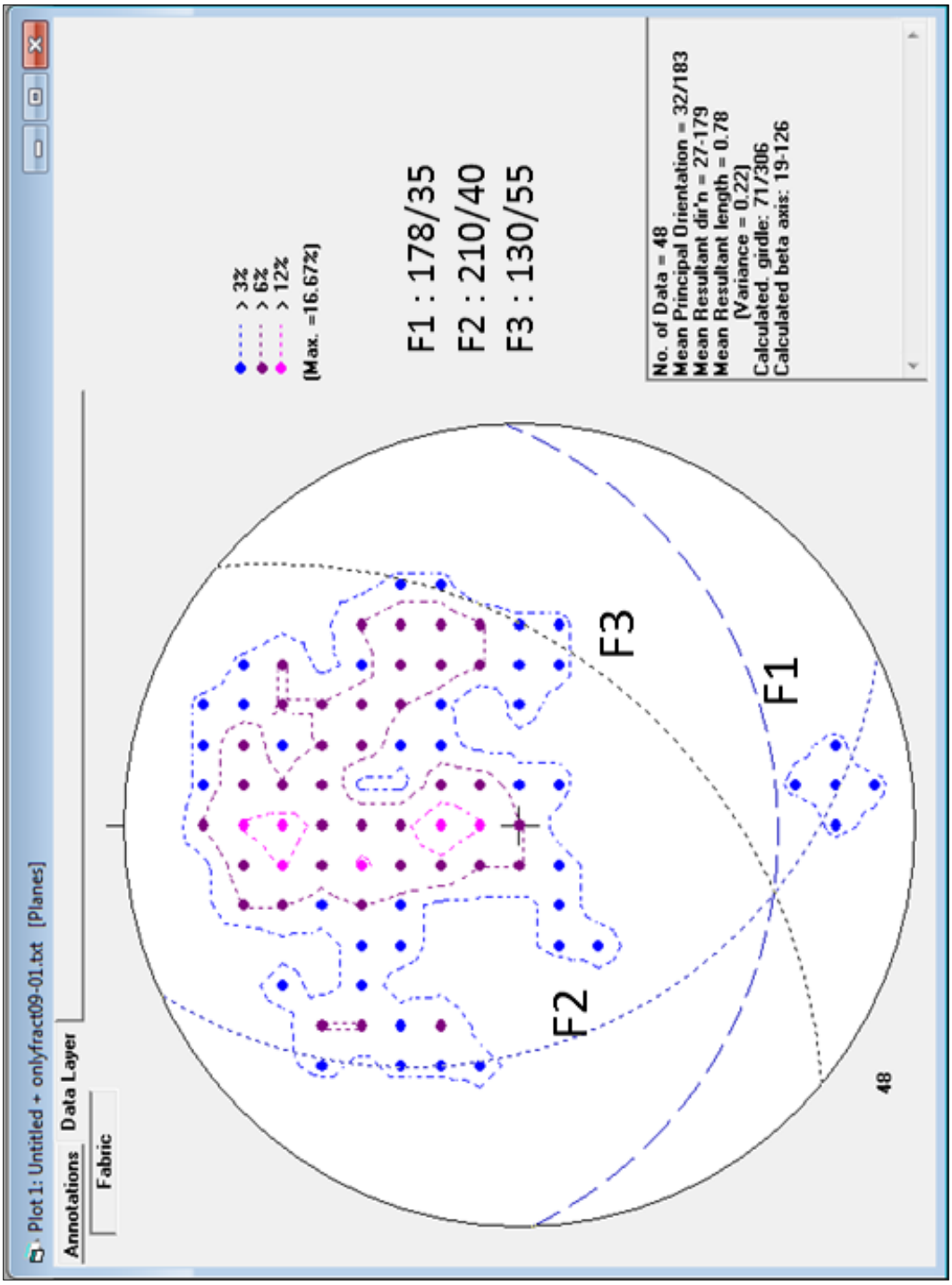

Figure 17. Stereographic projection from GEOrient, showing main dip planes of fractures logged within the #09-01 core. In this stereograph, schistosity is not taken into account in the data.

d) Mineralogy

An estimation of the mineralogy of the drill core was made using ERDAS 2010, as described in the methodology section. This study completes the descriptive part of the drill core, showing the estimated percentage of minerals by unsupervised classification of chosen control areas on the drill core (mainly muscovite, biotite, feldspar, and quartz), which can be identified "de visu." As a result of this mineralogy analysis several graphs were created where it is possible to see the variation of the mineral content with depth (Figure 18).

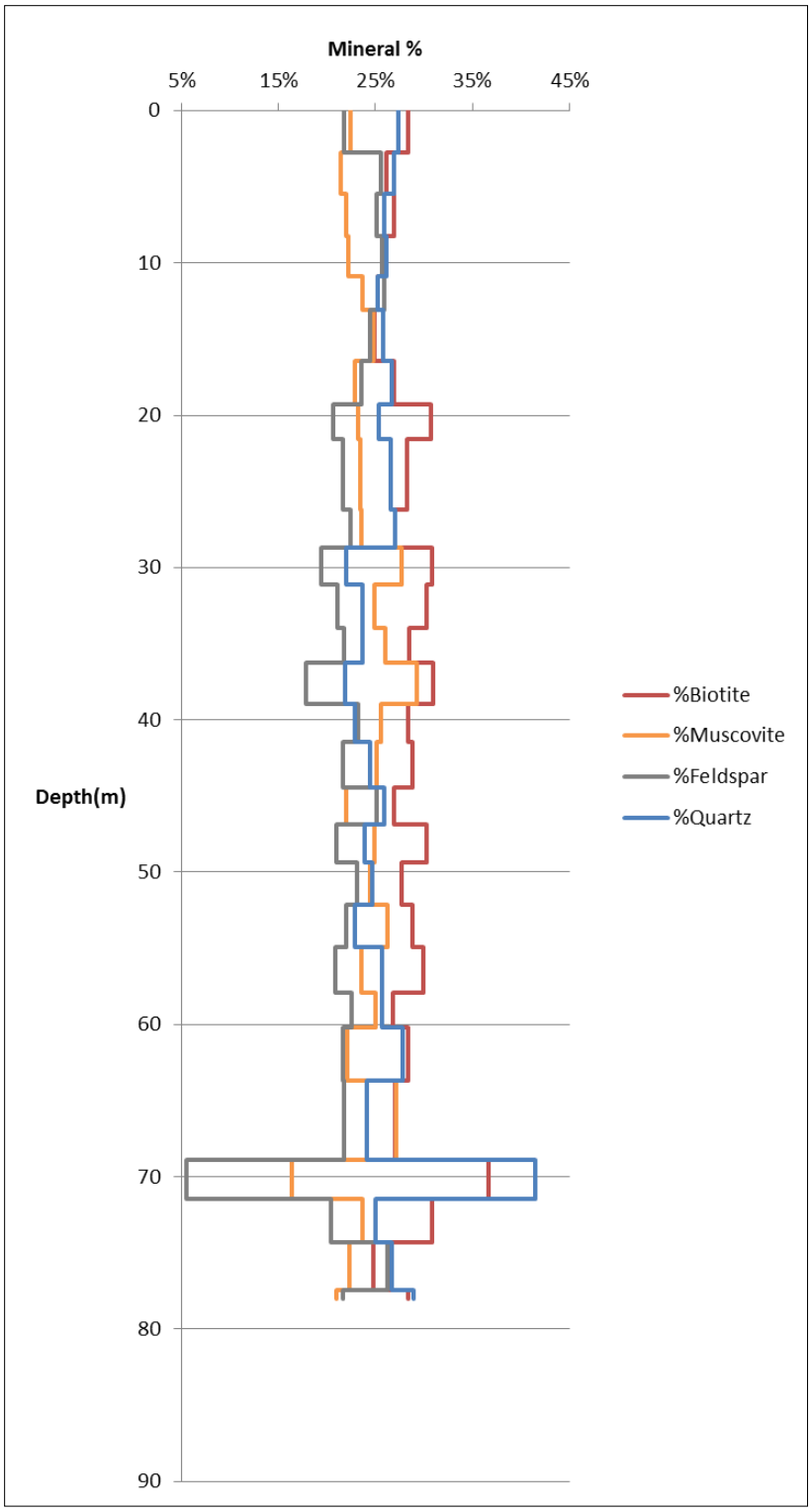

Figure 18. Biotite, muscovite, feldspar, and quartz percentage plotted versus depth. The segmented lines represent the length of each drill-core box.

Biotite and muscovite contents are constant at around 20 to 30 % over the entire core. This makes the percentage of micas in the core to be around 50%.

Quartz has a relation in percentage with feldspar though the estimation in feldspar records the lower percentages. They are also around 20 to 25 %, except for the areas of the core where we can find quartz veins. In these areas, the percentage of quartz increases, as can be expected.

There appears to be a slight correlation between the percentage of micas and the RQD through the core (Figure 19). As we go through the micas curve in the figure below, normally, if the percentage of micas increase so does the RQD in that section, for example in boxes 8, 11, 14, 18, 24, and 26. In the other hand, if the percentage of micas decrease also decreases the RQD, as for example in boxes 7, 9, 12, 13, 15 ,17 ,19 ,22, 25, and 27.

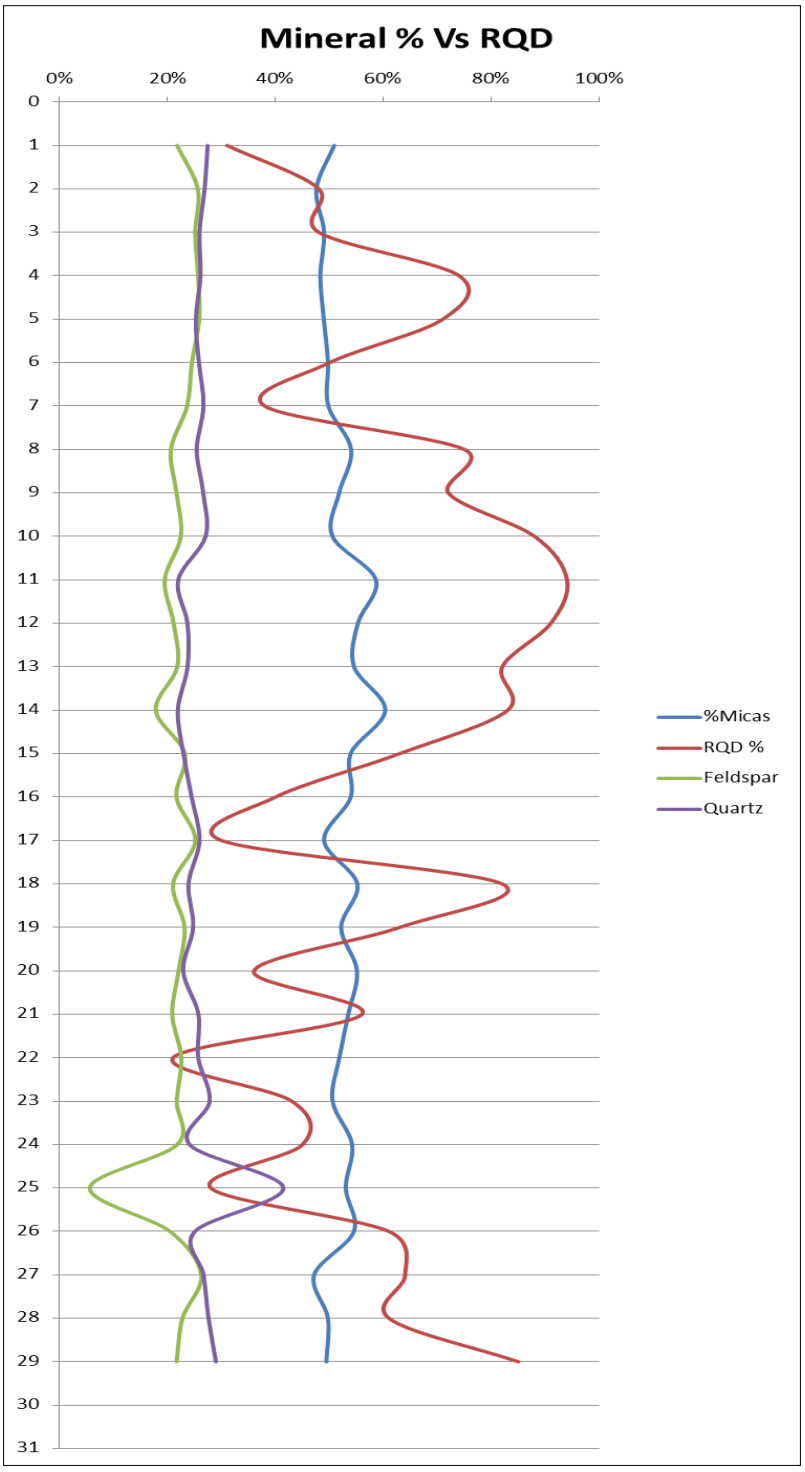

Figure 19. Mineral percentage versus RQD. In this case muscovite and biotite % has been combined to obtain the percentage of micas through the core. The relation between micas % and RQD can be seen here. Increasing percent of micas also increases the RQD, and vice versa.

e) Thin sections

Most of the thin sections observed tend to have strong foliation texture, except for those thin sections that have been taken from quartz veins which show high-strain grain texture, which are half way to granulitic. These grains are in a recrystallization process showing serrated contacts and subdomains of quartz grain bands (for more on the thin sections, see the Appendix).

Most major minerals observed are quartz, muscovite, biotite and feldspar (plagioclase and albite). The minor minerals are garnets and hornblende.

It is interesting the high presence of subhedral to anhedral micro garnets (< 0.1 mm) visible only in the thin sections closest to the surface (0 to 45.7 m; Figure 20). Below that depth, the garnets are nearly absent.

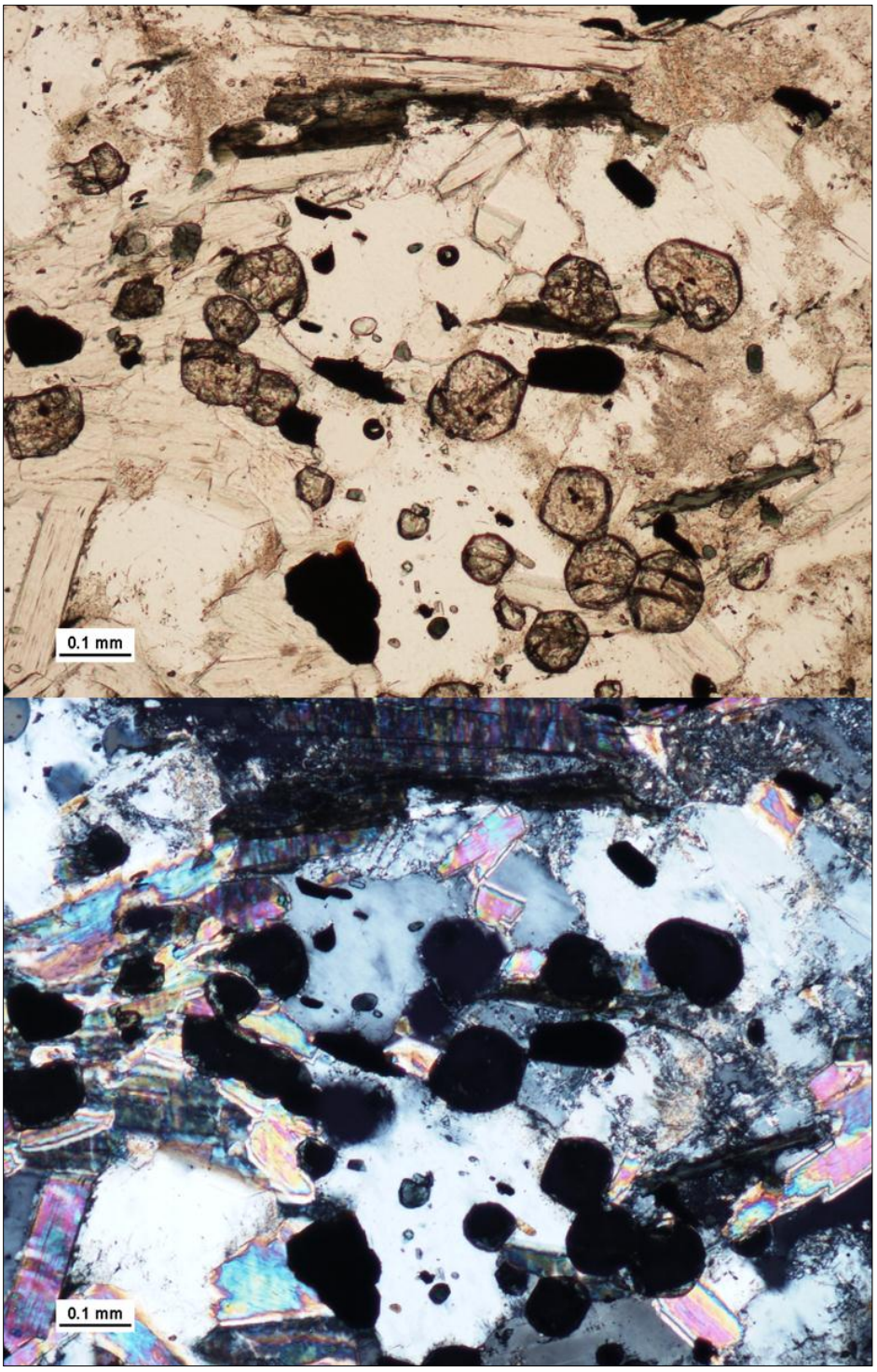

Figure 20. Presence of very small garnets ("micro garnets") in drill core #09-01 at 61.2 ft. (18.7m) depth. The occurrence of garnets decreases with depth, being practically nonexistent below 150 ft. (45.7m).

2. Fracture inventory of the study area.

A fracture inventory of several parts in the crater rim has been made, along with the surrounding areas of the crater. In the map below (Figure 21), the schistosity planes (black symbols) and the fractures directions (red symbols) are indicated.

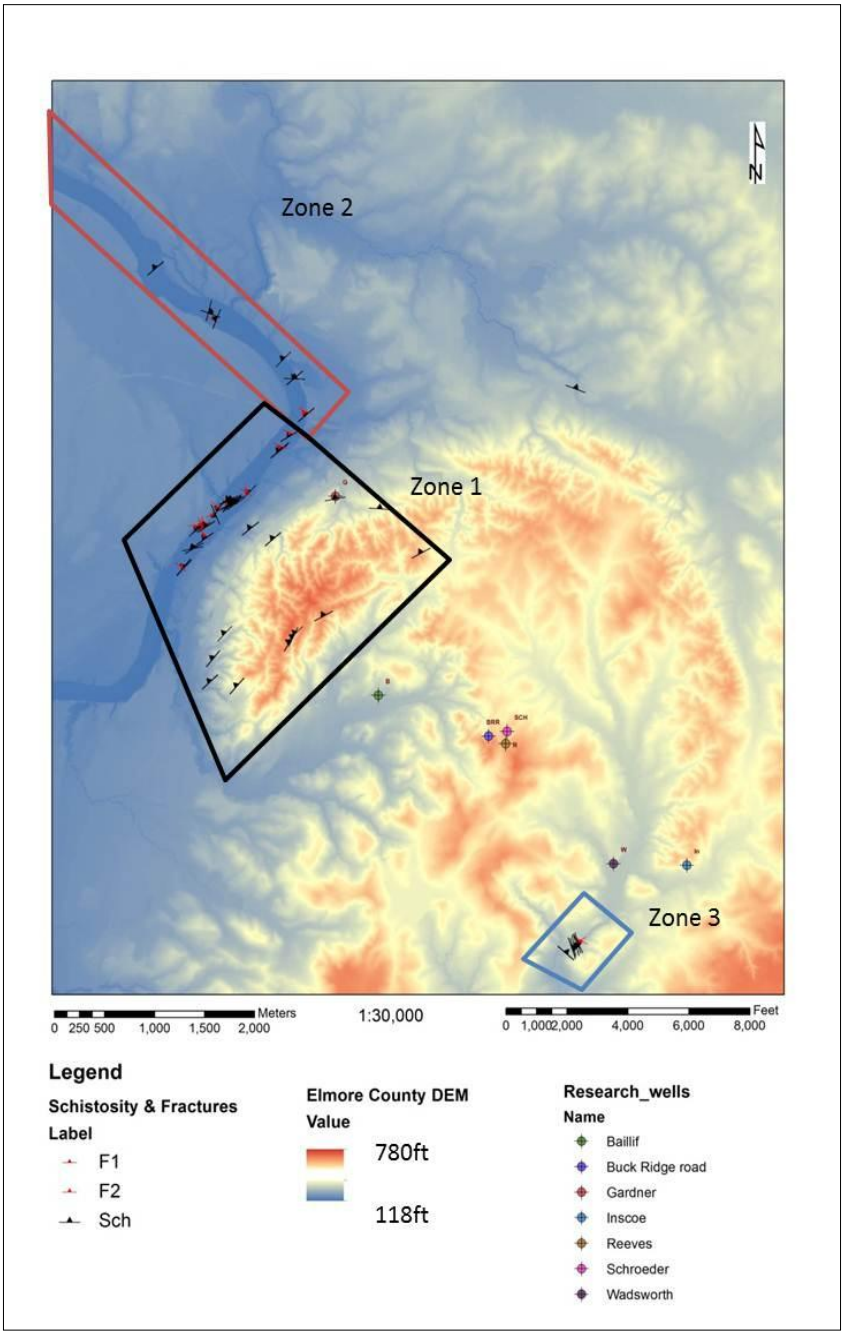

Figure 21. DEM of Wetumpka's rim area showing the inventory of fractures (red symbols) and schistosity (black symbols). This inventory has been separated into three zones; Zone 1 is the main area of study and covers the western rim; Zone 2 covers Coosa River; and Zone 3 cover the south eastern rim. In this DEM, higher areas correspond with bright colors while blue and more pale colors are the lower elevations. Research wells are plotted also in this figure.

All the measurements of orientation of fractures and schistosity from this side of the crater have been plotted in a stereographic projection to obtain an overview of the main fracture planes and schistosity planes (see Interpretations).

3. 3D resistivity

The outcome of the 3D resistivity survey is a resistivity rendered volume (10 m x 28 m x 6.5 m) as shown in Figure 22. The 3D resistivity volume is fully manageable and the sagittal, coronal, and transverse planes can be extracted out from the volume for a more detailed study.

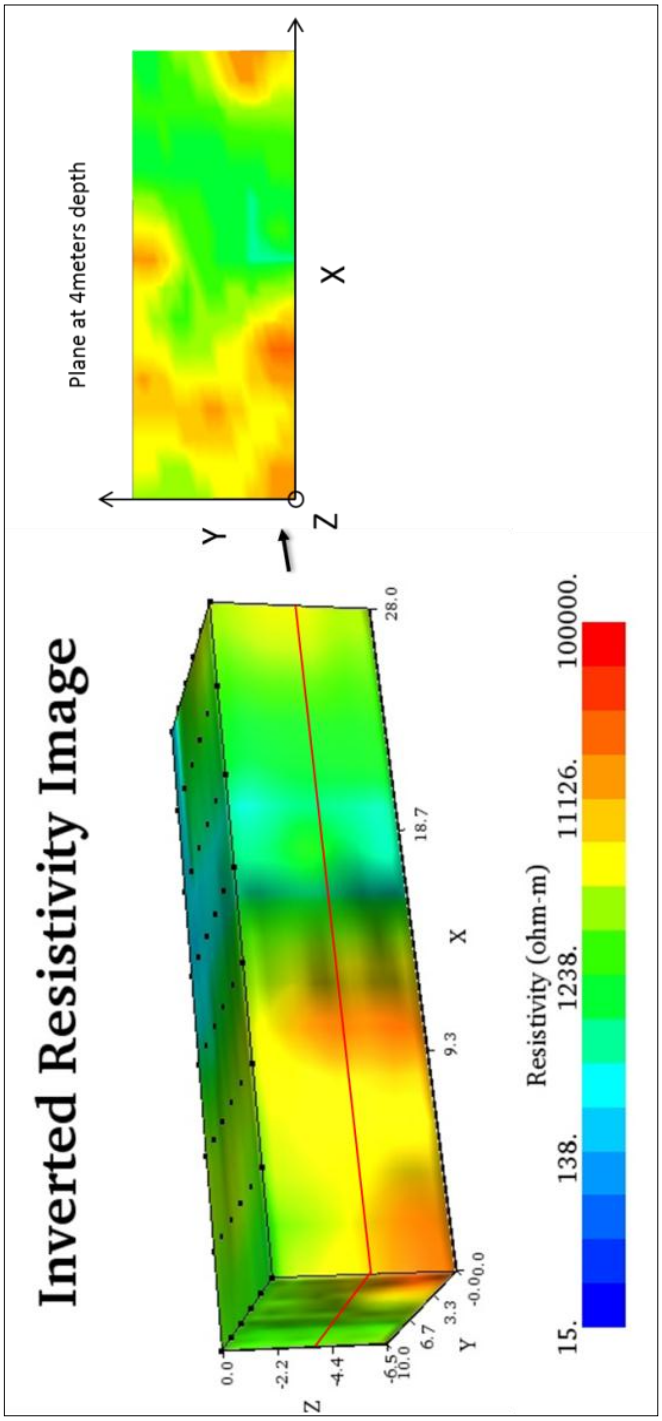

Figure 22. 3D resistivity rendered volume. The higher resistivity values (ohm-m) correspond with reddish-orange colors and the lower with green to blue colors. As an example, at right, one of the transverse planes has been taken out of the volume

4. LiDAR & GIS

a) Wetumpka DEM (Digital Elevation Model)

One of the results obtained from the LiDAR data for Elmore County (i.e., the data of The Atlantic Group, LLC) is an Elmore County DEM. As this is the most accurate topographic map ever made of this area (up to 2 m spatial resolution), this DEM is the base map and starting point for further studies on the geology of the Wetumpka impact crater.

Having these very precise geospatial and elevation data offers a great opportunity, because until now, there was no topographic map with that level of detail in the vicinity of Wetumpka. Lack of such a DEM constrained the geologic interpretation of the crater. Recently mapped and measured structures as well as hydrogeological fluvial patterns are shown in more detail in the DEM of Wetumpka.

There is an appreciable difference between the older DEM used prior to this study, and the new DEM obtained from LiDAR (Figure 23).

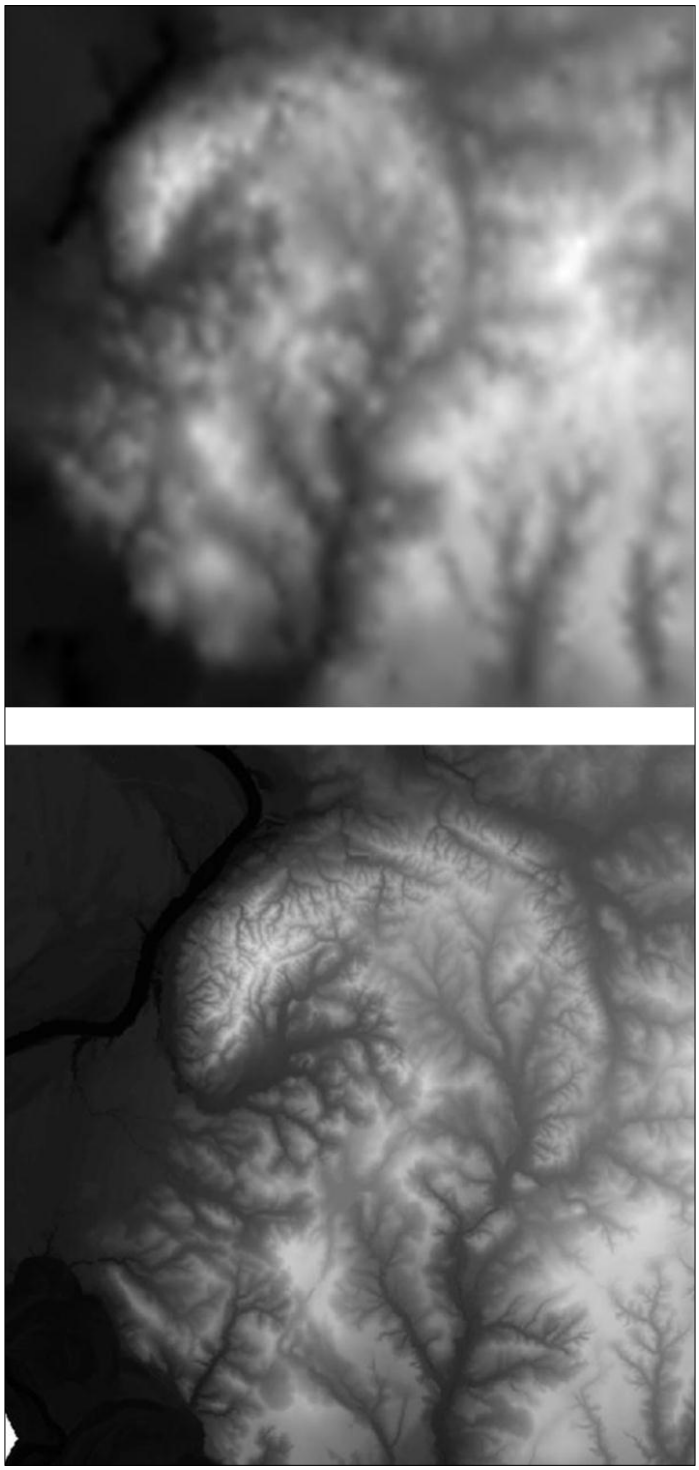

Figure 23. Differences in resolution between older DEM of Wetumpka (based on old US Geological Survey 7.5 minute quadrangles, (above) and the new DEM generated from 2010 LiDAR data that have a spatial resolution of 2 m (below).

The spatial resolution on the DEM generated from LIDAR, is higher than the DEM obtained from the US. Geological Survey quadrangle maps because the inverted relation between "coverage area / measurements density." The higher the measurement numbers per area, the smaller coverage area. This increment in the number of data points on a specific area is reflected into a less blurry image, i.e. a sharper, more detailed digital elevation model (Figure 23).

b) Detailed Cross-sections

A result of using a high-quality elevation model is a highly detailed elevation profile, which together with the DEM-based geological map, results in an interpretative geologic cross-section showing surface structure and stratigraphic relations of Wetumpka impact structure.

As an example, Figure 24 below presents two cross sections pertaining to Wetumpka impact structure.

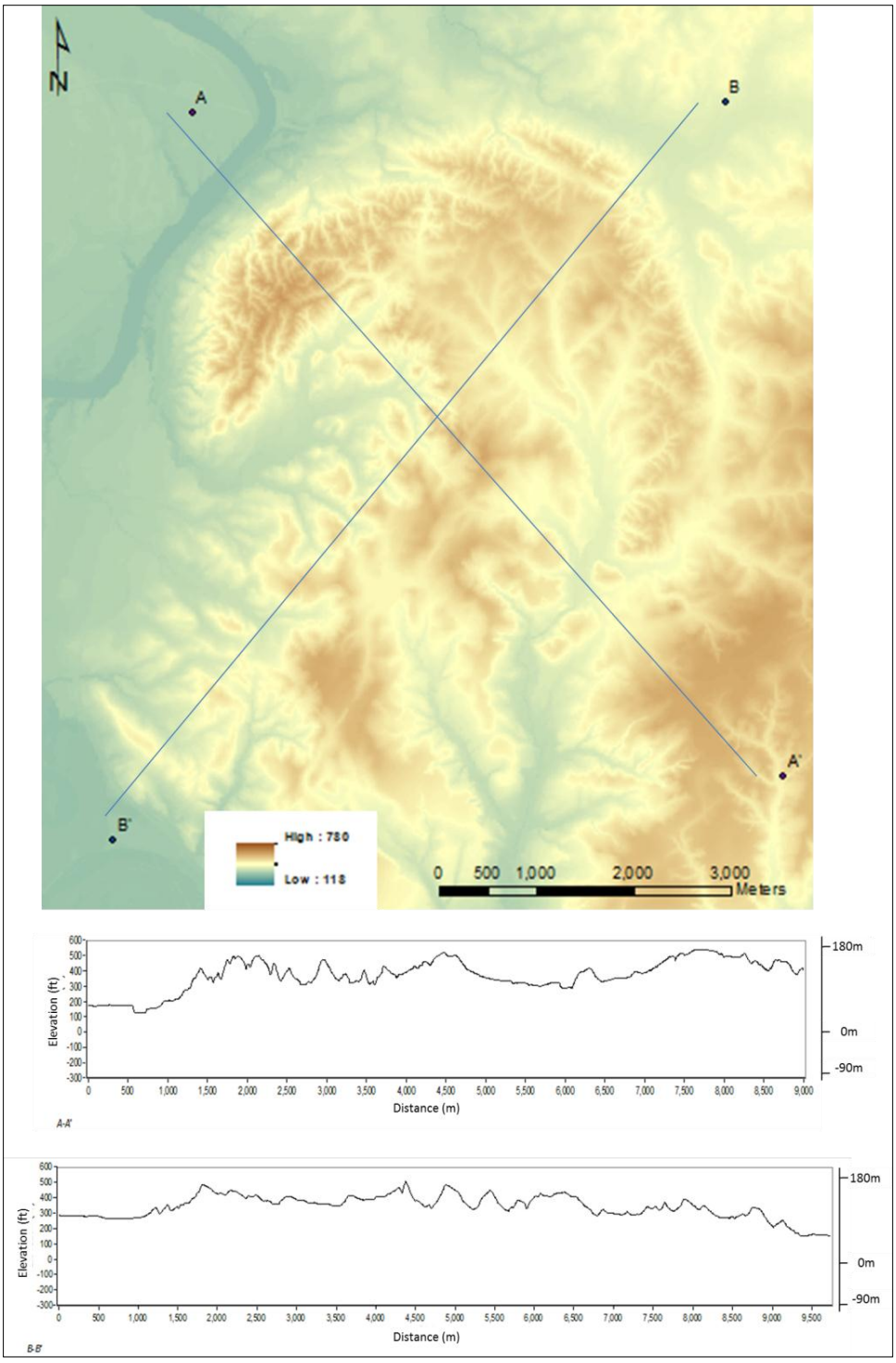

Figure 24. Two example elevation profiles of Wetumpka impact crater. At the top is a digital elevation model of the crater area where the lines of cross-sections AA' (NW-SE) and BB' (NE-SW) are marked. Below the map is AA’ and BB’ profile.

c) 3D map

Another of the features of digital elevation models is that the information contained in the image can be rendered 3-dimensionally, thus obtaining a complete 3D model of the topography of the area of study. This is interesting because it helps to provide an overview of the study area, to be able to measure distances and inclination of slopes, to have the flexibility to change points of views, and finally to be able to obtain an accurate photo-realism, and topographical relations between lithologies.

d) Slopes Map

This kind of map shows the different variation of slopes in Wetumpka area. The algorithm and the process are described in detail within the methods part of this thesis.

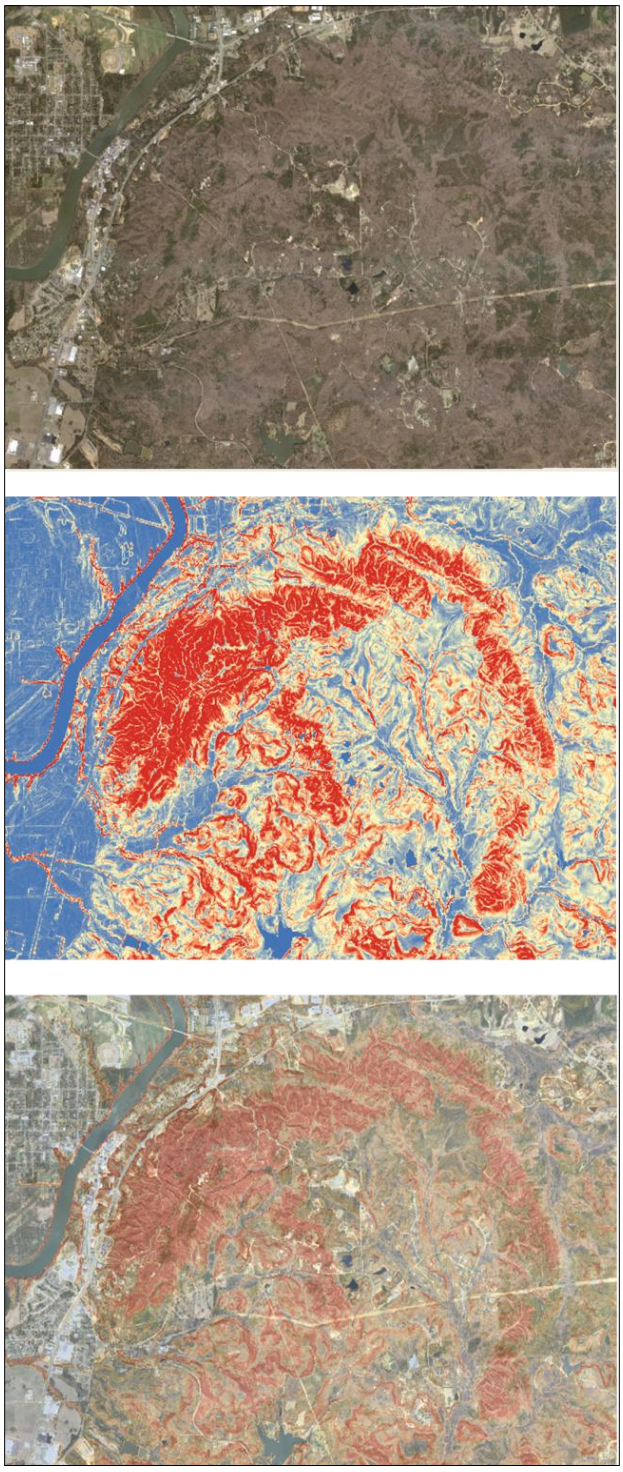

Figure 25. Image showing an aerial photograph of Wetumpka crater area (top), the slope map of the same area (center), and the combination of both images (bottom). High slopes areas are represented in red while low slopes or flat surfaces are in blue.

GIS offers many tools and combinations of possibilities, such as for example, combining high-detail orthophotos of Wetumpka crater with the slopes map. GIS allows us to make another map where we can observe areas that have a high slope, are difficult to access, or just to highlight main features. In Figure 25 we can see the process in which the orthophoto (top) has been overlaid with the slopes map (center) yielding a very useful aerial photograph with the slopes of the area (bottom), where the crater rim of Wetumpka becomes visible.

e) Aspect map

The aspect map is a derivative from the DEM where the cells have been classified according to their slope direction, thus giving the user an indication of where those surfaces are directed. This tool has many applications, nevertheless it here applied to the Wetumpka crater to discover structures because this algorithm has the special quality of highlighting structural features (Figure 26).

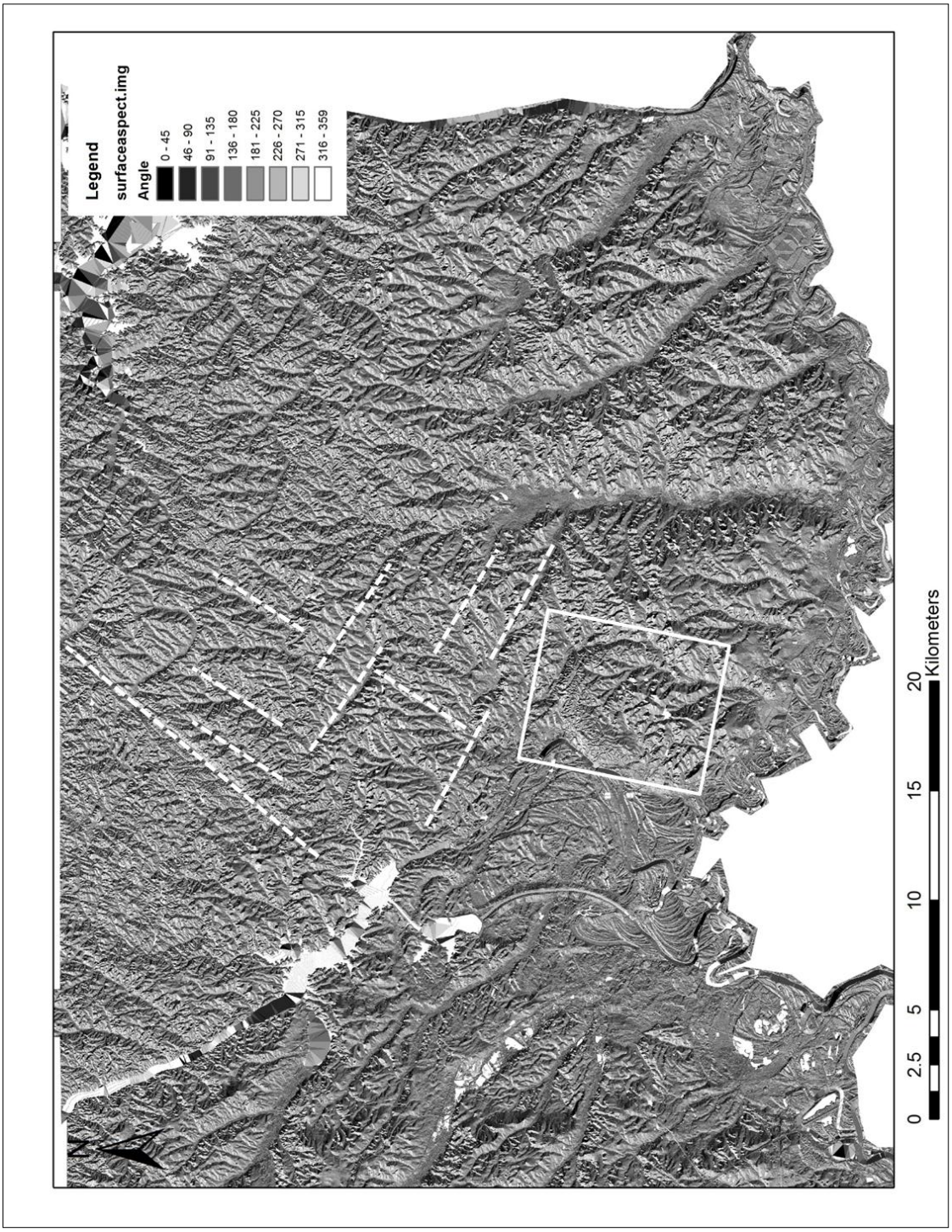

Figure 26. Aspect map of Elmore County. Some lineation (dashed lines) can be seen thanks to this derivative of the Elmore County DEM. The shape of Wetumpka crater (box) is also very well highlighted using this method.

f) Geologic map

The geologic map made by Neathery et al. (1976) was digitalized by Tiffany R. Davis (undergraduate student from the Geology and Geography Department, Auburn University) in 2010, and integrated with this new DEM to make a digital geological map. This digital geological map can be combined in GIS with others of the possible derivatives in order to have full perception of the geologic structure of Wetumpka and its relationship with topographic features. The digital geological map is presented in the next section of this thesis, and in more detail in the appendices.

INTERPRETATIONS

1. Drill core

Based on a detailed description of the drill core #09-01, there are a few interesting interpretations that can be made. For example, the schist in the core follows a fracture pattern that coincides with the schistosity of the rock in this area. Also, the dip angle of these fractures decreases with depth. A possible interpretation could be that this change of dip angle was caused by the excavation process during the impact causing a possible overturning of a rim flap. The dip angles would, consequently, be increasing near the hinge of the fold. Nevertheless this pattern needs to be confirmed on the other parts of the rim as well in order to make this a final assessment.

Also the breccia zone thickness in the core has been estimated to be approximately 12 ft (3 m), and is located between depth of 210 and 222 ft (located within drill-core box 25). This feature also supports a possible overturning of the rim flap. The interpretation of the mineral analysis is based mainly on the relation between micas percentage and RQD. The elastic properties of the micas could help the

rock to support high levels of stress in the rock without failure of the material, thus implying a higher RQD in most instances where the content of micas increases and lower where the content of micas decreases.

2. Fracture pattern in the area of study

The inventory of the fractures and schistosity of Wetumpka crater has been made mostly on the western part of the rim, a short reference section along Coosa River (Figure 27), and at the southeast part of the rim. These sites represent places where good exposures combined with safe access made the measurements possible.

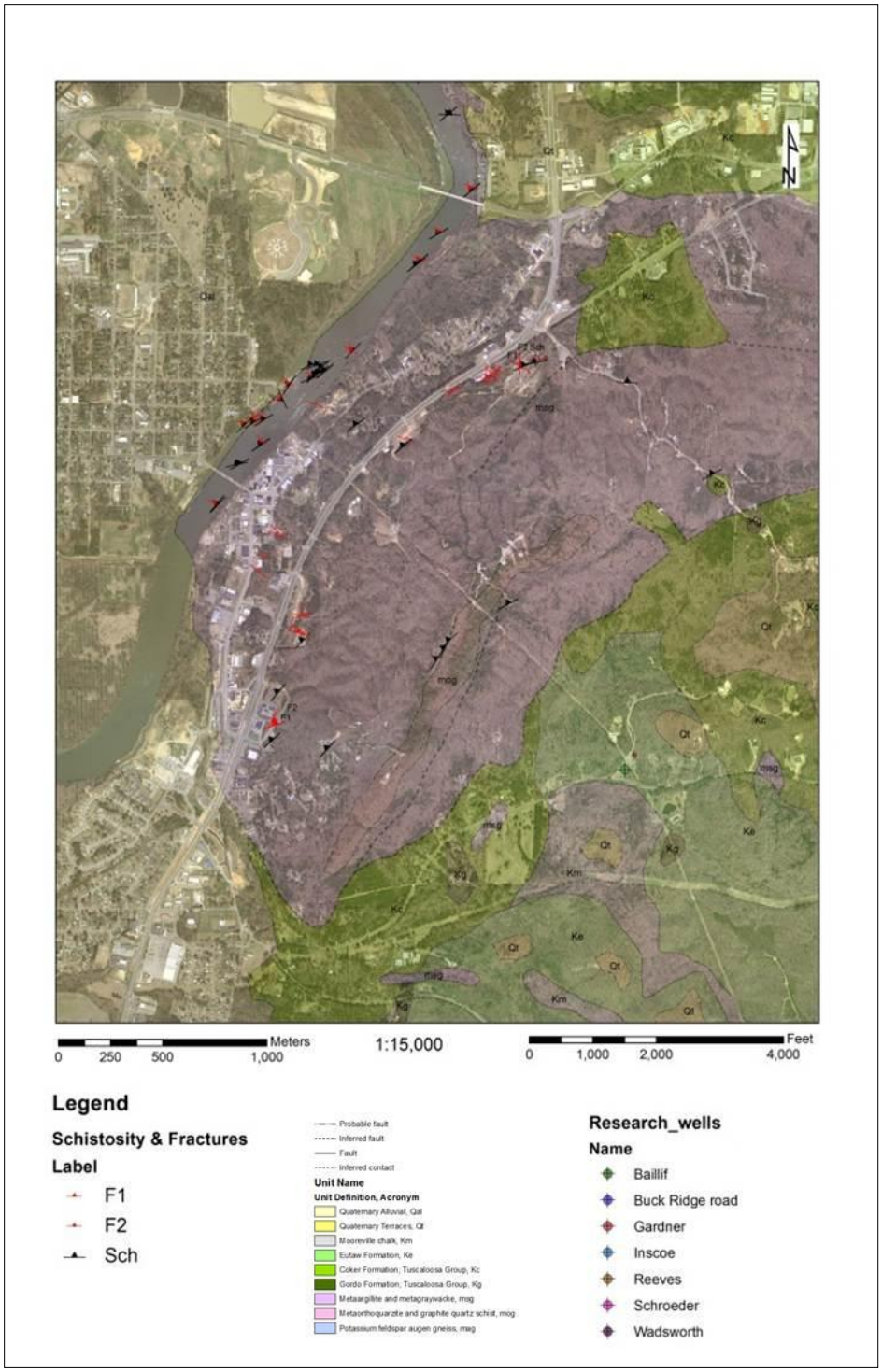

Figure 27. Detailed map showing the measures of dip and strike taken along the Coosa River and the western rim area. Fractures in the area are represented as red symbols and schistosity measures as black symbols.

The stereographic projection of the dip and strike on the western rim shows a consistent orientation of the schistosity planes. All the measurements are well grouped in a cloud of points, as we can see in the stereographic projection below (Figure 28). The stereographic projection shows also a calculated fold axis (β-axis) striking N37°.

In order to present a possible model accounting for all of the attitudinal data obtained from the stereographic projection and to better visualize the fold axis at this section of the western rim, a three-dimensional representation was made (Figure 29). One interpretation is that the fold axis in this case is in fact the same as the hinge of the overturned rim.

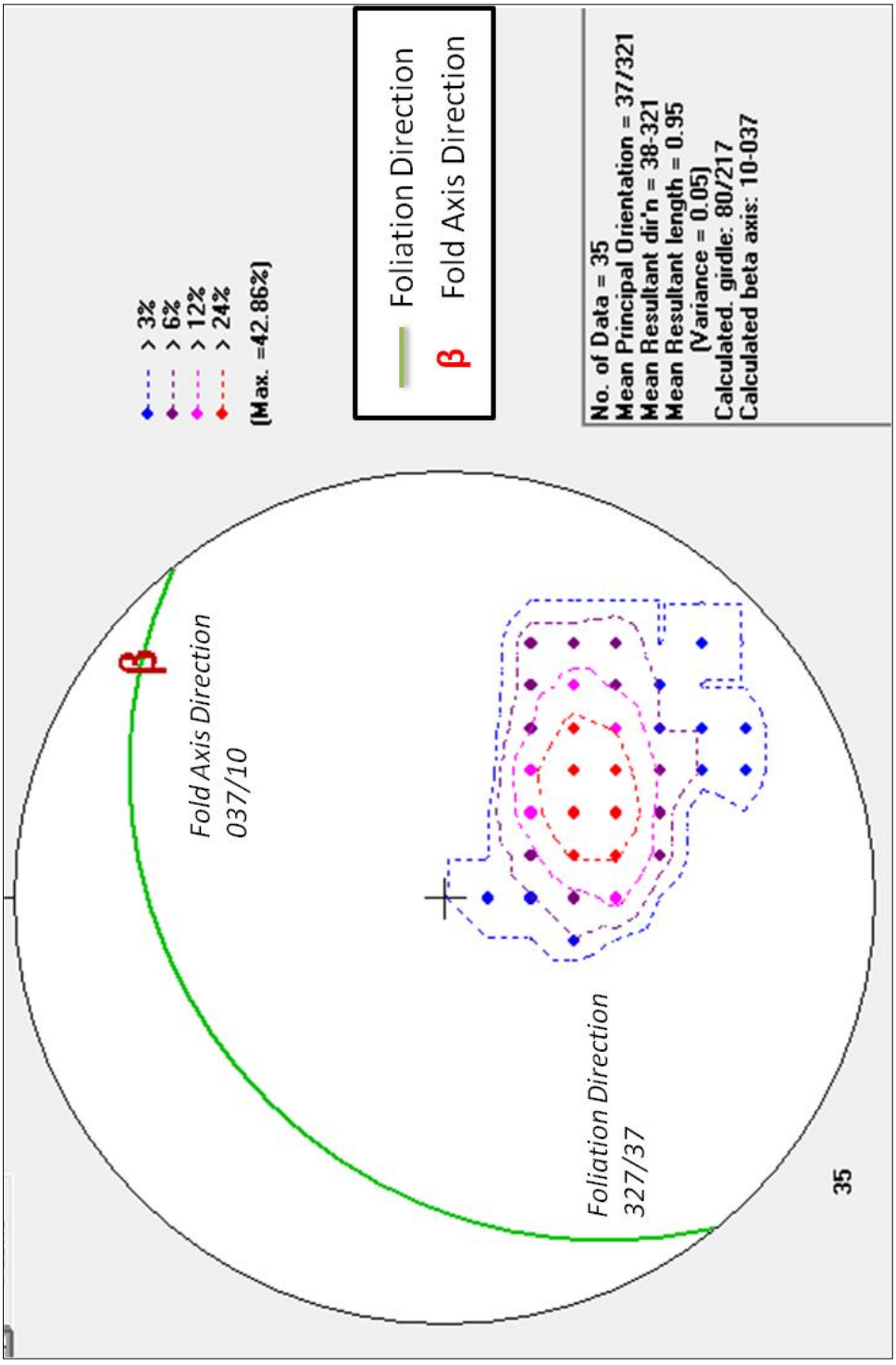

Figure 28. Stereographic projection of the measurements taken on the western rim area (Figure 19). This projection shows a strong directionality of the foliation towards NW (N327°/37°). The fold axis direction has been calculated also, which bears northeast (N037°).

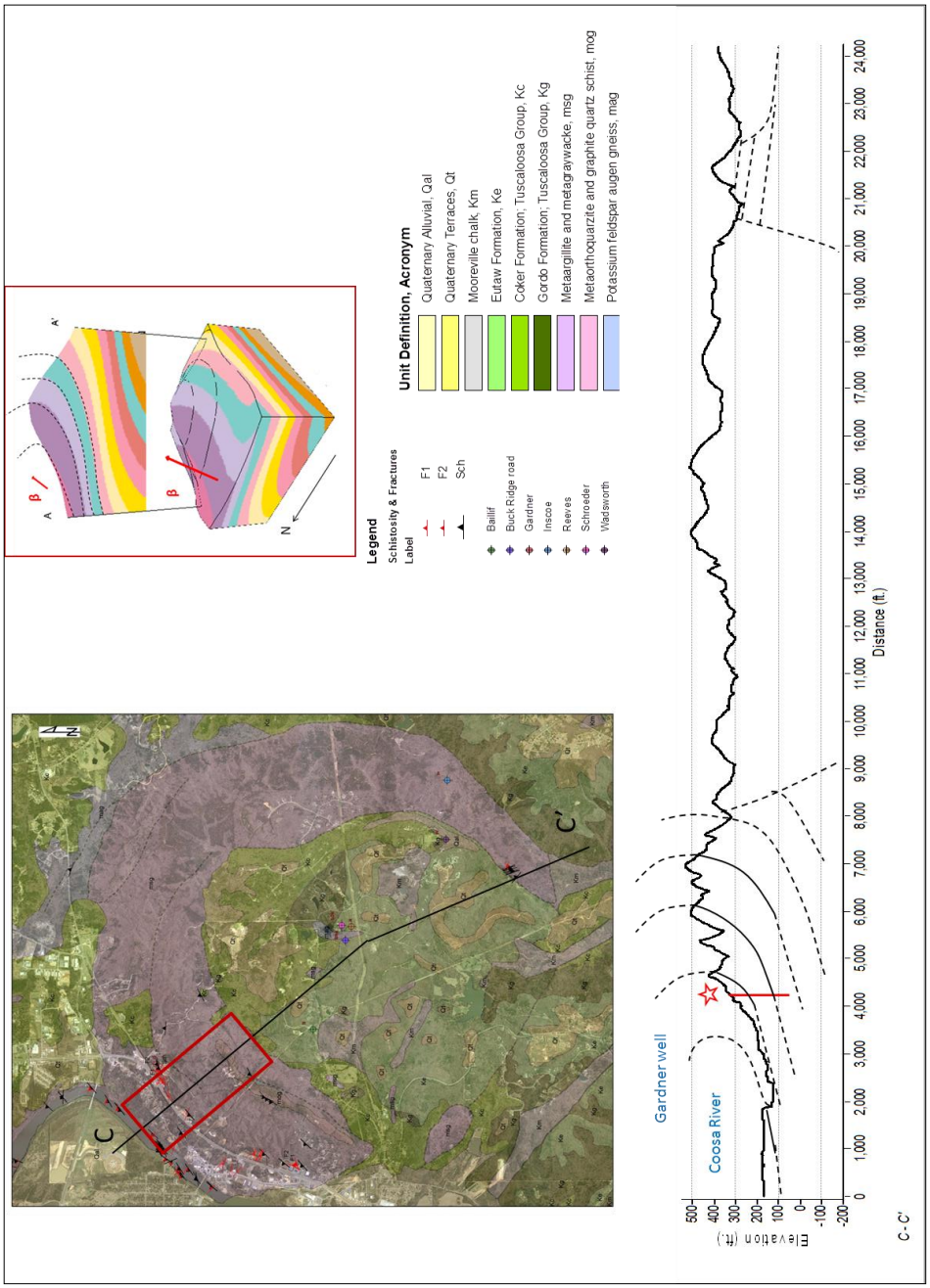

Figure 29. Sketch and cross-section illustrating the disposition of the schistosity and the suggested interpretation as a fold axis of the overturned flap at the investigated western section of the rim of Wetumpka. The upper right layered model represent the area content in the red box on the map (colors of the model do not represent geology) and is created using the online application from www.visiblegeology.com (Rowan, 2011).

Another set of measurements were taken upstream in the Coosa River area. This area is interesting because it is taking us away from the impact site and gives us an idea of the pre-existing structural conditions of the schist (i.e., structure before the impact). This area spanned a reach of the river going northwest from just south of the Bibb Graves Bridge down-town Wetumpka to north of Moccasin Gap on the Coosa River. This area possesses a different structural pattern than the one seen previously on the western rim. Here the schistosity planes are no longer concordant with the bedding planes of the schist. Besides the high level of agreement and continuity of the schistosity measured that we found through the western rim does no longer hold as we move northeast and away from the Bibb Graves Bridge, where the bedding planes are all folded creating a wave-like (undulating) pattern of folds, several meters from flank to flank (Figure 30).

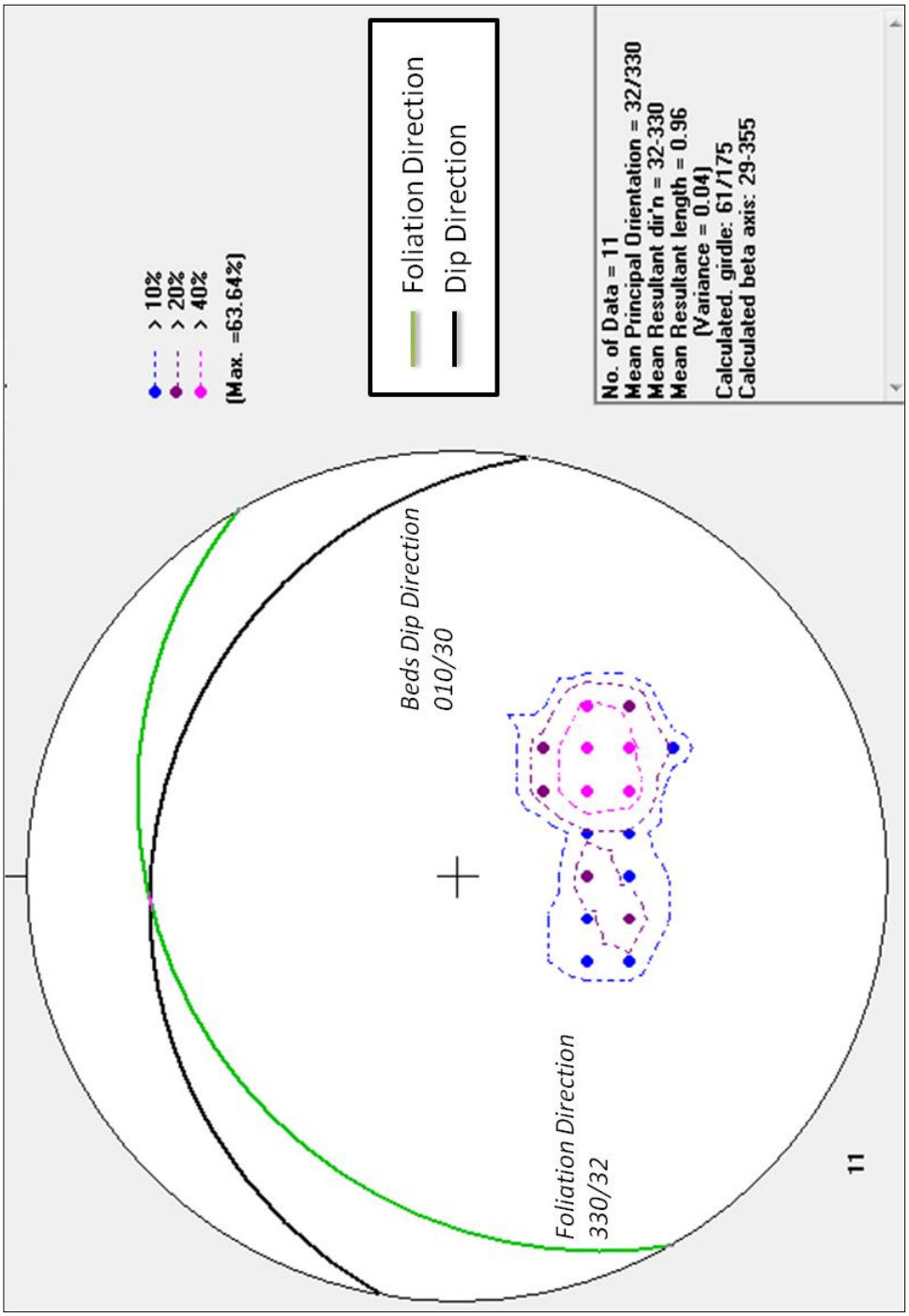

Figure 30. Stereographic projection of the measurements taken along the Coosa River section (just south of the Bibb Graves Bridge to north of Moccasin Gap in the Coosa River). In this figure, the foliation is no longer the dominant bedding plane that derives into two orientations.

It is still unknown if this area along the river could be considered as a good example of the pre-impact target appearance of the schist. More detailed mapping of the surrounding areas of Wetumpka is needed in order to fully understand how this schist's structure appeared by the time of the impact.

The other studied area is at the southeastern rim. It is a small area along Harwell Mill Creek where schist is well exposed. If we assume the same dip pattern of the western rim (layers dipping concentrically to the west) and extrapolate to the other sides of the rim, the expected dip direction in this part of the rim should dip concentrically in opposite direction relative to the center of the crater, i.e. a dip towards the southeast. However, the actual measurements taken in this area instead show a dip towards the east (N067°), as we can see on the stereographic projection below (Figure 31). There is not yet a final explanation for this discrepancy, but one idea is that this part of the rim has somehow been rotated from its original orientation with a dip towards the southeast to a more easterly dip.

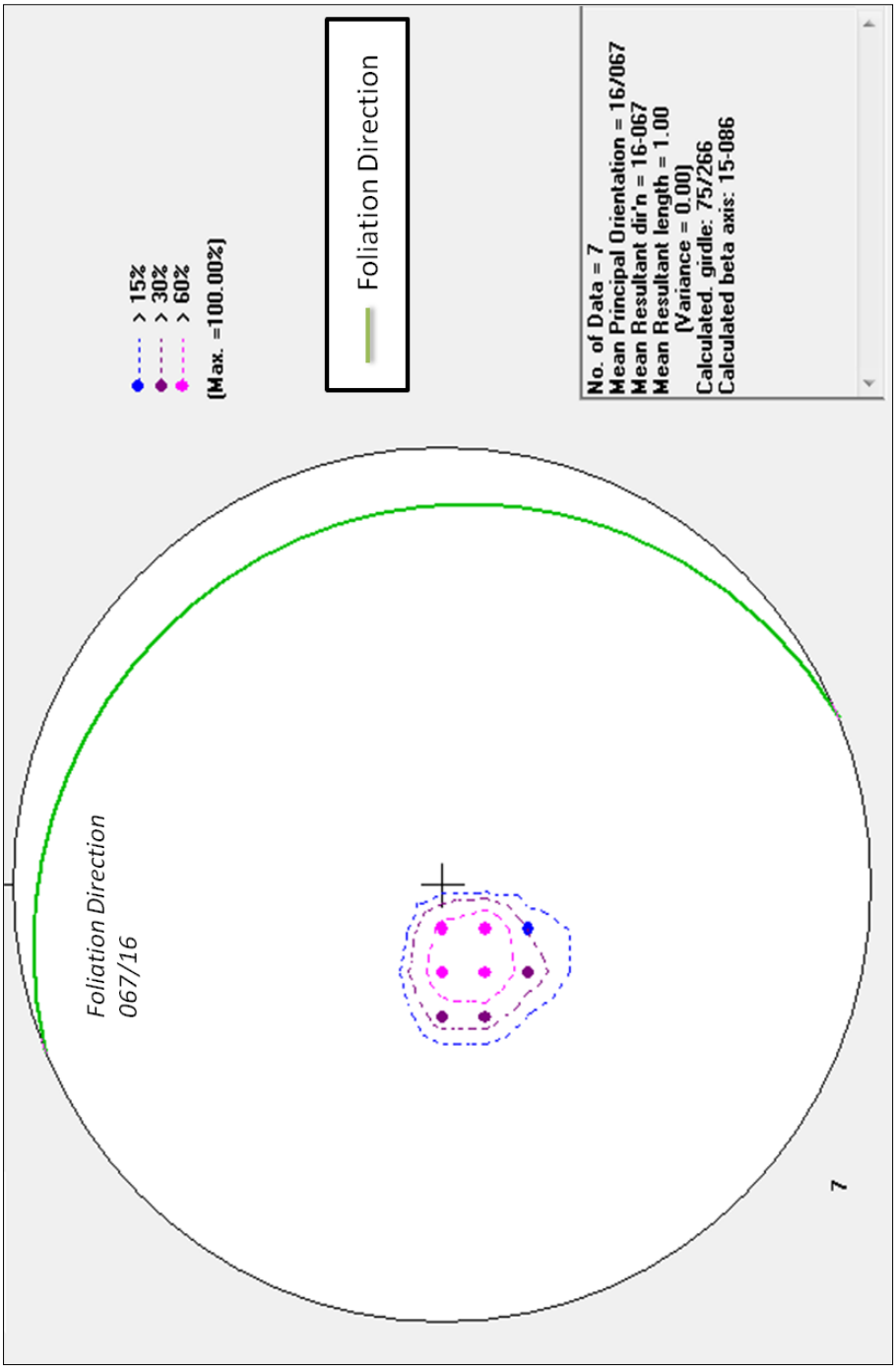

Figure 31. Stereographic projection of the measurements taken at the southeastern part of the rim. The picture shows a dominant foliation direction concordant with the bedding planes similarly as on the western rim. The measurements show a strong directionality toward the north east (N067°).

3. 3D resistivity

Shown in Figure 32 are the results obtained from the 3D resistivity, where reddish colors in the diagram are the higher resistivity areas while the green and blue are those of lower resistivity. The results indicate that rocks of high resistivity are covered by a layer of low resistivity material.The lower unit is to interpreted to correspond to solid schist rock, which is covered by an upper unit of saprolite, a weathered material of generally low resistivity.

Elongated anomalies in the F1 and F2 directions appear in the depth slices within the lower unit, and these are interpreteted as fractures that are concordant in direction of fractures measured in the surrounding areas.

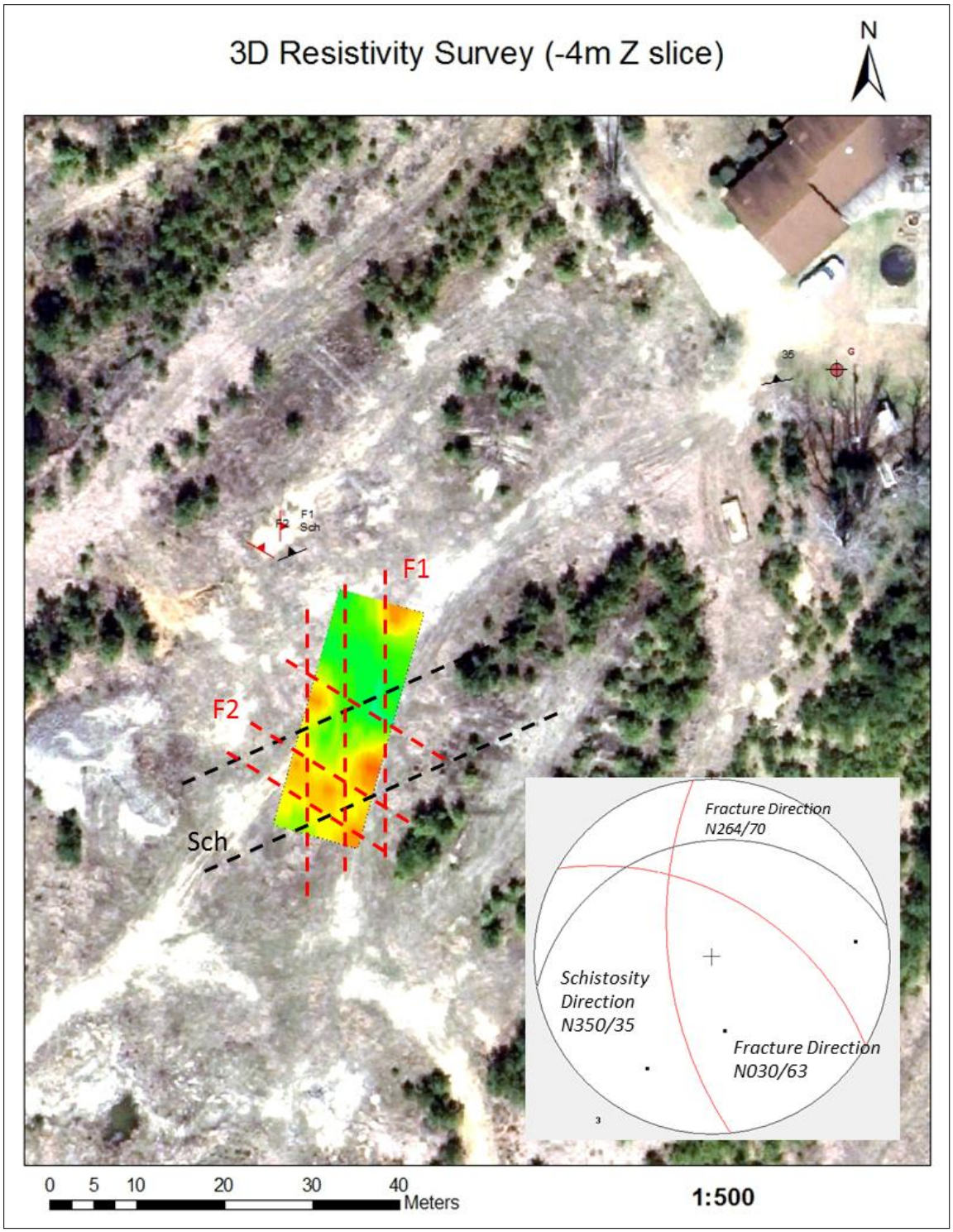

Figure 32. Aerial photograph of an area on the western rim with the local resistivity map superimposed. The resistivity map shows the resistivity surface at 4 m depth**.**

From these interpretations, it is inferred that the fractures have a high development not only in depth but also transversally through the rim. The bisector angle between the two fracture families points directly to the center of the crater. Nevertheless, it is unknown if in fact all these fractures are in some way related to the impact process. This could be determined if the same families of fractures are mapped on the remaining parts of the rim as well.

4. LiDAR and DEMs

The interpretations from LiDAR and DEM images have been very helpful not only in order to have a more accurate view of Wetumpka impact crater, but also of the geomorphological features of the surroundings of the crater.

The digital elevation map (Figure 33) shows a high-resolution image of the limits of Wetumpka impact crater. It also shows different patterns of structural lineaments. Also, there is a noticeable variance in topographic texture between the rim and the inner part of the crater. The rim shares two main characteristics: it is formed by highly weathered schist, and it has a complex network of fractures. These two features create short, antecedent and trellis fluvial patterns (Figure 33). Meanwhile, the inner part of the crater is formed by slumped and resurged sedimentary material (King et al., 2002; 2006), therefore the interior sediments and impact breccias result in a consequent (dendritic) pattern.

Interpretations of the topographic texture and the fluvial patterns in the rim and in the inner crater could be useful to re-evaluate the previously mapped boundaries between formations in the 1976 geologic map (Neathery et al., 1976).

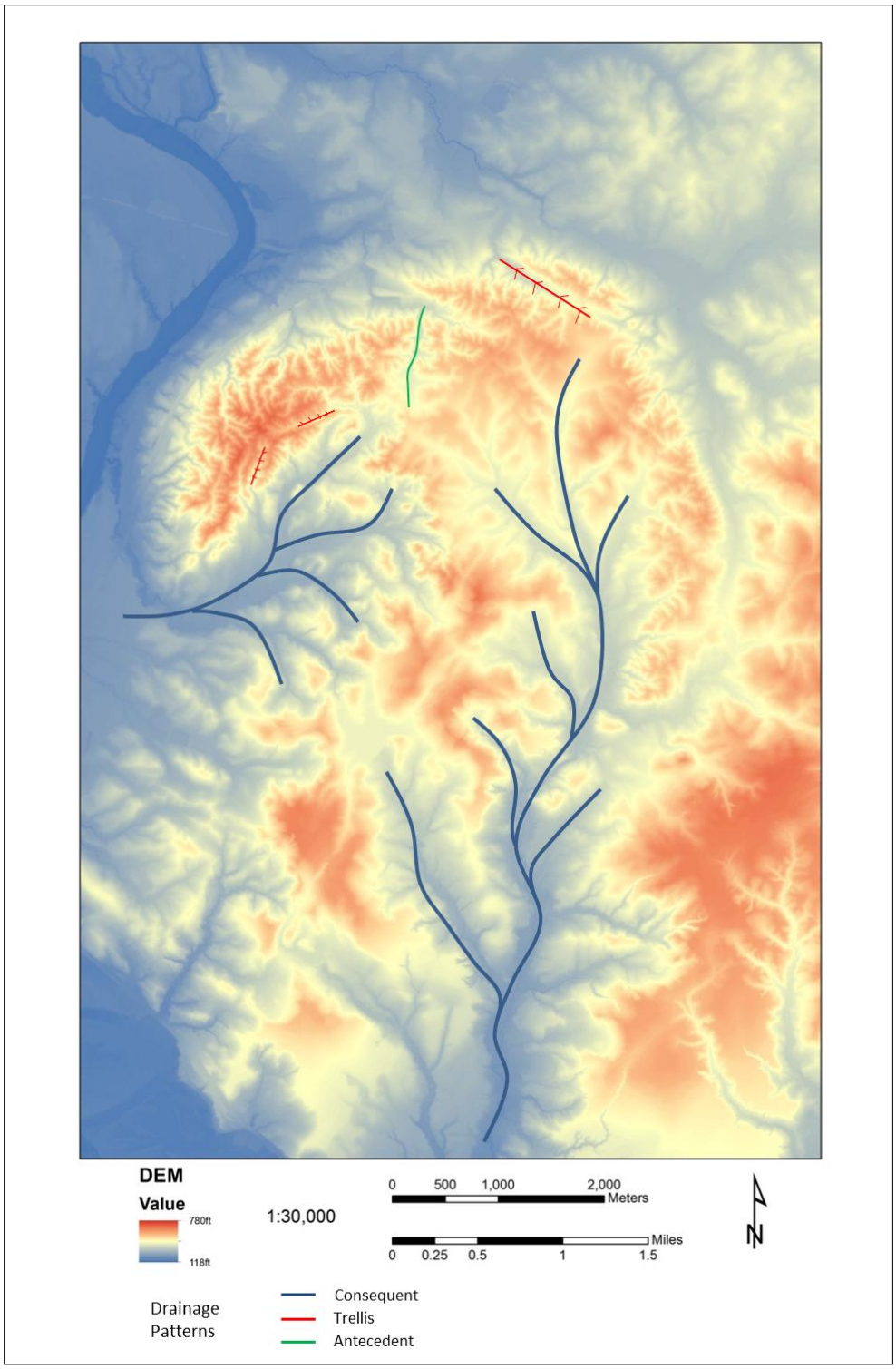

Figure 33. Digital elevation model of Wetumpka at a scale which shows the fluvial patterns mentioned in the text (antecedent and trellis versus consequent).

If we look closely at the slopes map derived from Wetumpka DEM (Figure 34), it is easy to see that the highest slopes of the crater follow a semi-round shape that coincides well with the unit boundaries of the 1976 geologic map. It seems that the western rim high slopes (reddish color) of the crater are following the Emuckfaw Group outcrop, which makes up the rim. This relation between high slopes and Emuckfaw Group (mica-schist) in the rim also seems to help to define the topographic boundaries of the rim.

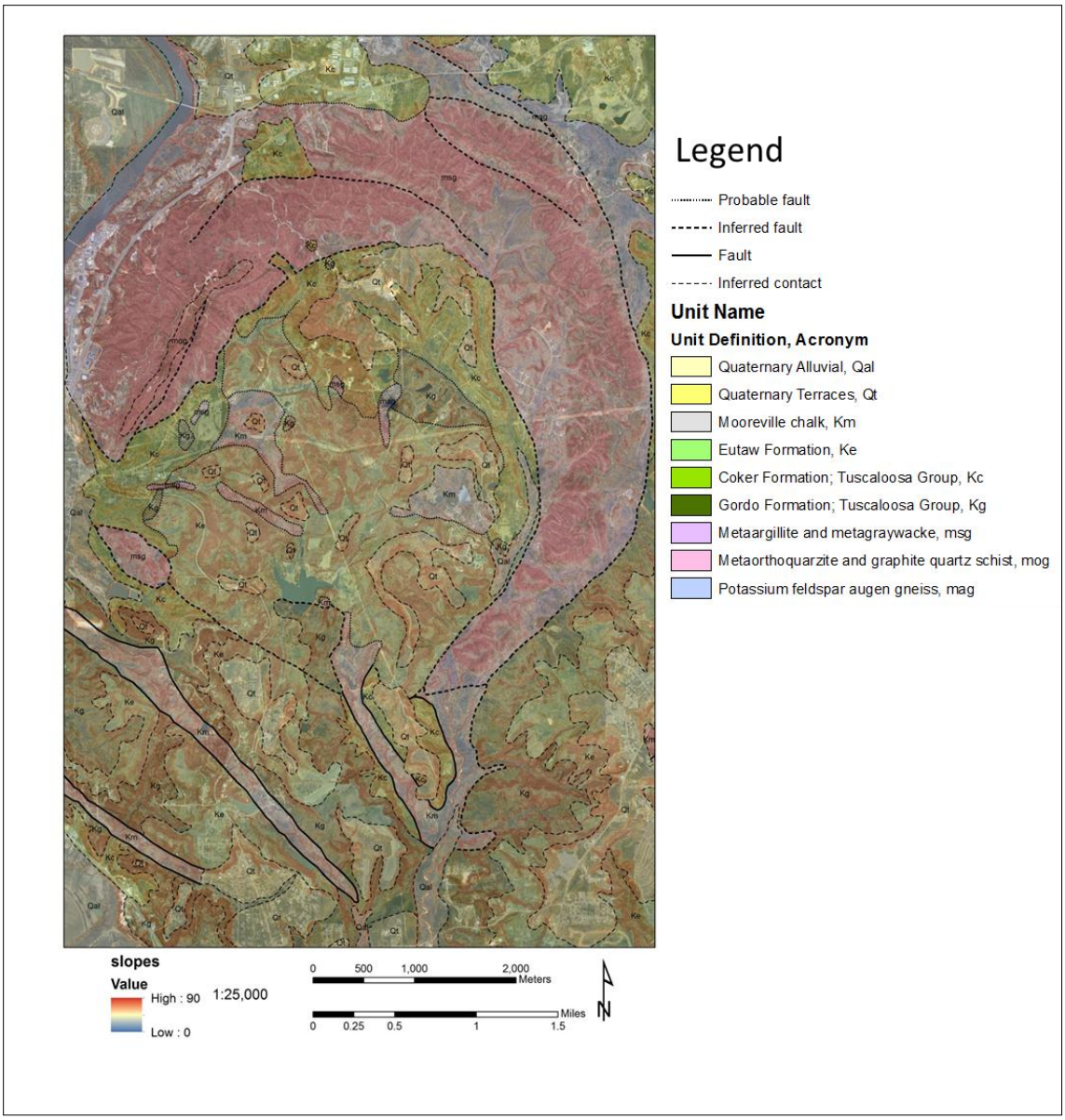

Figure 34. Map showing the 1976 geologic map units and the relative value of the slopes (see value scale) obtained from the Wetumpka LiDAR-based DEM, which is plotted on a high resolution orthophoto of the Wetumpka area. Geologic map was digitized from Neathery et al. (1976).

So far the interpretations of the DEM and their derivatives indicate that there are parts of the rim that can be defined more accurately. According to the information obtained from these tools, it should be considered that the rim in the northern and eastern sides is narrower than it was thought at first, although not enough information about the eastern rim is available at present.

CONCLUSIONS

Drill core

The detailed description of drill core #09-01 includes detailed photographs, fracture analysis, RQD, mineralogy composition, drill core log and a recompilation of all the information gathered from the drill core into a database. This fulfills the first objective of this master thesis, which was to provide a comprehensive drill core description in narrative and digital form for drill core #09-01.

The lithology of the drill core rock is classified as moderately fractured mica schist with quartz veins. The mineralogy described in the core is principally lamellar minerals such as muscovite and biotite, as well as and hornblende (>50% in composition); in addition, quartz and feldspar also occurs (<25%). There is presence of minor minerals such as micro-garnets and other accessory minerals (not identified).

The dip direction of the schistosity in the core is N350° and it is consistent with the measurements taken in the near vicinity of the drill site. This direction does not change with depth, but the dip angle decreases with depth. The other fractures found in the drill core are a total of 48 that can be separated into 3 families.

Regarding the mineral content study of the core, it seems to have a correlation between the percentage of micas (muscovite and biotite) and the RQD calculated, thus the increment of micas also increases the RQD values decreasing the number of fractures

The fracture distribution and appearance throughout the drill-core, e.g. their decrease in dip angle with depth, the breccia zone, and the elasto-plastic behavior of the rock inferred by the high content of micas, support a possible interpretation of the rim formation by rim flap overturning on western Wetumpka impact.

Even though there is much to be done to fully understand the rim formation in Wetumpka, this drill-core description could help future researchers to complete the study of the rim of the Wetumpka impact structure.

Fracture pattern of the investigated western section of the Wetumpka crater rim

The fracture inventory of the western section of the Wetumpka rim adds more data to supplement the information gathered by the drill core #09-01 in the rim. The results and interpretations obtained from the stereographic projection suggest an apparent fold axis on the western section of the rim, which could be inferred as the hinge of the overturned flap. This hints to a stimulating idea regarding the process by which the rim was formed.

3D resistivity

The main point of this survey was to discern whether the fractures are constant through the rim or if they are a result of weathering processes and landslide. The fractures detected with the 3D resistivity survey are consistent with the fractures measured on outcrop in the surrounding area and display a fracture development radial to the western part of the rim.

LiDAR

With this new data we have obtained a powerful tool for future research not only in the Wetumpka area but also all over Elmore County. It offers many new possibilities to study the rock formations, hydrology, and geography of this area. It is now possible for new thematic maps to be made for the purposes of geologic interpretation.

New structures and patterns such as faults and foliations and the related consequent, trellis, and antecedent drainage patterns are now evident on the new Wetumpka DEM.

The elevation model shows inconsistencies with the geologic map that need to be rectified.

In summary, DEMs generated from LiDAR are helping to virtually plan new areas of study on the crater, create a geo-database with sample coordinates and photos of easy access and draw cross-sections for a better understanding of the geology and formation of the crater.

Future work

New structural research on the northern and eastern sections of the rim could help in conjunction to the structural analysis conducted in this work to answer some questions and give some new ideas of the formation of the rim, and maybe also provide hints to the possible trajectory of the asteroid.

The study should be expanded to other locations beyond the apparent limits of Wetumpka crater to provide reference data on the mica schist (Emuckfaw Group) that forms Wetumpka's rim.

REFERENCES

Advanced Geosciences, Inc., 2006, Instruction Manual for The SuperSting™with Swift™ automatic resistivity and IP system, Austin, Texas.

Advanced Geosciences, Inc., 2007, Instruction Manual for EarthImager 3D Version 1.3.9 Resistivity Inversion Software, Austin, Texas.

Bellian, J.A., Kerans, C. and Jennette D.C., 2005, Digital outcrop models: applications of terrestrial scanning lidar technology in stratigraphic modeling Bureau of Economic Geology, *USA*,. Journal of Sedimentary Research, vol. 75, no. 2, p. 166–176.

Burger, H.R., 1992, Exploration Geophysics Of The Shallow Subsurface, Prentice-Hall, New Jersey, p. 289-293.

Burrough, P.A., and McDonell, R.A., 1998, Principles of Geographical Information Systems, Oxford University Press, New York, p. 190.

Deere, D.U., 1964, Technical description of rock cores, Rock Mechanics Engineering Geology, 1 p. 16-22.

Deere, D.U., 1989, Rock quality designation (RQD) after twenty years, U.S. Army Corps of Engineers Contract Report GL-89-1, Vicksburg MS, Waterways Experiment Station, 92p.

Horton, J.W., Jr., Powars, D.S., and Gohn,G.S., 2005, Studies of the Chesapeake Bay impact structure - The USGS-NASA Langley core hole, Hampton, Virginia, and related coreholes and geophysical surveys, United States Geological Survey Professional Paper 1688, 464p.

King Jr., D.T., J. Ormö, L.W. Petruny, and T.L. Neathery, 2006, Role of the sea water in the formation of the Late Cretaceous Wetumpka impact structure, inner Gulf Coastal Plain of Alabama, USA, Meteoritics and Planetary Science, p. 1625-1631.

King Jr., D.T., T.L. Neathery, and L.W. Petruny, 2003, Crater-filling sediments of the wetumpka marine-target impact crater (Alabama, USA), In Cratering in Marine Environments and on Ice (eds. H. Dypvik, and P. Claeys, eds.), Berlin, Springer-Verlag, p. 97-113.

King Jr., D.T., T.L. Neathery, L.W. Petruny, C. Koeberl, and W.E. Hames, 2002, Shallow marine-impact origin for the Wetumpka structure (Alabama, USA), Earth and Planetary Science Letters, p. 541-549

King Jr., D.T., and Ormö, J., 2007, Marine Impact Craters on Earth: Field Investigation of the Wetumpka Impact Crater, a Well-Preserved Marine Impact Crater, and the K-T Boundary in the Alabama Gulf Coastal Plain: Wetumpka, Alabama, Guidebook and Abstracts, p. 119.

King Jr., D.T., and Ormö, J., 2011, The marine-target Wetumpka impact structure examined in the field and by shallow core-hole drilling, in Garry, W.B., and Bleacher, J.E., eds., Analogs for Planetary Exploration: Geological Society of America Special Paper 483, p. 287–300, doi:10.11 30/2011.2483(19).

King Jr., D.T., Petruny, L.W., and Neathery, T.L., 2004, The horseshoe-shaped rim of Wetumpka marine impact crater—From oblique impact or heterogeneity in the rim?: Geological Society of America Abstracts with Programs, v. 36, no. 5, p. 266–267.

Neathery T.L., Bentley R.D., and Lines G.C., 1976b, Cryptoexplosive structure near Wetumpka, Alabama, Geological Society of America Bulletin, v.87, p. 567-573.

Neathery, T.L., King, D.T., Jr., and Wolf, L.W., 1997, The Wetumpka impact structure and related features, Alabama Geological Society Guidebook 34c, Alabama Geological Society, Tuscaloosa, AL, United States (USA).

Nelson, A. 2000, Geological mapping of Wetumpka impact crater area, Elmore County, Alabama [M.S. thesis]: Alabama, Auburn University, Unpublished, p. 187.

Ormö J., King Jr., D.T., R.S. Harris, L.W. Petruny, and J.K. Markin, 2010, Sediment-Laden Flow of Mooreville Chalk Within the Interior of Wetumpka Marine Target Impact Structure, Alabama: Evidence for a Shallow Water Resurge, Lunar and Planetary Science.

Ormö, J., Sturkell, E., and Lindström, M., 2007, Sedimentological analysis of resurge deposits at the Lockne and Tvären craters: Clues to flow dynamics: Meteoritics & Planetary Science, v. 42, p. 1929–1943.

The Atlantic Group, LLC., 2010, LiDAR Data Acquisition report, The Atlantic Group, LLC., Remote Sensing and Land Information Solutions, Huntsville, Alabama, p. 27.

Rowan C., 2011, Visible Geology: http://app.visiblegeology.com/ (October 2011).

Wolf, L.W., Plescia, J., and Steltenpohl, M.G., 1997, Geophysical investigation of a "suspect" impact crater in Wetumpka, Alabama, in Neathery, T.L., King, D.T., Jr., and Wolf, L.W., eds., The Wetumpka impact structure and related features, Alabama Geological Society Guidebook 34c: Tuscaloosa, Alabama Geological Society, p. 57-68.

APPENDICES

The Appendix is presented in three parts. Part A is the drill core log. Part B is the thin section documentation section. Part C is the digital geological map. These parts are also available in higher resolution on the CD enclosed with this thesis. Additional files like the digital photographs of the drill core are also available on this enclosed CD.

A) Drill core

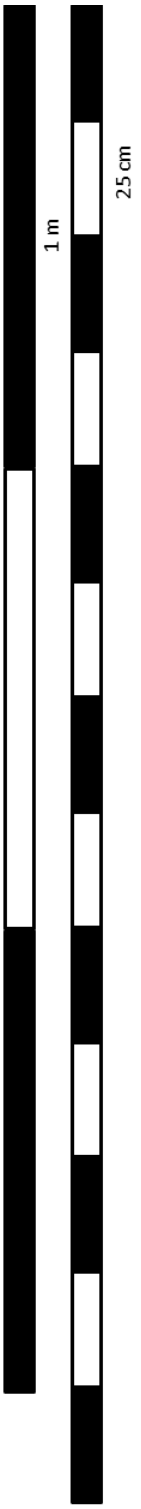

0 m
0 Ft

2.74 m
9 Ft

Drill Core Box 1

Total core Run (m)	Total Core Recovery (m)	Total Core Recovery %	RQD %
2.743	2.38	77.45	31.17

Description sheet

Box N.	1

1. Grain size	Fine	Medium	Coarse grained	Very Coarse Grained	Porphyroblastic	Granoblastic	Porphyroclastic
Sets	<0.75mm	0.75-1mm	1-2mm	>2mm	Containing crystals that are larger than the enclosing matrix	Composed of crystals of the same size. Fine to medium grained metamorphic rocks Al poor.	Coarse, relict, deformed crystals set in a fine grained, mylonitic matrix.
Top-1	x				x		
Top-2	x				x		
Middle	x				x		
Bottom-1	x				x		
Bottom-2	x				x		

2. Layering. (Foliation)	Isotropic	Compositional layering	Gneissosity	Schistosity	Cleavage	Mylonitic layering
Sets	Not layered	Foliation defined by alternating layers composed of different minerals. Easy to recognize by differences in colors of layers.	Compositional layering in with granoblastic layers of roughly equidimensional grains(quartz and feldspar) alternate with more schistose layers of platy or elongate grains.	Foliation defined by aligned minerals. Commonly platy minerals(micas, chlorite...) or prismatic (amphibole, tourmaline). They posses a preferred orientation.	Schistosity surfaces that are planar along which the rock may break(cleave) into tabular or platy fragments. Slaty cleavage is perfectly planar. Crenulation cleavage is defined by cm- to mm scale periodic folds.	Foliation defined by layers of microbreccia with glassy appearance and or highly strained and elongated grains of quartz and or feldspar.
Top-1	x					
Top-2	x					
Middle				x		
Bottom-1				x		
Bottom-2				x		

Box 1

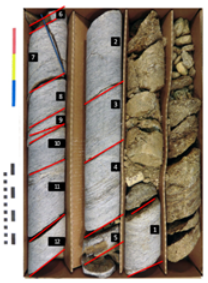

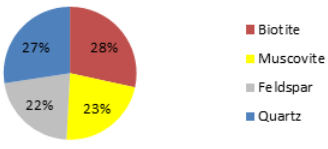

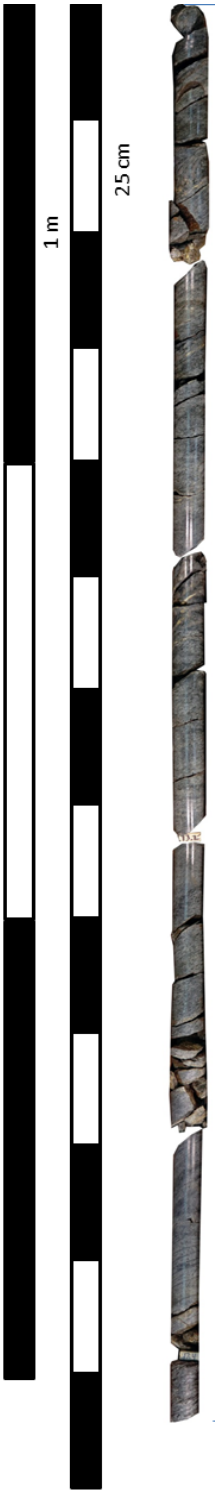

2.74 m
9 Ft

5.46 m
17.9 Ft

Drill Core Box 2

Total core Run (m)	Total Core Recovery (m)	Total Core Recovery %	RQD %
2.713	2.38	87.55	48.11

Description sheet

Box N.	2

1. Grain size	Fine	Medium	Coarse grained	Very Coarse Grained	Porphyroblastic	Granoblastic	Porphyroclastic
Sets	<0.75mm	0.75-1mm	1-2mm	>2mm	Containing crystals that are larger than the enclosing matrix	Composed of crystals of the same size. Fine to medium grained metamorphic rocks Al poor.	Coarse, relict, deformed crystals set in a fine grained, mylonitic matrix.
Top-1	x				x		
Top-2	x				x		
Middle	x				x		
Bottom-1	x				x		
Bottom-2	x				x		

2. Layering. (Foliation)	Isotropic	Compositional layering	Gneissosity	Schistosity	Cleavage	Mylonitic layering
Sets	Not layered	Foliation defined by alternating layers composed of different minerals. Easy to recognize by differences in colors of layers.	Compositional layering in with granoblastic layers of roughly equidimensional grains(quartz and feldspar) alternate with more schistose layers of platy or elongate grains.	Foliation defined by aligned minerals. Commonly platy minerals(micas, chlorite...) or prismatic (amphibole, tourmaline). They posses a preferred orientation.	Schistosity surfaces that are planar along which the rock may break(cleave) into tabular or platy fragments. Slaty cleavage is perfectly planar. Crenulation cleavage is defined by cm- to mm scale periodic folds.	Foliation defined by layers of microbreccia with glassy appearance and or highly strained and elongated grains of quartz and or feldspar.
Top-1				x		
Top-2				x		
Middle				x		
Bottom-1				x		
Bottom-2				x		

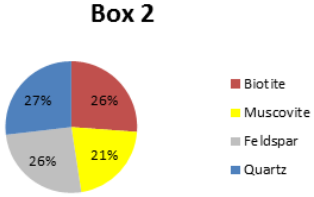

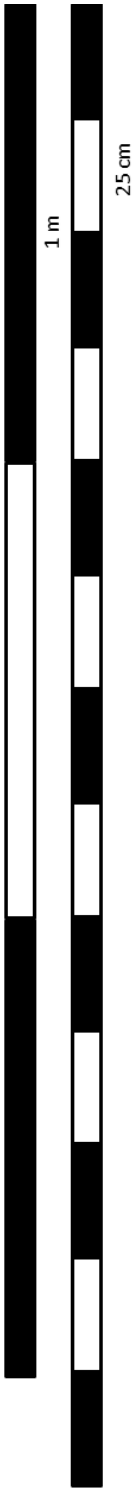

5.46 m
17.9 Ft

8.23 m
27 Ft

Drill Core Box 3

Total core Run (m)	Total Core Recovery (m)	Total Core Recovery %	RQD %
2.774	2.50	89.95	48.31

Description sheet

Box N.	3

1. Grain size	Fine	Medium	Coarse grained	Very Coarse Grained	Porphyroblastic	Granoblastic	Porphyroclastic
Sets	<0.75mm	0.75-1mm	1-2mm	>2mm	Containing crystals that are larger than the enclosing matrix	Composed of crystals of the same size. Fine to medium grained metamorphic rocks Al poor.	Coarse, relict, deformed crystals set in a fine grained, mylonitic matrix.
Top-1	x				x		
Top-2	x				x		
Middle	x				x		
Bottom-1	x				x		
Bottom-2	x				x		

2. Layering. (Foliation)	Isotropic	Compositional layering	Gneissosity	Schistosity	Cleavage	Mylonitic layering
Sets	Not layered	Foliation defined by alternating layers composed of different minerals. Easy to recognize by differences in colors of layers.	Compositional layering in with granoblastic layers of roughly equidimensional grains(quartz and feldspar) alternate with more schistose layers of platy or elongate grains.	Foliation defined by aligned minerals. Commonly platy minerals(micas, chlorite...) or prismatic (amphibole, tourmaline). They posses a preferred orientation.	Schistosity surfaces that are planar along which the rock may break(cleave) into tabular or platy fragments. Slaty cleavage is perfectly planar. Crenulation cleavage is defined by cm- to mm scale periodic folds.	Foliation defined by layers of microbreccia with glassy appearance and or highly strained and elongated grains of quartz and or feldspar.
Top-1				x		
Top-2	x			x		
Middle				x		
Bottom-1				x		
Bottom-2				x		

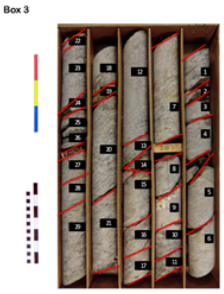

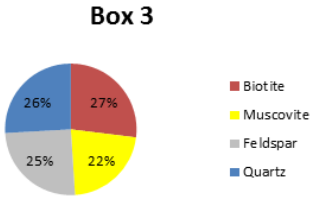

10.85 m
35.6 Ft

Drill Core Box 4

Total core Run (m)	Total Core Recovery (m)	Total Core Recovery %	RQD %
2.621	2.53	96.33	73.63

Description sheet

Box N.	4

1. Grain size	Fine	Medium	Coarse grained	Very Coarse Grained	Porphyroblastic	Granoblastic	Porphyroclastic
Sets	<0.75mm	0.75-1mm	1-2mm	>2mm	Containing crystals that are larger than the enclosing matrix	Composed of crystals of the same size. Fine to medium grained metamorphic rocks Al poor.	Coarse, relict, deformed crystals set in a fine grained, mylonitic matrix.
Top-1	x				x		
Top-2	x				x		
Middle	x				x		
Bottom-1	x				x		
Bottom-2	x				x		

2. Layering. (Foliation)	Isotropic	Compositional layering	Gneissosity	Schistosity	Cleavage	Mylonitic layering
Sets	Not layered	Foliation defined by alternating layers composed of different minerals. Easy to recognize by differences in colors of layers.	Compositional layering in with granoblastic layers of roughly equidimensional grains(quartz and feldspar) alternate with more schistose layers of platy or elongate grains.	Foliation defined by aligned minerals. Commonly platy minerals(micas, chlorite...) or prismatic (amphibole, tourmaline). They posses a preferred orientation.	Schistosity surfaces that are planar along which the rock may break(cleave) into tabular or platy fragments. Slaty cleavage is perfectly planar. Crenulation cleavage is defined by cm- to mm scale periodic folds.	Foliation defined by layers of microbreccia with glassy appearance and or highly strained and elongated grains of quartz and or feldspar.
Top-1				x		
Top-2				x		
Middle				x		
Bottom-1				x		
Bottom-2				x		

Box 4

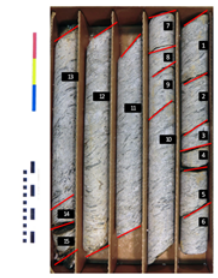

10.85 m
35.6 Ft

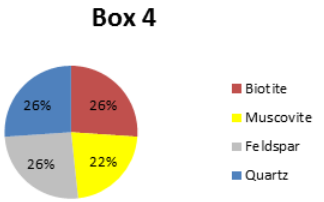

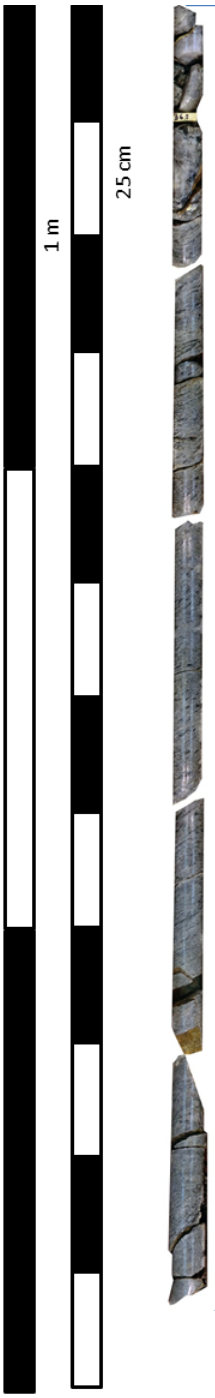

10.85 m
35.6 Ft

Drill Core Box 5

Total core Run (m)	Total Core Recovery (m)	Total Core Recovery %	RQD %
2.256	2.25	99.53	71.49

Description sheet

Box N.	5

1. Grain size	Fine	Medium	Coarse grained	Very Coarse Grained	Porphyroblastic	Granoblastic	Porphyroclastic
Sets	<0.75mm	0.75-1mm	1-2mm	>2mm	Containing crystals that are larger than the enclosing matrix	Composed of crystals of the same size. Fine to medium grained metamorphic rocks Al poor.	Coarse, relict, deformed crystals set in a fine grained, mylonitic matrix.
Top-1	x				x		
Top-2	x				x		
Middle	x				x		
Bottom-1	x				x		
Bottom-2	x				x		

2. Layering. (Foliation)	Isotropic	Compositional layering	Gneissosity	Schistosity	Cleavage	Mylonitic layering
Sets	Not layered	Foliation defined by alternating layers composed of different minerals. Easy to recognize by differences in colors of layers.	Compositional layering in with granoblastic layers of roughly equidimensional grains(quartz and feldspar) alternate with more schistose layers of platy or elongate grains.	Foliation defined by aligned minerals. Commonly platy minerals(micas, chlorite...) or prismatic (amphibole, tourmaline). They posses a preferred orientation.	Schistosity surfaces that are planar along which the rock may break(cleave) into tabular or platy fragments. Slaty cleavage is perfectly planar. Crenulation cleavage is defined by cm- to mm scale periodic folds.	Foliation defined by layers of microbreccia with glassy appearance and or highly strained and elongated grains of quartz and or feldspar.
Top-1				x		
Top-2				x		
Middle				x		
Bottom-1				x		
Bottom-2				x		

13.11 m
43 Ft

Box 5

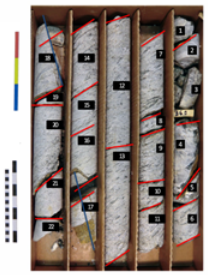

Box 5

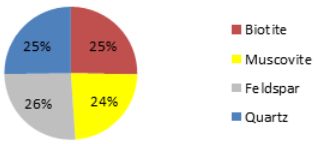

13.11 m
43 Ft

Drill Core Box 6

Total core Run (m)	Total Core Recovery (m)	Total Core Recovery %	RQD %
3.53	2.42	72.15	49.51

Description sheet

Box N.	6

1. Grain size	Fine	Medium	Coarse grained	Very Coarse Grained	Porphyroblastic	Granoblastic	Porphyroclastic
Sets	<0.75mm	0.75-1mm	1-2mm	>2mm	Containing crystals that are larger than the enclosing matrix	Composed of crystals of the same size. Fine to medium grained metamorphic rocks Al poor.	Coarse, relict, deformed crystals set in a fine grained, mylonitic matrix.
Top-1	x				x		
Top-2	x				x		
Middle	x				x		
Bottom-1	x				x		
Bottom-2	x				x		

2. Layering. (Foliation)	Isotropic	Compositional layering	Gneissosity	Schistosity	Cleavage	Mylonitic layering
Sets	Not layered	Foliation defined by alternating layers composed of different minerals. Easy to recognize by differences in colors of layers.	Compositional layering in with granoblastic layers of roughly equidimensional grains(quartz and feldspar) alternate with more schistose layers of platy or elongate grains.	Foliation defined by aligned minerals. Commonly platy minerals(micas, chlorite...) or prismatic (amphibole, tourmaline). They posses a preferred orientation.	Schistosity surfaces that are planar along which the rock may break(cleave) into tabular or platy fragments. Slaty cleavage is perfectly planar. Crenulation cleavage is defined by cm- to mm scale periodic folds.	Foliation defined by layers of microbreccia with glassy appearance and or highly strained and elongated grains of quartz and or feldspar.
Top-1				x		
Top-2				x		
Middle				x		
Bottom-1				x		
Bottom-2				x		

16.46 m
54 Ft

Box 6

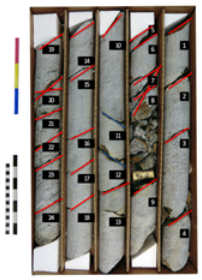

Box 6

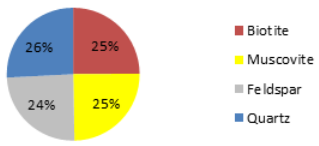

16.46 m
54 Ft

Drill Core Box 7

Total core Run (m)	Total Core Recovery (m)	Total Core Recovery %	RQD %
2.80	2.11	75.3	38.09

Description sheet

Box N.	7

1. Grain size	Fine	Medium	Coarse grained	Very Coarse Grained	Porphyroblastic	Granoblastic	Porphyroclastic
Sets	<0.75mm	0.75-1mm	1-2mm	>2mm	Containing crystals that are larger than the enclosing matrix	Composed of crystals of the same size. Fine to medium grained metamorphic rocks Al poor.	Coarse, relict, deformed crystals set in a fine grained, mylonitic matrix.
Top-1	x				x		
Top-2	x				x		
Middle	x				x		
Bottom-1	x				x		
Bottom-2	x				x		

2. Layering. (Foliation)	Isotropic	Compositional layering	Gneissosity	Schistosity	Cleavage	Mylonitic layering
Sets	Not layered	Foliation defined by alternating layers composed of different minerals. Easy to recognize by differences in colors of layers.	Compositional layering in with granoblastic layers of roughly equidimensional grains(quartz and feldspar) alternate with more schistose layers of platy or elongate grains.	Foliation defined by aligned minerals. Commonly platy minerals(micas, chlorite...) or prismatic (amphibole, tourmaline). They posses a preferred orientation.	Schistosity surfaces that are planar along which the rock may break(cleave) into tabular or platy fragments. Slaty cleavage is perfectly planar. Crenulation cleavage is defined by cm- to mm scale periodic folds.	Foliation defined by layers of microbreccia with glassy appearance and or highly strained and elongated grains of quartz and or feldspar.
Top-1				x		
Top-2				x		
Middle				x		
Bottom-1				x		
Bottom-2				x		

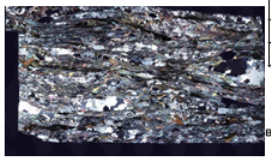

Box 7

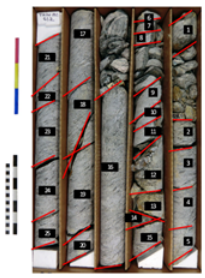

Thin section
(61.2Ft.)

19.26 m
63.2 Ft

Box 7

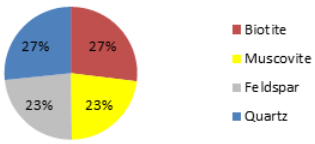

19.35 m
63.5 Ft

Thin section
(65.2 Ft.)

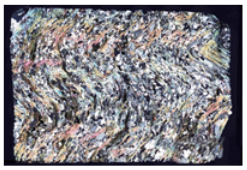

21.58 m
70.8 Ft

Drill Core Box 8

Total core Run (m)	Total Core Recovery (m)	Total Core Recovery %	RQD %
2.23	2.15	96.6	75

Description sheet

Box N.	8

1. Grain size	Fine	Medium	Coarse grained	Very Coarse Grained	Porphyroblastic	Granoblastic	Porphyroclastic
Sets	<0.75mm	0.75-1mm	1-2mm	>2mm	Containing crystals that are larger than the enclosing matrix	Composed of crystals of the same size. Fine to medium grained metamorphic rocks Al poor.	Coarse, relict, deformed crystals set in a fine grained, mylonitic matrix.
Top-1	x				x		
Top-2	x				x		
Middle	x				x		
Bottom-1	x				x		
Bottom-2	x				x		

2. Layering. (Foliation)	Isotropic	Compositional layering	Gneissosity	Schistosity	Cleavage	Mylonitic layering
Sets	Not layered	Foliation defined by alternating layers composed of different minerals. Easy to recognize by differences in colors of layers.	Compositional layering in with granoblastic layers of roughly equidimensional grains(quartz and feldspar) alternate with more schistose layers of platy or elongate grains.	Foliation defined by aligned minerals. Commonly platy minerals(micas, chlorite...) or prismatic (amphibole, tourmaline). They posses a preferred orientation.	Schistosity surfaces that are planar along which the rock may break(cleave) into tabular or platy fragments. Slaty cleavage is perfectly planar. Crenulation cleavage is defined by cm- to mm scale periodic folds.	Foliation defined by layers of microbreccia with glassy appearance and or highly strained and elongated grains of quartz and or feldspar.
Top-1				x		
Top-2				x		
Middle				x		
Bottom-1				x		
Bottom-2				x		

Box 8

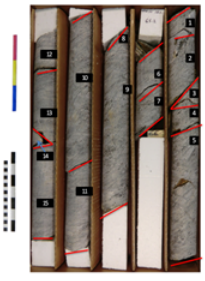

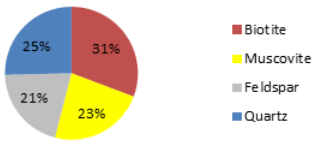

21.61 m
70.9 Ft

Drill Core Box 9

Total core Run (m)	Total Core Recovery (m)	Total Core Recovery %	RQD %
2.35	2.28	97.2	72

Description sheet

Box N.	9

1. Grain size	Fine	Medium	Coarse grained	Very Coarse Grained	Porphyroblastic	Granoblastic	Porphyroclastic
Sets	<0.75mm	0.75-1mm	1-2mm	>2mm	Containing crystals that are larger than the enclosing matrix	Composed of crystals of the same size. Fine to medium grained metamorphic rocks Al poor.	Coarse, relict, deformed crystals set in a fine grained, mylonitic matrix.
Top-1	x				x		
Top-2	x				x		
Middle	x				x		
Bottom-1	x				x		
Bottom-2	x				x		

2. Layering. (Foliation)	Isotropic	Compositional layering	Gneissosity	Schistosity	Cleavage	Mylonitic layering
Sets	Not layered	Foliation defined by alternating layers composed of different minerals. Easy to recognize by differences in colors of layers.	Compositional layering in with granoblastic layers of roughly equidimensional grains(quartz and feldspar) alternate with more schistose layers of platy or elongate grains.	Foliation defined by aligned minerals. Commonly platy minerals(micas, chlorite...) or prismatic (amphibole, tourmaline). They posses a preferred orientation.	Schistosity surfaces that are planar along which the rock may break(cleave) into tabular or platy fragments. Slaty cleavage is perfectly planar. Crenulation cleavage is defined by cm- to mm scale periodic folds.	Foliation defined by layers of microbreccia with glassy appearance and or highly strained and elongated grains of quartz and or feldspar.
Top-1				x		
Top-2				x		
Middle				x		
Bottom-1				x		
Bottom-2				x		

23.96 m
78.6 Ft

Box 9

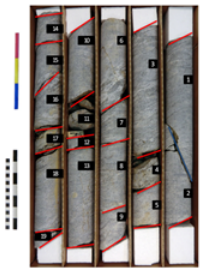

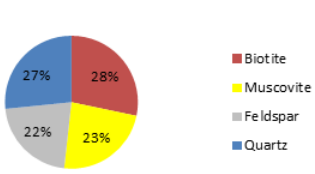

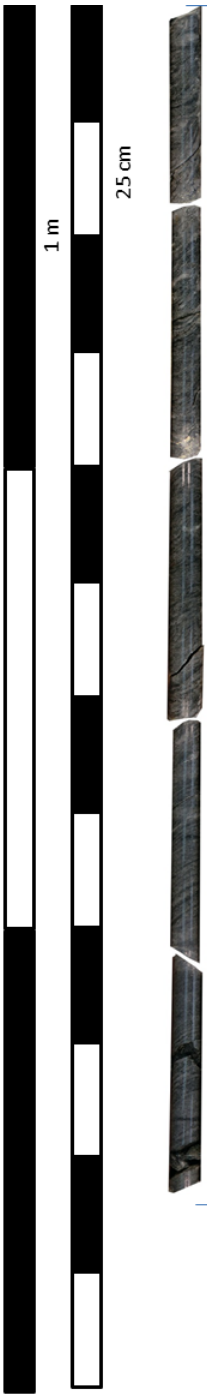

23.96 m
78.6 Ft

Drill Core Box 10

Total core Run (m)	Total Core Recovery (m)	Total Core Recovery %	RQD %
2.26	2.22	98.2	87.8

Description sheet

Box N.	10

1. Grain size	Fine	Medium	Coarse grained	Very Coarse Grained	Porphyroblastic	Granoblastic	Porphyroclastic
Sets	<0.75mm	0.75-1mm	1-2mm	>2mm	Containing crystals that are larger than the enclosing matrix	Composed of crystals of the same size. Fine to medium grained metamorphic rocks Al poor.	Coarse, relict, deformed crystals set in a fine grained, mylonitic matrix.
Top-1	x				x		
Top-2	x				x		
Middle	x				x		
Bottom-1	x				x		
Bottom-2	x				x		

2. Layering. (Foliation)	Isotropic	Compositional layering	Gneissosity	Schistosity	Cleavage	Mylonitic layering
Sets	Not layered	Foliation defined by alternating layers composed of different minerals. Easy to recognize by differences in colors of layers.	Compositional layering in with granoblastic layers of roughly equidimensional grains(quartz and feldspar) alternate with more schistose layers of platy or elongate grains.	Foliation defined by aligned minerals. Commonly platy minerals(micas, chlorite...) or prismatic (amphibole, tourmaline). They posses a preferred orientation.	Schistosity surfaces that are planar along which the rock may break(cleave) into tabular or platy fragments. Slaty cleavage is perfectly planar. Crenulation cleavage is defined by cm- to mm scale periodic folds.	Foliation defined by layers of microbreccia with glassy appearance and or highly strained and elongated grains of quartz and or feldspar.
Top-1				x		
Top-2				x		
Middle				x		
Bottom-1				x		
Bottom-2				x		

26.21 m
86 Ft

Box 10

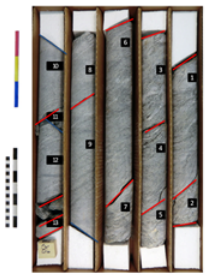

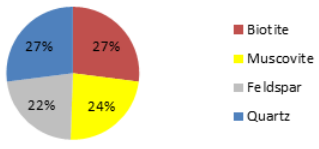

Drill Core Box 11

26.21 m
86 Ft

Total core Run (m)	Total Core Recovery (m)	Total Core Recovery %	RQD %
2.47	2.47	100	94.1

Description sheet

Box N.	11

1. Grain size	Fine	Medium	Coarse grained	Very Coarse Grained	Porphyrobl astic	Granoblastic	Porphyrocla stic
Sets	<0.75mm	0.75-1mm	1-2mm	>2mm	Containing crystals that are larger than the enclosing matrix	Composed of crystals of the same size. Fine to medium grained metamorphic rocks Al poor.	Coarse, relict, deformed crystals set in a fine grained, mylonitic matrix.
Top-1	x				x		
Top-2	x				x		
Middle	x				x		
Bottom-1	x				x		
Bottom-2	x				x		

2. Layering. (Foliation)	Isotropic	Compositional layering	Gneissosity	Schistosity	Cleavage	Mylonitic layering
Sets	Not layered	Foliation defined by alternating layers composed of different minerals. Easy to recognize by differences in colors of layers.	Compositional layering in with granoblastic layers of roughly equidimensional grains(quartz and feldspar) alternate with more schistose layers of platy or elongate grains.	Foliation defined by aligned minerals. Commonly platy minerals(micas, chlorite...) or prismatic (amphibole, tourmaline). They posses a preferred orientation.	Schistosity surfaces that are planar along which the rock may break(cleave) into tabular or platy fragments. Slaty cleavage is perfectly planar. Crenulation cleavage is defined by cm- to mm scale periodic folds.	Foliation defined by layers of microbreccia with glassy appearance and or highly strained and elongated grains of quartz and or feldspar.
Top-1				x		
Top-2				x		
Middle				x		
Bottom-1				x		
Bottom-2				x		

28.68 m
94.1 Ft

Box 11

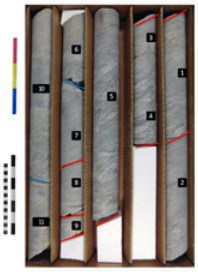

Box 11

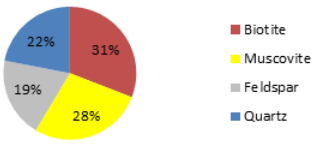

28.68 m
94.1 Ft

Thin section
(98Ft.)

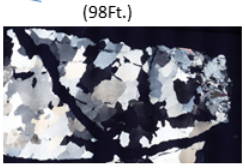

31.09 m
102 Ft

Drill Core Box 12

Total core Run (m)	Total Core Recovery (m)	Total Core Recovery %	RQD %
2.41	2.18	90.5	60.8

Description sheet

Box N.	12

1. Grain size	Fine	Medium	Coarse grained	Very Coarse Grained	Porphyroblastic	Granoblastic	Porphyroclastic
Sets	<0.75mm	0.75-1mm	1-2mm	>2mm	Containing crystals that are larger than the enclosing matrix	Composed of crystals of the same size. Fine to medium grained metamorphic rocks Al poor.	Coarse, relict, deformed crystals set in a fine grained, mylonitic matrix.
Top-1	x				x		
Top-2	x				x		
Middle	x				x		
Bottom-1	x				x		
Bottom-2	x				x		

2. Layering. (Foliation)	Isotropic	Compositional layering	Gneissosity	Schistosity	Cleavage	Mylonitic layering
Sets	Not layered	Foliation defined by alternating layers composed of different minerals. Easy to recognize by differences in colors of layers.	Compositional layering in with granoblastic layers of roughly equidimensional grains(quartz and feldspar) alternate with more schistose layers of platy or elongate grains.	Foliation defined by aligned minerals. Commonly platy minerals(micas, chlorite...) or prismatic (amphibole, tourmaline). They posses a preferred orientation.	Schistosity surfaces that are planar along which the rock may break(cleave) into tabular or platy fragments. Slaty cleavage is perfectly planar. Crenulation cleavage is defined by cm- to mm scale periodic folds.	Foliation defined by layers of microbreccia with glassy appearance and or highly strained and elongated grains of quartz and or feldspar.
Top-1				x		
Top-2				x		
Middle				x		
Bottom-1				x		
Bottom-2				x		

Box 12

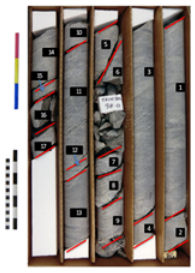

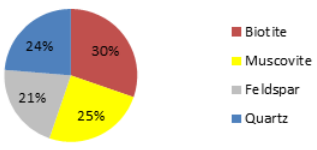

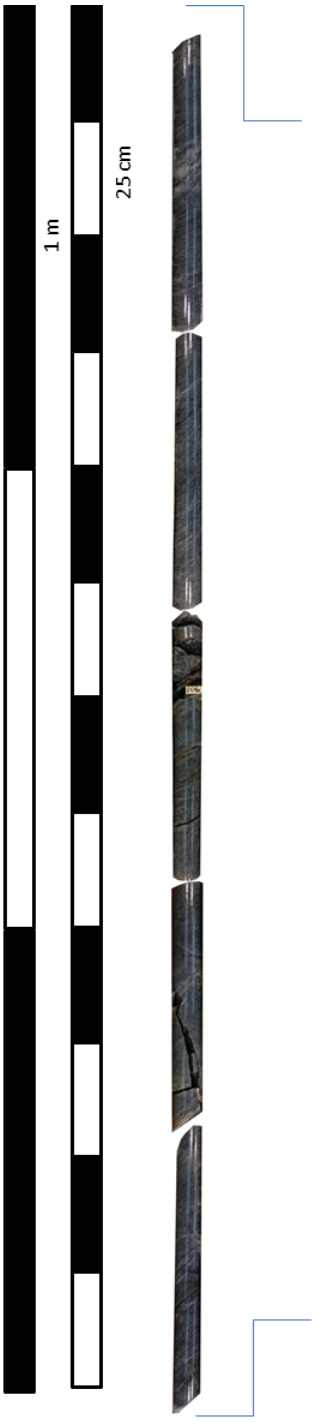

31.09 m
102 Ft

Drill Core Box 13

Total core Run (m)	Total Core Recovery (m)	Total Core Recovery %	RQD %
2.86	2.55	89.0	82.2

Description sheet

Box N.	13

1. Grain size	Fine	Medium	Coarse grained	Very Coarse Grained	Porphyroblastic	Granoblastic	Porphyroclastic
Sets	<0.75mm	0.75-1mm	1-2mm	>2mm	Containing crystals that are larger than the enclosing matrix	Composed of crystals of the same size. Fine to medium grained metamorphic rocks Al poor.	Coarse, relict, deformed crystals set in a fine grained, mylonitic matrix.
Top-1	x				x		
Top-2	x				x		
Middle	x				x		
Bottom-1	x				x		
Bottom-2	x				x		

2. Layering. (Foliation)	Isotropic	Compositional layering	Gneissosity	Schistosity	Cleavage	Mylonitic layering
Sets	Not layered	Foliation defined by alternating layers composed of different minerals. Easy to recognize by differences in colors of layers.	Compositional layering in with granoblastic layers of roughly equidimensional grains(quartz and feldspar) alternate with more schistose layers of platy or elongate grains.	Foliation defined by aligned minerals. Commonly platy minerals(micas, chlorite...) or prismatic (amphibole, tourmaline). They posses a preferred orientation.	Schistosity surfaces that are planar along which the rock may break(cleave) into tabular or platy fragments. Slaty cleavage is perfectly planar. Crenulation cleavage is defined by cm- to mm scale periodic folds.	Foliation defined by layers of microbreccia with glassy appearance and or highly strained and elongated grains of quartz and or feldspar.
Top-1				x		
Top-2				x		
Middle				x		
Bottom-1				x		
Bottom-2				x		

Box 13

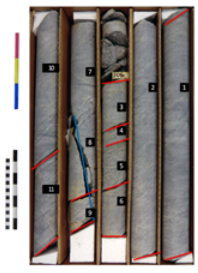

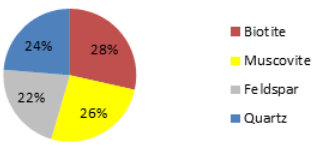

33.95 m
111.4 Ft

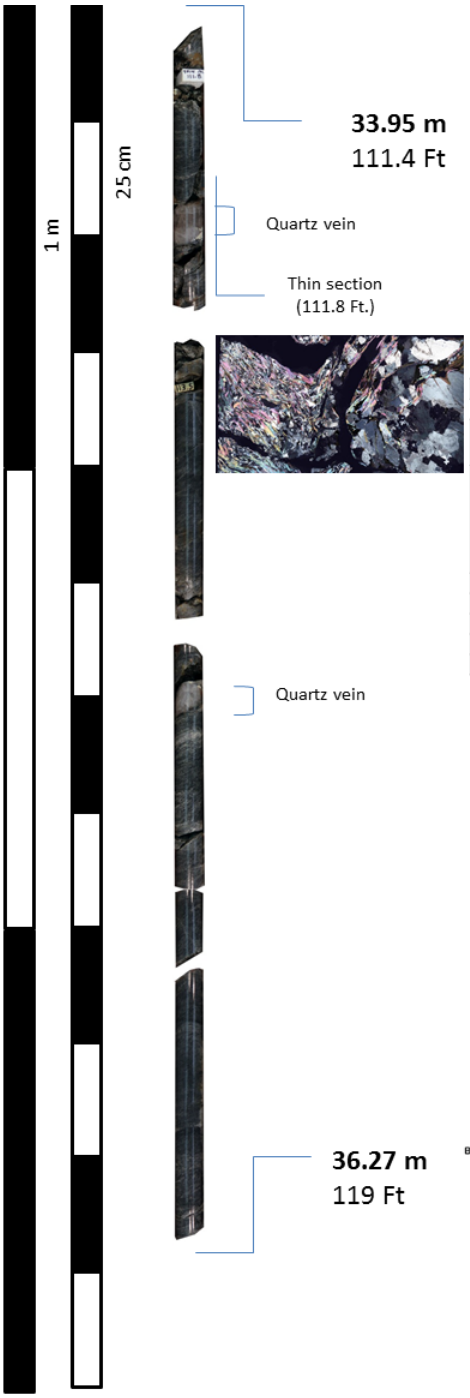

Drill Core Box 14

Total core Run (m)	Total Core Recovery (m)	Total Core Recovery %	RQD %
2.32	2.15	92.8	82.8

Description sheet

Box N.	14

1. Grain size	Fine	Medium	Coarse grained	Very Coarse Grained	Porphyroblastic	Granoblastic	Porphyroclastic
Sets	<0.75mm	0.75-1mm	1-2mm	>2mm	Containing crystals that are larger than the enclosing matrix	Composed of crystals of the same size. Fine to medium grained metamorphic rocks Al poor.	Coarse, relict, deformed crystals set in a fine grained, mylonitic matrix.
Top-1	x				x		
Top-2	x				x		
Middle	x				x		
Bottom-1	x				x		
Bottom-2	x				x		

2. Layering. (Foliation)	Isotropic	Compositional layering	Gneissosity	Schistosity	Cleavage	Mylonitic layering
Sets	Not layered	Foliation defined by alternating layers composed of different minerals. Easy to recognize by differences in colors of layers.	Compositional layering in with granoblastic layers of roughly equidimensional grains(quartz and feldspar) alternate with more schistose layers of platy or elongate grains.	Foliation defined by aligned minerals. Commonly platy minerals(micas, chlorite...) or prismatic (amphibole, tourmaline). They posses a preferred orientation.	Schistosity surfaces that are planar along which the rock may break(cleave) into tabular or platy fragments. Slaty cleavage is perfectly planar. Crenulation cleavage is defined by cm- to mm scale periodic folds.	Foliation defined by layers of microbreccia with glassy appearance and or highly strained and elongated grains of quartz and or feldspar.
Top-1				x		
Top-2				x		
Middle				x		
Bottom-1				x		
Bottom-2				x		

Box 14

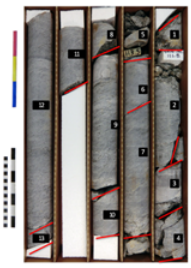

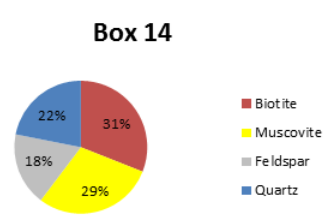

36.27 m
119 Ft

Quartz vein

38.98 m
127.9 Ft

Drill Core Box 15

Total core Run (m)	Total Core Recovery (m)	Total Core Recovery %	RQD %
2.72	2.52	92.9	62.7

Description sheet

Box N.	15

1. Grain size	Fine	Medium	Coarse grained	Very Coarse Grained	Porphyroblastic	Granoblastic	Porphyroclastic
Sets	<0.75mm	0.75-1mm	1-2mm	>2mm	Containing crystals that are larger than the enclosing matrix	Composed of crystals of the same size. Fine to medium grained metamorphic rocks Al poor.	Coarse, relict, deformed crystals set in a fine grained, mylonitic matrix.
Top-1	x				x		
Top-2	x				x		
Middle	x				x		
Bottom-1	x				x		
Bottom-2	x				x		

2. Layering. (Foliation)	Isotropic	Compositional layering	Gneissosity	Schistosity	Cleavage	Mylonitic layering
Sets	Not layered	Foliation defined by alternating layers composed of different minerals. Easy to recognize by differences in colors of layers.	Compositional layering in with granoblastic layers of roughly equidimensional grains(quartz and feldspar) alternate with more schistose layers of platy or elongate grains.	Foliation defined by aligned minerals. Commonly platy minerals(micas, chlorite...) or prismatic (amphibole, tourmaline). They posses a preferred orientation.	Schistosity surfaces that are planar along which the rock may break(cleave) into tabular or platy fragments. Slaty cleavage is perfectly planar. Crenulation cleavage is defined by cm- to mm scale periodic folds.	Foliation defined by layers of microbreccia with glassy appearance and or highly strained and elongated grains of quartz and or feldspar.
Top-1				x		
Top-2				x		
Middle				x		
Bottom-1				x		
Bottom-2				x		

Box 15

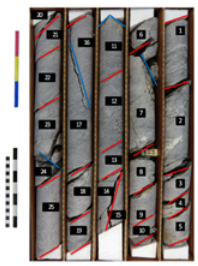

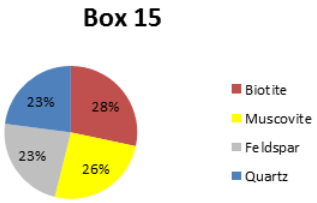

38.98 m
127.9 Ft

Drill Core Box 16

Total core Run (m)	Total Core Recovery (m)	Total Core Recovery %	RQD %
2.47	2.41	97.6	39.7

Description sheet

Box N.	16

1. Grain size	Fine	Medium	Coarse grained	Very Coarse Grained	Porphyroblastic	Granoblastic	Porphyroclastic
Sets	<0.75mm	0.75-1mm	1-2mm	>2mm	Containing crystals that are larger than the enclosing matrix	Composed of crystals of the same size. Fine to medium grained metamorphic rocks Al poor.	Coarse, relict, deformed crystals set in a fine grained, mylonitic matrix.
Top-1	x				x		
Top-2	x				x		
Middle	x				x		
Bottom-1	x				x		
Bottom-2	x				x		

2. Layering. (Foliation)	Isotropic	Compositional layering	Gneissosity	Schistosity	Cleavage	Mylonitic layering
Sets	Not layered	Foliation defined by alternating layers composed of different minerals. Easy to recognize by differences in colors of layers.	Compositional layering in with granoblastic layers of roughly equidimensional grains(quartz and feldspar) alternate with more schistose layers of platy or elongate grains.	Foliation defined by aligned minerals. Commonly platy minerals(micas, chlorite...) or prismatic (amphibole, tourmaline). They posses a preferred orientation.	Schistosity surfaces that are planar along which the rock may break(cleave) into tabular or platy fragments. Slaty cleavage is perfectly planar. Crenulation cleavage is defined by cm- to mm scale periodic folds.	Foliation defined by layers of microbreccia with glassy appearance and or highly strained and elongated grains of quartz and or feldspar.
Top-1				x		
Top-2				x		
Middle				x		
Bottom-1				x		
Bottom-2				x		

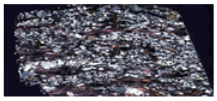

Box 16

Thin section
(135.8 Ft.)

41.45 m
136 Ft

Box 16

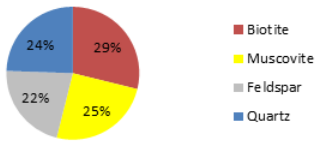

41.54 m
136.3 Ft

Drill Core Box 17

Total core Run (m)	Total Core Recovery (m)	Total Core Recovery %	RQD %
2.9	2.27	78.2	29.5

Description sheet

Box N.	17

1. Grain size	Fine	Medium	Coarse grained	Very Coarse Grained	Porphyroblastic	Granoblastic	Porphyroclastic
Sets	<0.75mm	0.75-1mm	1-2mm	>2mm	Containing crystals that are larger than the enclosing matrix	Composed of crystals of the same size. Fine to medium grained metamorphic rocks Al poor.	Coarse, relict, deformed crystals set in a fine grained, mylonitic matrix.
Top-1	x				x		
Top-2	x				x		
Middle	x				x		
Bottom-1	x				x		
Bottom-2	x				x		

Thin section
(141Ft.)

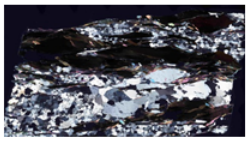

Quartz vein

2. Layering. (Foliation)	Isotropic	Compositional layering	Gneissosity	Schistosity	Cleavage	Mylonitic layering
Sets	Not layered	Foliation defined by alternating layers composed of different minerals. Easy to recognize by differences in colors of layers.	Compositional layering in with granoblastic layers of roughly equidimensional grains(quartz and feldspar) alternate with more schistose layers of platy or elongate grains.	Foliation defined by aligned minerals. Commonly platy minerals(micas, chlorite...) or prismatic (amphibole, tourmaline). They posses a preferred orientation.	Schistosity surfaces that are planar along which the rock may break(cleave) into tabular or platy fragments. Slaty cleavage is perfectly planar. Crenulation cleavage is defined by cm- to mm scale periodic folds.	Foliation defined by layers of microbreccia with glassy appearance and or highly strained and elongated grains of quartz and or feldspar.
Top-1				x		
Top-2				x		
Middle				x		
Bottom-1				x		
Bottom-2				x		

Box 17

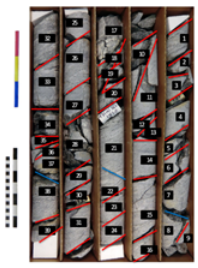

44.44 m
145.8 Ft

Box 17

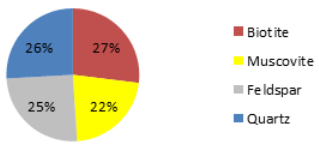

44.44 m
145.8 Ft

Drill Core Box 18

Total core Run (m)	Total Core Recovery (m)	Total Core Recovery %	RQD %
2.44	2.42	99.2	82.23

Description sheet

Box N.	18

1. Grain size	Fine	Medium	Coarse grained	Very Coarse Grained	Porphyroblastic	Granoblastic	Porphyroclastic
Sets	<0.75mm	0.75-1mm	1-2mm	>2mm	Containing crystals that are larger than the enclosing matrix	Composed of crystals of the same size. Fine to medium grained metamorphic rocks Al poor.	Coarse, relict, deformed crystals set in a fine grained, mylonitic matrix.
Top-1	x				x		
Top-2	x				x		
Middle	x				x		
Bottom-1	x				x		
Bottom-2	x				x		

2. Layering. (Foliation)	Isotropic	Compositional layering	Gneissosity	Schistosity	Cleavage	Mylonitic layering
Sets	Not layered	Foliation defined by alternating layers composed of different minerals. Easy to recognize by differences in colors of layers.	Compositional layering in with granoblastic layers of roughly equidimensional grains(quartz and feldspar) alternate with more schistose layers of platy or elongate grains.	Foliation defined by aligned minerals. Commonly platy minerals(micas, chlorite...) or prismatic (amphibole, tourmaline). They posses a preferred orientation.	Schistosity surfaces that are planar along which the rock may break(cleave) into tabular or platy fragments. Slaty cleavage is perfectly planar. Crenulation cleavage is defined by cm- to mm scale periodic folds.	Foliation defined by layers of microbreccia with glassy appearance and or highly strained and elongated grains of quartz and or feldspar.
Top-1				x		
Top-2				x		
Middle				x		
Bottom-1				x		
Bottom-2				x		

46.88 m
153.8 Ft

Box 18

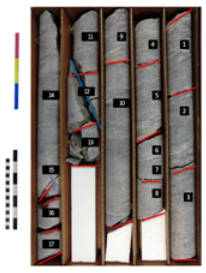

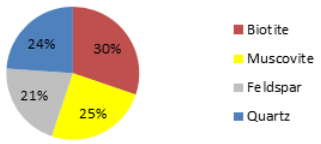

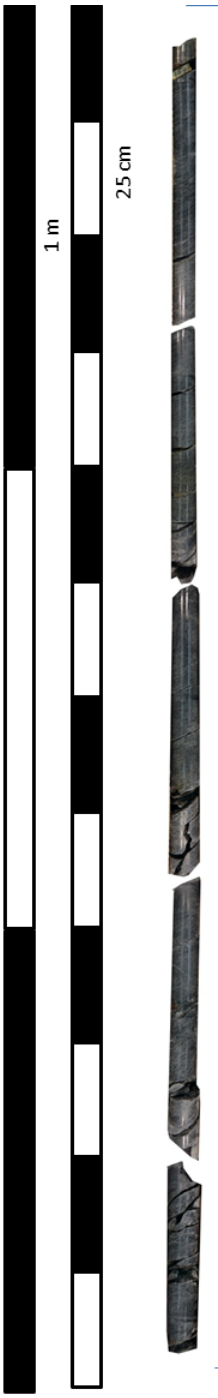

46.88 m
153.8 Ft

Drill Core Box 19

Total core Run (m)	Total Core Recovery (m)	Total Core Recovery %	RQD %
2.5	2.5	100	63.4

Description sheet

Box N.	19

1. Grain size	Fine	Medium	Coarse grained	Very Coarse Grained	Porphyroblastic	Granoblastic	Porphyroclastic
Sets	<0.75mm	0.75-1mm	1-2mm	>2mm	Containing crystals that are larger than the enclosing matrix	Composed of crystals of the same size. Fine to medium grained metamorphic rocks Al poor.	Coarse, relict, deformed crystals set in a fine grained, mylonitic matrix.
Top-1	x				x		
Top-2	x				x		
Middle	x				x		
Bottom-1	x				x		
Bottom-2	x				x		

2. Layering. (Foliation)	Isotropic	Compositional layering	Gneissosity	Schistosity	Cleavage	Mylonitic layering
Sets	Not layered	Foliation defined by alternating layers composed of different minerals. Easy to recognize by differences in colors of layers.	Compositional layering in with granoblastic layers of roughly equidimensional grains(quartz and feldspar) alternate with more schistose layers of platy or elongate grains.	Foliation defined by aligned minerals. Commonly platy minerals(micas, chlorite...) or prismatic (amphibole, tourmaline). They posses a preferred orientation.	Schistosity surfaces that are planar along which the rock may break(cleave) into tabular or platy fragments. Slaty cleavage is perfectly planar. Crenulation cleavage is defined by cm- to mm scale periodic folds.	Foliation defined by layers of microbreccia with glassy appearance and or highly strained and elongated grains of quartz and or feldspar.
Top-1				x		
Top-2				x		
Middle				x		
Bottom-1				x		
Bottom-2				x		

Box 19

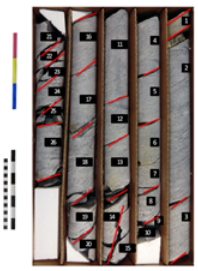

49.38 m
162 Ft

Box 19

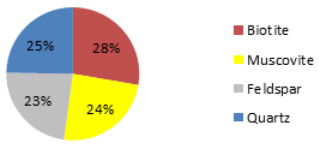

49.38 m
162 Ft

Drill Core Box 20

Total core Run (m)	Total Core Recovery (m)	Total Core Recovery %	RQD %
2.7	2.4	86.53	36.05

Description sheet

Box N.	20

1. Grain size	Fine	Medium	Coarse grained	Very Coarse Grained	Porphyroblastic	Granoblastic	Porphyroclastic
Sets	<0.75mm	0.75-1mm	1-2mm	>2mm	Containing crystals that are larger than the enclosing matrix	Composed of crystals of the same size. Fine to medium grained metamorphic rocks Al poor.	Coarse, relict, deformed crystals set in a fine grained, mylonitic matrix.
Top-1	x				x		
Top-2	x				x		
Middle	x				x		
Bottom-1	x				x		
Bottom-2	x				x		

2. Layering. (Foliation)	Isotropic	Compositional layering	Gneissosity	Schistosity	Cleavage	Mylonitic layering
Sets	Not layered	Foliation defined by alternating layers composed of different minerals. Easy to recognize by differences in colors of layers.	Compositional layering in with granoblastic layers of roughly equidimensional grains(quartz and feldspar) alternate with more schistose layers of platy or elongate grains.	Foliation defined by aligned minerals. Commonly platy minerals(micas, chlorite...) or prismatic (amphibole, tourmaline). They posses a preferred orientation.	Schistosity surfaces that are planar along which the rock may break(cleave) into tabular or platy fragments. Slaty cleavage is perfectly planar. Crenulation cleavage is defined by cm- to mm scale periodic folds.	Foliation defined by layers of microbreccia with glassy appearance and or highly strained and elongated grains of quartz and or feldspar.
Top-1				x		
Top-2				x		
Middle				x		
Bottom-1				x		
Bottom-2				x		

Box 20

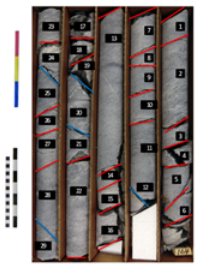

52.15 m
171.1 Ft

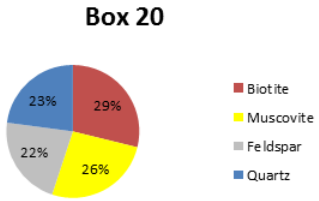

52.15 m
171.1 Ft

Drill Core Box 21

Total core Run (m)	Total Core Recovery (m)	Total Core Recovery %	RQD %
2.77	2.44	87.97	54.42

Description sheet

Box N.	21

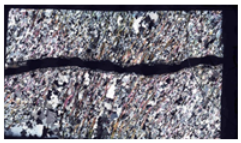

Thin section
(174.7 Ft.)

1. Grain size	Fine	Medium	Coarse grained	Very Coarse Grained	Porphyroblastic	Granoblastic	Porphyroclastic
Sets	<0.75mm	0.75-1mm	1-2mm	>2mm	Containing crystals that are larger than the enclosing matrix	Composed of crystals of the same size. Fine to medium grained metamorphic rocks Al poor.	Coarse, relict, deformed crystals set in a fine grained, mylonitic matrix.
Top-1	x				x		
Top-2	x				x		
Middle	x				x		
Bottom-1	x				x		
Bottom-2	x				x		

2. Layering. (Foliation)	Isotropic	Compositional layering	Gneissosity	Schistosity	Cleavage	Mylonitic layering
Sets	Not layered	Foliation defined by alternating layers composed of different minerals. Easy to recognize by differences in colors of layers.	Compositional layering in with granoblastic layers of roughly equidimensional grains(quartz and feldspar) alternate with more schistose layers of platy or elongate grains.	Foliation defined by aligned minerals. Commonly platy minerals(micas, chlorite...) or prismatic (amphibole, tourmaline). They posses a preferred orientation.	Schistosity surfaces that are planar along which the rock may break(cleave) into tabular or platy fragments. Slaty cleavage is perfectly planar. Crenulation cleavage is defined by cm- to mm scale periodic folds.	Foliation defined by layers of microbreccia with glassy appearance and or highly strained and elongated grains of quartz and or feldspar.
Top-1				x		
Top-2				x		
Middle				x		
Bottom-1				x		
Bottom-2				x		

Box 21

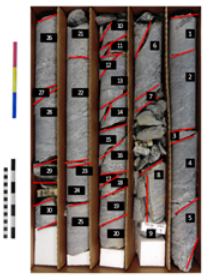

54.92 m
180.2 Ft

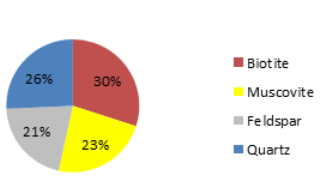

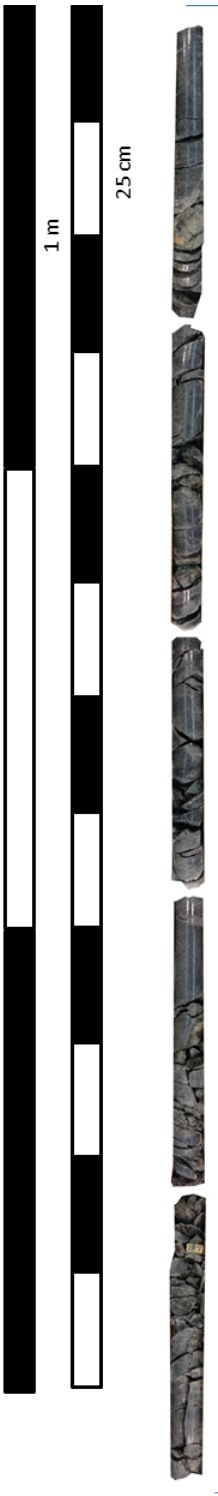

54.92 m
180.2 Ft

Drill Core Box 22

Total core Run (m)	Total Core Recovery (m)	Total Core Recovery %	RQD %
2.99	2.29	67.96	21.1

Description sheet

Box N.	22

1. Grain size	Fine	Medium	Coarse grained	Very Coarse Grained	Porphyroblastic	Granoblastic	Porphyroclastic
Sets	<0.75mm	0.75-1mm	1-2mm	>2mm	Containing crystals that are larger than the enclosing matrix	Composed of crystals of the same size. Fine to medium grained metamorphic rocks Al poor.	Coarse, relict, deformed crystals set in a fine grained, mylonitic matrix.
Top-1	x				x		
Top-2	x				x		
Middle	x				x		
Bottom-1	x				x		
Bottom-2	x				x		

2. Layering. (Foliation)	Isotropic	Compositional layering	Gneissosity	Schistosity	Cleavage	Mylonitic layering
Sets	Not layered	Foliation defined by alternating layers composed of different minerals. Easy to recognize by differences in colors of layers.	Compositional layering in with granoblastic layers of roughly equidimensional grains(quartz and feldspar) alternate with more schistose layers of platy or elongate grains.	Foliation defined by aligned minerals. Commonly platy minerals(micas, chlorite...) or prismatic (amphibole, tourmaline). They posses a preferred orientation.	Schistosity surfaces that are planar along which the rock may break(cleave) into tabular or platy fragments. Slaty cleavage is perfectly planar. Crenulation cleavage is defined by cm- to mm scale periodic folds.	Foliation defined by layers of microbreccia with glassy appearance and or highly strained and elongated grains of quartz and or feldspar.
Top-1				x		
Top-2				x		
Middle				x		
Bottom-1				x		
Bottom-2				x		

Box 22

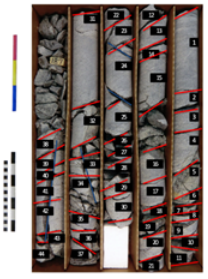

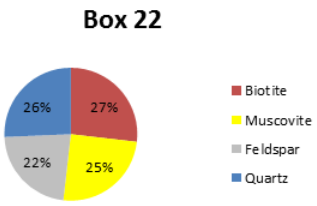

57.91 m
190 Ft

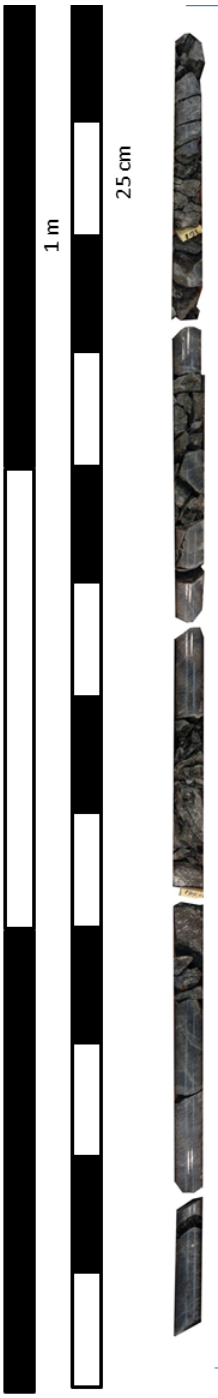

57.91 m
190 Ft

Drill Core Box 23

Total core Run (m)	Total Core Recovery (m)	Total Core Recovery %	RQD %
2.29	1.64	71.52	42.9

Description sheet

Box N.	23

1. Grain size	Fine	Medium	Coarse grained	Very Coarse Grained	Porphyroblastic	Granoblastic	Porphyroclastic
Sets	<0.75mm	0.75-1mm	1-2mm	>2mm	Containing crystals that are larger than the enclosing matrix	Composed of crystals of the same size. Fine to medium grained metamorphic rocks Al poor.	Coarse, relict, deformed crystals set in a fine grained, mylonitic matrix.
Top-1	x				x		
Top-2	x				x		
Middle	x				x		
Bottom-1	x				x		
Bottom-2	x				x		

2. Layering. (Foliation)	Isotropic	Compositional layering	Gneissosity	Schistosity	Cleavage	Mylonitic layering
Sets	Not layered	Foliation defined by alternating layers composed of different minerals. Easy to recognize by differences in colors of layers.	Compositional layering in with granoblastic layers of roughly equidimensional grains(quartz and feldspar) alternate with more schistose layers of platy or elongate grains.	Foliation defined by aligned minerals. Commonly platy minerals(micas, chlorite...) or prismatic (amphibole, tourmaline). They posses a preferred orientation.	Schistosity surfaces that are planar along which the rock may break(cleave) into tabular or platy fragments. Slaty cleavage is perfectly planar. Crenulation cleavage is defined by cm- to mm scale periodic folds.	Foliation defined by layers of microbreccia with glassy appearance and or highly strained and elongated grains of quartz and or feldspar.
Top-1				x		
Top-2				x		
Middle				x		
Bottom-1				x		
Bottom-2				x		

Box 23

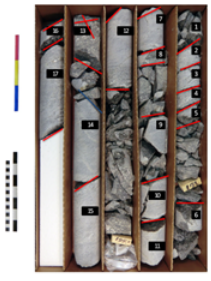

60.2 m
197.5 Ft

Box 23

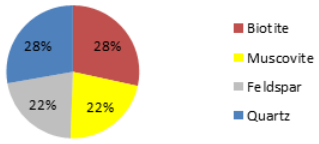

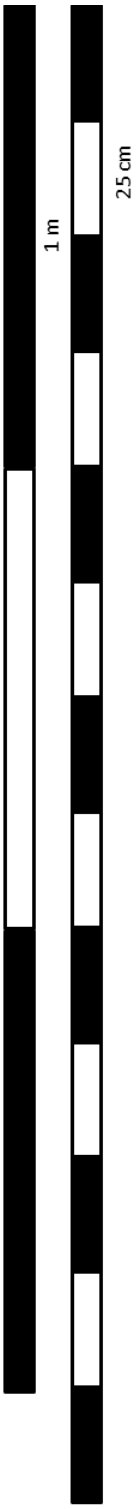

60.2 m
197.5 Ft

Drill Core Box 24

Total core Run (m)	Total Core Recovery (m)	Total Core Recovery %	RQD %
3.505	2.21	62.91	44.8

Description sheet

Box N.	24

1. Grain size	Fine	Medium	Coarse grained	Very Coarse Grained	Porphyroblastic	Granoblastic	Porphyroclastic
Sets	<0.75mm	0.75-1mm	1-2mm	>2mm	Containing crystals that are larger than the enclosing matrix	Composed of crystals of the same size. Fine to medium grained metamorphic rocks Al poor.	Coarse, relict, deformed crystals set in a fine grained, mylonitic matrix.
Top-1	x				x		
Top-2	x				x		
Middle	x				x		
Bottom-1	x				x		
Bottom-2	x				x		

2. Layering. (Foliation)	Isotropic	Compositional layering	Gneissosity	Schistosity	Cleavage	Mylonitic layering
Sets	Not layered	Foliation defined by alternating layers composed of different minerals. Easy to recognize by differences in colors of layers.	Compositional layering in with granoblastic layers of roughly equidimensional grains(quartz and feldspar) alternate with more schistose layers of platy or elongate grains.	Foliation defined by aligned minerals. Commonly platy minerals(micas, chlorite...) or prismatic (amphibole, tourmaline). They posses a preferred orientation.	Schistosity surfaces that are planar along which the rock may break(cleave) into tabular or platy fragments. Slaty cleavage is perfectly planar. Crenulation cleavage is defined by cm- to mm scale periodic folds.	Foliation defined by layers of microbreccia with glassy appearance and or highly strained and elongated grains of quartz and or feldspar.
Top-1				x		
Top-2				x		
Middle				x		
Bottom-1				x		
Bottom-2				x		

Box 24

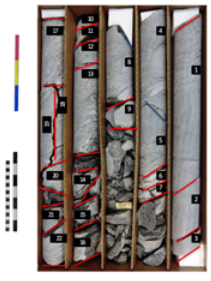

63.7 m
209 Ft

Box 24

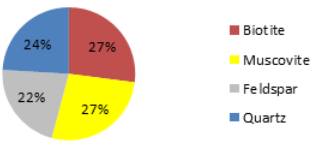

63.7 m
209 Ft

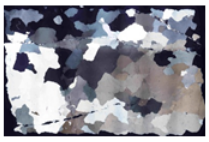

Quartz vein

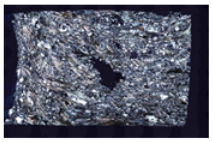

Thin sections (216 and 222 Ft.)

Breccia and sand zone ± 3.5m (12ft)

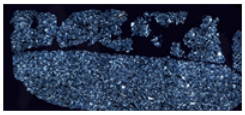

Thin section (breccia and sand zone)

68.88 m
226 Ft

Drill Core Box 25

Total core Run (m)	Total Core Recovery (m)	Total Core Recovery %	RQD %
5.182	1.64	31.55	28

Description sheet

Box N.	25

1. Grain size	Fine	Medium	Coarse grained	Very Coarse Grained	Porphyroblastic	Granoblastic	Porphyroclastic
Sets	<0.75mm	0.75-1mm	1-2mm	>2mm	Containing crystals that are larger than the enclosing matrix	Composed of crystals of the same size. Fine to medium grained metamorphic rocks Al poor.	Coarse, relict, deformed crystals set in a fine grained, mylonitic matrix.
Top-1	x						
Top-2	x						
Middle	x				x		
Bottom-1	x				x		
Bottom-2	x				x		

2. Layering. (Foliation)	Isotropic	Compositional layering	Gneissosity	Schistosity	Cleavage	Mylonitic layering
Sets	Not layered	Foliation defined by alternating layers composed of different minerals. Easy to recognize by differences in colors of layers.	Compositional layering in with granoblastic layers of roughly equidimensional grains(quartz and feldspar) alternate with more schistose layers of platy or elongate grains.	Foliation defined by aligned minerals. Commonly platy minerals(micas, chlorite...) or prismatic (amphibole, tourmaline). They posses a preferred orientation.	Schistosity surfaces that are planar along which the rock may break(cleave) into tabular or platy fragments. Slaty cleavage is perfectly planar. Crenulation cleavage is defined by cm- to mm scale periodic folds.	Foliation defined by layers of microbreccia with glassy appearance and or highly strained and elongated grains of quartz and or feldspar.
Top-1	x					
Top-2	x					
Middle				x		
Bottom-1				x		
Bottom-2				x		

Box 25

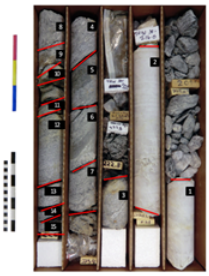

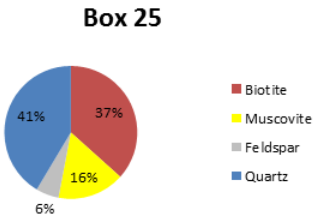

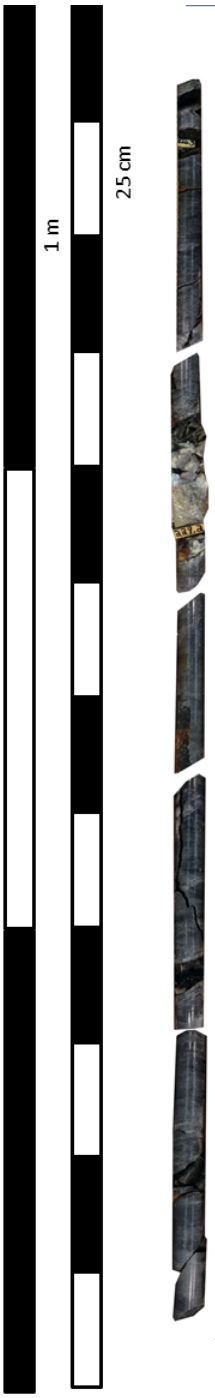

68.88 m
226 Ft

Drill Core Box 26

Total core Run (m)	Total Core Recovery (m)	Total Core Recovery %	RQD %
2.59	2.03	78.16	61.4

Description sheet

Box N.	26

1. Grain size	Fine	Medium	Coarse grained	Very Coarse Grained	Porphyroblastic	Granoblastic	Porphyroclastic
Sets	<0.75mm	0.75-1mm	1-2mm	>2mm	Containing crystals that are larger than the enclosing matrix	Composed of crystals of the same size. Fine to medium grained metamorphic rocks Al poor.	Coarse, relict, deformed crystals set in a fine grained, mylonitic matrix.
Top-1	x				x		
Top-2	x				x		
Middle	x				x		
Bottom-1	x				x		
Bottom-2	x				x		

2. Layering. (Foliation)	Isotropic	Compositional layering	Gneissosity	Schistosity	Cleavage	Mylonitic layering
Sets	Not layered	Foliation defined by alternating layers composed of different minerals. Easy to recognize by differences in colors of layers.	Compositional layering in with granoblastic layers of roughly equidimensional grains(quartz and feldspar) alternate with more schistose layers of platy or elongate grains.	Foliation defined by aligned minerals. Commonly platy minerals(micas, chlorite...) or prismatic (amphibole, tourmaline). They posses a preferred orientation.	Schistosity surfaces that are planar along which the rock may break(cleave) into tabular or platy fragments. Slaty cleavage is perfectly planar. Crenulation cleavage is defined by cm- to mm scale periodic folds.	Foliation defined by layers of microbreccia with glassy appearance and or highly strained and elongated grains of quartz and or feldspar.
Top-1				x		
Top-2				x		
Middle				x		
Bottom-1				x		
Bottom-2				x		

71.48 m
234.5 Ft

Box 26

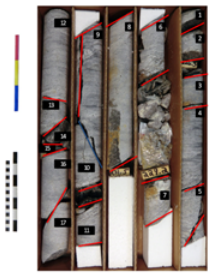

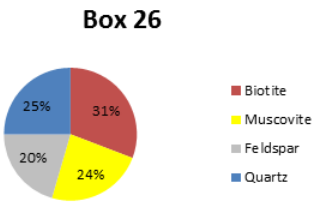

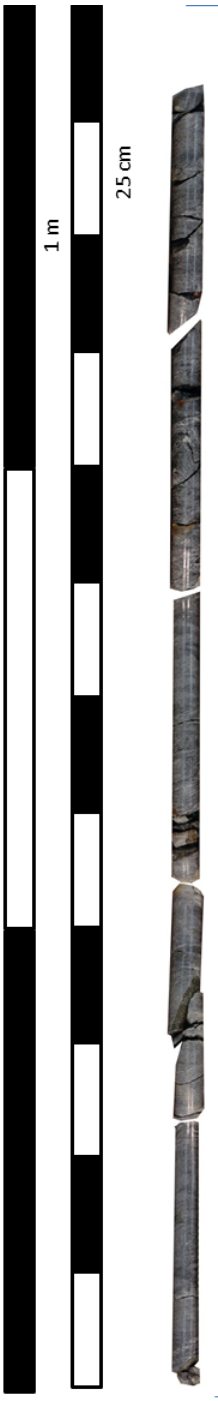

71.48 m
234.5 Ft

74.34 m
243.9 Ft

Drill Core Box 27

Total core Run (m)	Total Core Recovery (m)	Total Core Recovery %	RQD %
2.865	2.33	81.32	63.7

Description sheet

Box N.	27

1. Grain size	Fine	Medium	Coarse grained	Very Coarse Grained	Porphyroblastic	Granoblastic	Porphyroclastic
Sets	<0.75mm	0.75-1mm	1-2mm	>2mm	Containing crystals that are larger than the enclosing matrix	Composed of crystals of the same size. Fine to medium grained metamorphic rocks Al poor.	Coarse, relict, deformed crystals set in a fine grained, mylonitic matrix.
Top-1	x				x		
Top-2	x				x		
Middle	x				x		
Bottom-1	x				x		
Bottom-2	x				x		

2. Layering. (Foliation)	Isotropic	Compositional layering	Gneissosity	Schistosity	Cleavage	Mylonitic layering
Sets	Not layered	Foliation defined by alternating layers composed of different minerals. Easy to recognize by differences in colors of layers.	Compositional layering in with granoblastic layers of roughly equidimensional grains(quartz and feldspar) alternate with more schistose layers of platy or elongate grains.	Foliation defined by aligned minerals. Commonly platy minerals(micas, chlorite...) or prismatic (amphibole, tourmaline). They posses a preferred orientation.	Schistosity surfaces that are planar along which the rock may break(cleave) into tabular or platy fragments. Slaty cleavage is perfectly planar. Crenulation cleavage is defined by cm- to mm scale periodic folds.	Foliation defined by layers of microbreccia with glassy appearance and or highly strained and elongated grains of quartz and or feldspar.
Top-1				x		
Top-2				x		
Middle				x		
Bottom-1				x		
Bottom-2				x		

Box 27

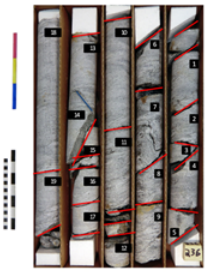

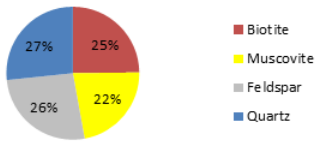

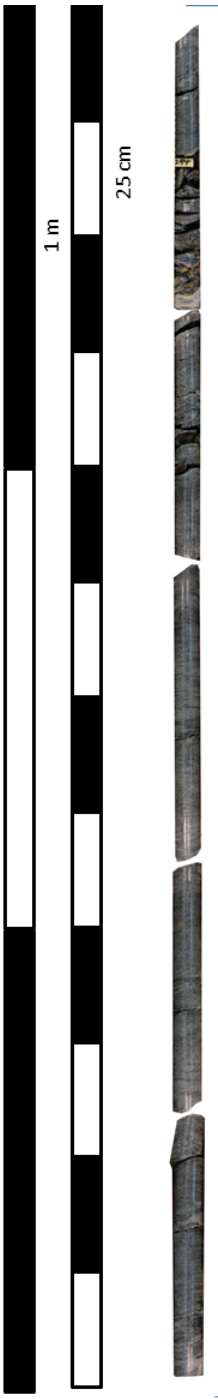

74.22 m
243.5 Ft

Drill Core Box 28

Total core Run (m)	Total Core Recovery (m)	Total Core Recovery %	RQD %
3.231	2.35	72.58	61.13

Description sheet

Box N.	27

1. Grain size	Fine	Medium	Coarse grained	Very Coarse Grained	Porphyroblastic	Granoblastic	Porphyroclastic
Sets	<0.75mm	0.75-1mm	1-2mm	>2mm	Containing crystals that are larger than the enclosing matrix	Composed of crystals of the same size. Fine to medium grained metamorphic rocks Al poor.	Coarse, relict, deformed crystals set in a fine grained, mylonitic matrix.
Top-1	x				x		
Top-2	x				x		
Middle	x				x		
Bottom-1	x				x		
Bottom-2	x				x		

2. Layering. (Foliation)	Isotropic	Compositional layering	Gneissosity	Schistosity	Cleavage	Mylonitic layering
Sets	Not layered	Foliation defined by alternating layers composed of different minerals. Easy to recognize by differences in colors of layers.	Compositional layering in with granoblastic layers of roughly equidimensional grains(quartz and feldspar) alternate with more schistose layers of platy or elongate grains.	Foliation defined by aligned minerals. Commonly platy minerals(micas, chlorite...) or prismatic (amphibole, tourmaline). They posses a preferred orientation.	Schistosity surfaces that are planar along which the rock may break(cleave) into tabular or platy fragments. Slaty cleavage is perfectly planar. Crenulation cleavage is defined by cm- to mm scale periodic folds.	Foliation defined by layers of microbreccia with glassy appearance and or highly strained and elongated grains of quartz and or feldspar.
Top-1				x		
Top-2				x		
Middle				x		
Bottom-1				x		
Bottom-2				x		

Box 28

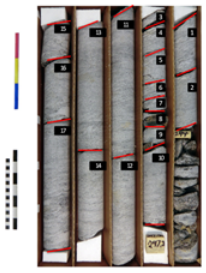

77.45 m
254.1 Ft

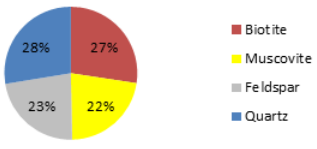

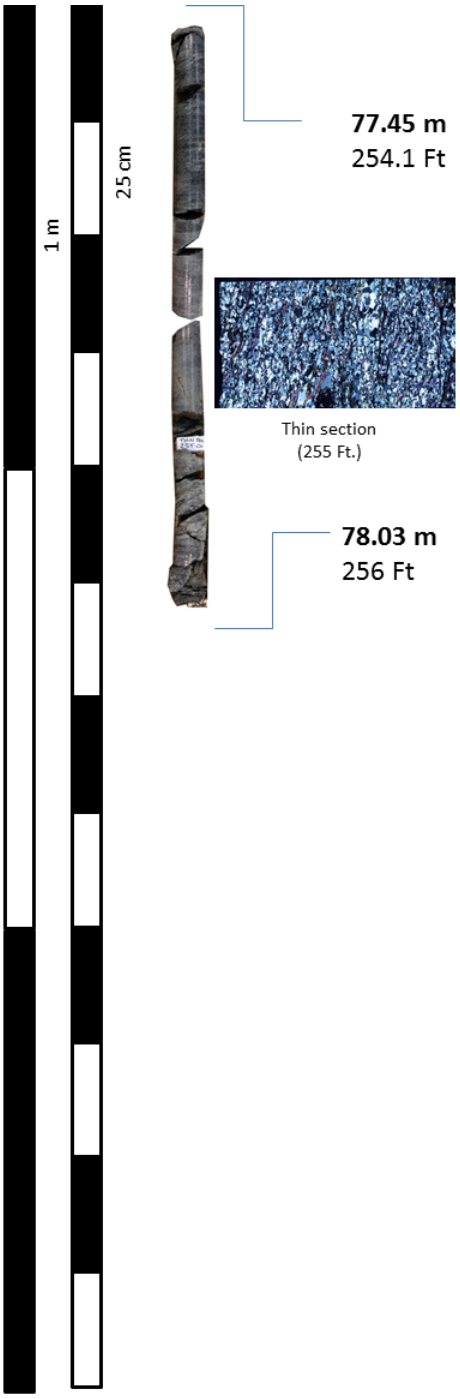

Drill Core Box 29

Total core Run (m)	Total Core Recovery (m)	Total Core Recovery %	RQD %
0.579	0.89	100	84.61

Description sheet

Box N.	29

1. Grain size	Fine	Medium	Coarse grained	Very Coarse Grained	Porphyrobl astic	Granoblastic	Porphyrocla stic
Sets	<0.75mm	0.75-1mm	1-2mm	>2mm	Containing crystals that are larger than the enclosing matrix	Composed of crystals of the same size. Fine to medium grained metamorphic rocks Al poor.	Coarse, relict, deformed crystals set in a fine grained, mylonitic matrix.
Top-1	x				x		
Top-2	x				x		
Middle	x				x		
Bottom-1	x				x		
Bottom-2	x				x		

2. Layering. (Foliation)	Isotropic	Compositional layering	Gneissosity	Schistosity	Cleavage	Mylonitic layering
Sets	Not layered	Foliation defined by alternating layers composed of different minerals. Easy to recognize by differences in colors of layers.	Compositional layering in with granoblastic layers of roughly equidimensional grains(quartz and feldspar) alternate with more schistose layers of platy or elongate grains.	Foliation defined by aligned minerals. Commonly platy minerals(micas, chlorite...) or prismatic (amphibole, tourmaline). They posses a preferred orientation.	Schistosity surfaces that are planar along which the rock may break(cleave) into tabular or platy fragments. Slaty cleavage is perfectly planar. Crenulation cleavage is defined by cm- to mm scale periodic folds.	Foliation defined by layers of microbreccia with glassy appearance and or highly strained and elongated grains of quartz and or feldspar.
Top-1				x		
Top-2				x		
Middle				x		
Bottom-1				x		
Bottom-2				x		

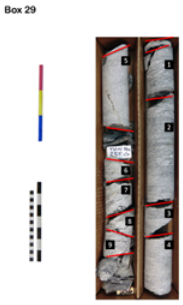

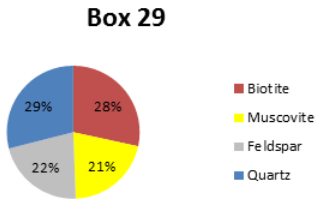

B) Thin Sections

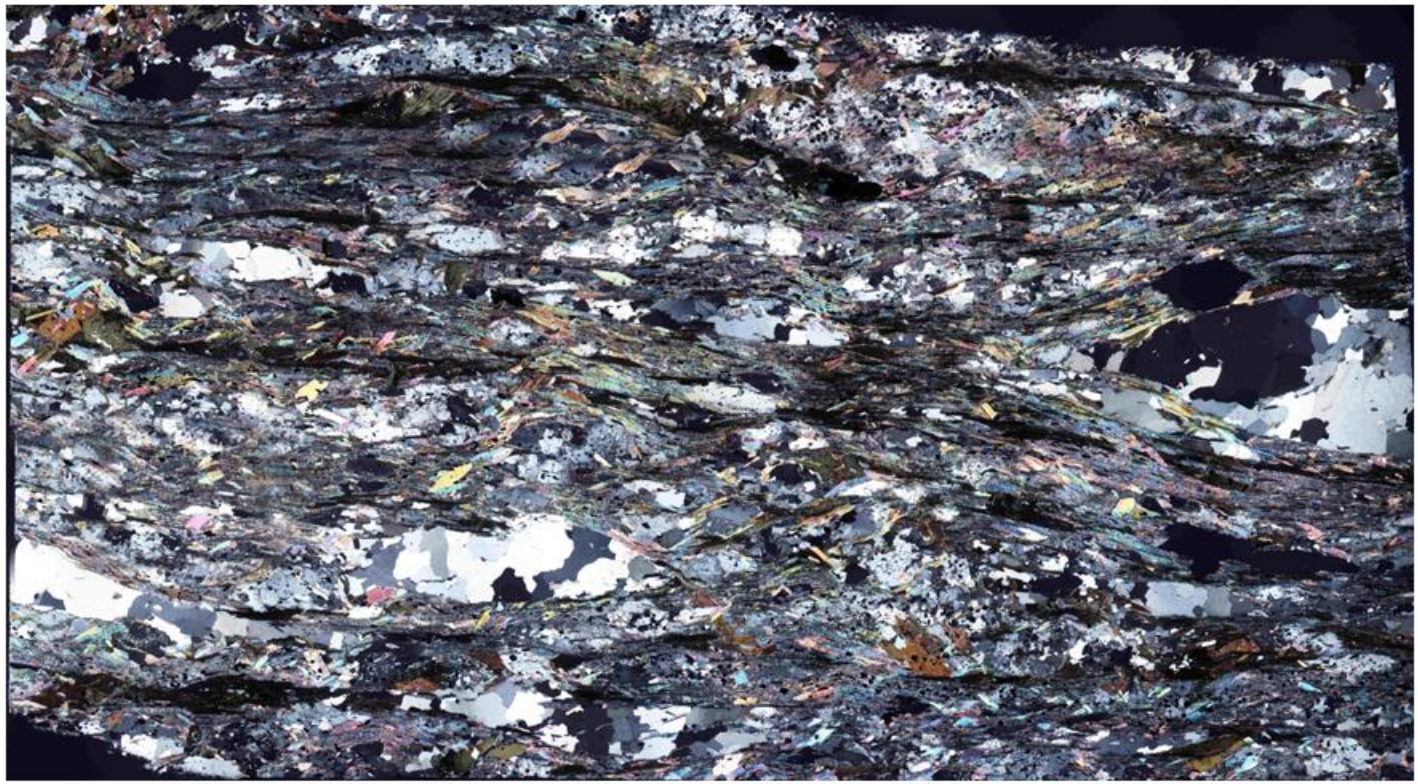

Thin Section	09-01(61.2)
Rock Name	Mica Schist
Grain Size	< 1mm
Texture	Foliated

Mayor Mineralogy	% present	Size(mm) Min.	Max.	Av.	Color	Habit & Cleavage	Comments
Quartz	20	0.1	1.5	1	Colorless	Anhedral crystals	Undulose extinction, dynamic recrystallization.
Muscovite	30	0.1	1	0.5	Colorless	Long skinny flakes. Single Cleavage	Low relief, lack of color
Biotite	20	0.1	1	0.5	Pleochroic	Long skinny flakes. Single Cleavage	Brown in PP
Feldspar	20	0.1	1.5	1	Colorless	Altered giving it a grainy or grayish appearance	Dirty weathered quartz looking
Minor Mineralogy	**% present**	**Size(mm) Min.**	**Max.**	**Av.**	**Color**	**Habit & Cleavage**	**Comments**
Acc. Min	5	0.01	0.5	0.5	Opaque	Scattered, probably metallic minerals such magnetite, hematite...	
Garnet	5	0.01	0.1	0.1	Colorless	Irregularly fractured, Subhedral to euhedral	Scattered groups
Hornblende	5	1	1	1	Greenish	Flakes, similar to biotite or muscovite. Single Cleavage	

Thin Section	09-01 (65.2)
Rock Name	Mica Schist
Grain Size	< 1mm
Texture	Crenulated

Mayor Mineralogy	% present	Size(mm) Min.	Max.	Av.	Color	Habit & Cleavage	Comments
Quartz	20	0.1	1	0.25	Colorless	Anhedral crystals	Undulose extinction, dynamic recrystallization
Muscovite	20	0.1	1.5	0.5	Colorless	Long skinny flakes. Single Cleavage	Low relief, lack of color
Biotite	20	0.1	1.5	0.5	Pleochroic	Long skinny flakes. Single Cleavage	Brown in PP
Feldspar	20	0.1	1.5	1	Colorless	Altered giving it a grainy or grayish appearance	Dirty weathered quartz looking
Minor Mineralogy	% present	Size(mm) Min.	Max.	Av.	Color	Habit & Cleavage	Comments
acc. Min	5	0.1	1	0.1	Opaque		Scattered, probably metallic minerals such magnetite
Garnet	5	0.01	0.1	0.05	Colorless	Irregularly fractured, Subhedral to euhedral	Scattered groups
Hornblende	10	0.5	1	0.5	Greenish	Flakes, similar to biotite or muscovite. Single Cleavage	

Thin Section	09-01 (98)
Rock Name	Mica Schist
Grain Size	>2mm
Texture	Highly Strain

Mayor Mineralogy	% present	Size(mm) Min.	Max.	Av.	Color	Habit & Cleavage	Comments
Quartz	100	1	3	2	Colorless	Anhedral crystals	Undulose extinction separated by subgrains band domains, recrystallizing, serrated contacts

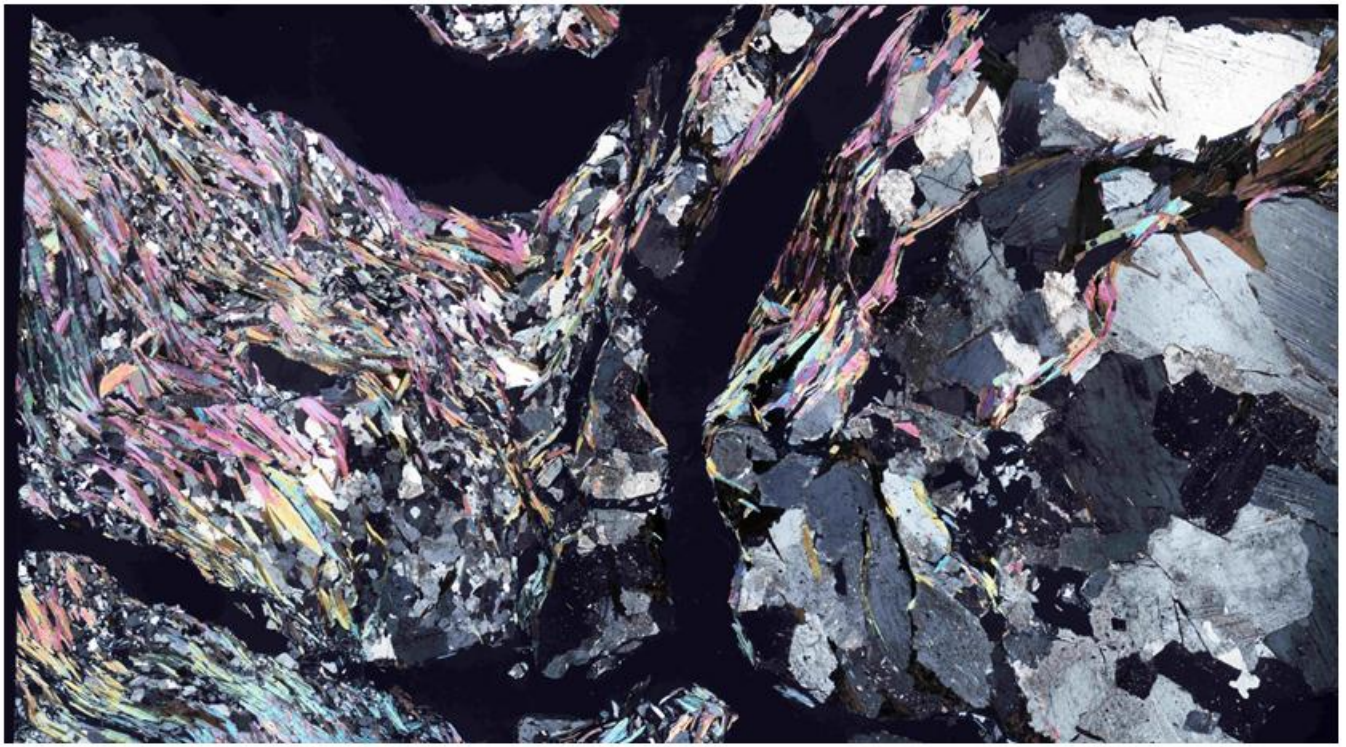

Thin Section	09-01 (111.8)
Rock Name	Mica Schist
Grain Size	<1mm to>2mm
Texture	Foliated

Mayor Mineralogy	% present	Size(mm) Min.	Max.	Av.	Color	Habit & Cleavage	Comments
Quartz	20	0.1	2	0.5	Colorless	Anhedral crystals	recrystallized, serrated contacts, some grains show degradation signs
Muscovite	25	0.1	1	1	Colorless		Low relief, lack of color
Biotite	25	0.1	1	0.5	Pleochroic		Brown in PP
Plagioclase (albite)	20	0.5	0.5	0.5	Lack of color	Euhedral crystals, twinning in some grains	Dirty weathered quartz looking, White with bare eyes
Minor Mineralogy	% present	Size(mm) Min.	Max.	Av.	Color	Habit & Cleavage	Comments
Acc. Min	5	1	0.1	0.5	Opaque		Scattered, probably metallic minerals such magnetite
Hornblende	5	0.5	1	0.5	Greenish	Flakes, similar to biotite or muscovite.Single Cleavage	

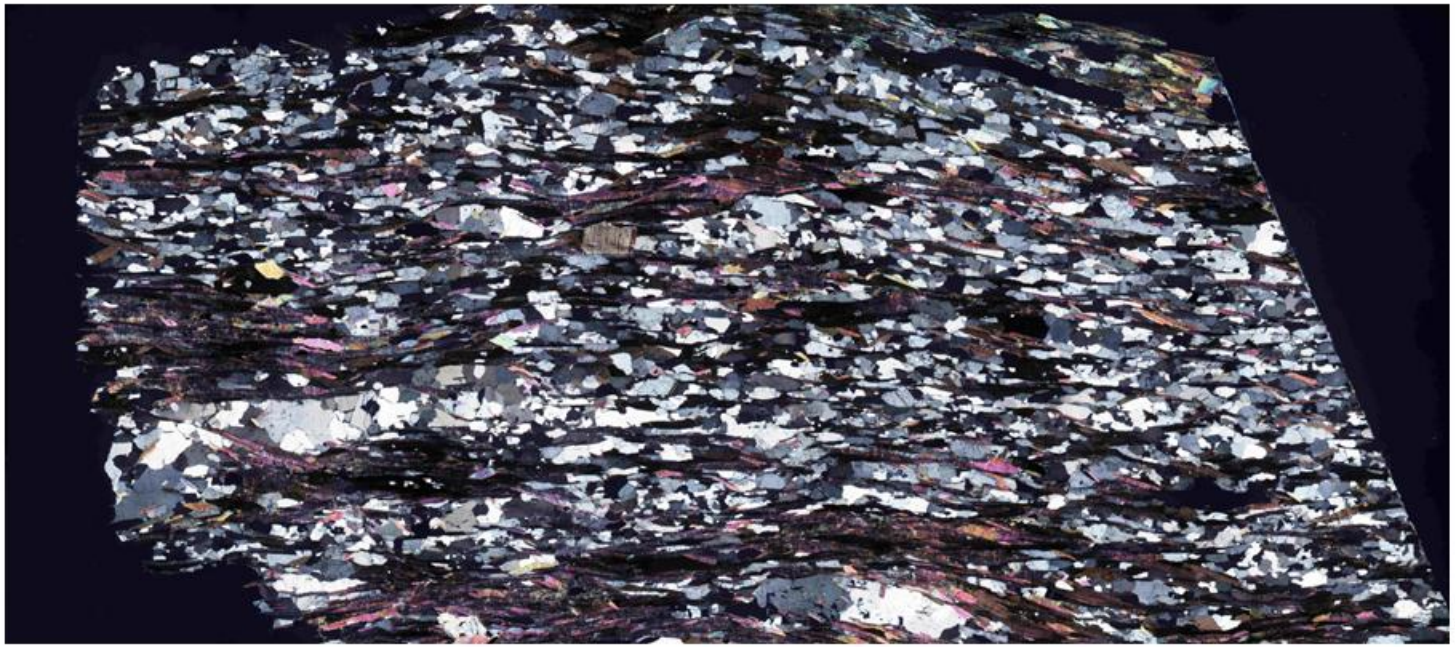

Thin Section	09-01 (135.8)
Rock Name	Mica Schist
Grain Size	<1mm
Texture	Fioliated

Mayor Mineralogy	% present	Size(mm) Min.	Max.	Av.	Color	Habit & Cleavage	Comments
Quartz	25	0.1	2	0.5	Colorless	Anhedral crystals	recrystallized, various grains have serrated contacts.
Muscovite	20	0.1	2	1	Colorless		Low relief, lack of color
Biotite	20	0.1	2	1	Pleochroic		Brown in PP
eldspar	20	0.1	1.5	1	Colorless	Altered giving it a grainy or grayish appearance	Dirty weathered quartz looking
Minor Mineralogy	**% present**	**Size(mm) Min.**	**Max.**	**Av.**	**Color**	**Habit & Cleavage**	**Comments**
acc. Min	5	0	0	0	Opaque		Scattered, probably metallic minerals such magnetite
Hornblende	5	0.5	1	0.5	Greenish	Flakes, similar to biotite or muscovite.Single Cleavage	
Garnet	5	0.01	0.1	0.1	Colorless	Irregularly fractured, Subhedral to euhedral	Not as few as in other thin sections but bigger in size

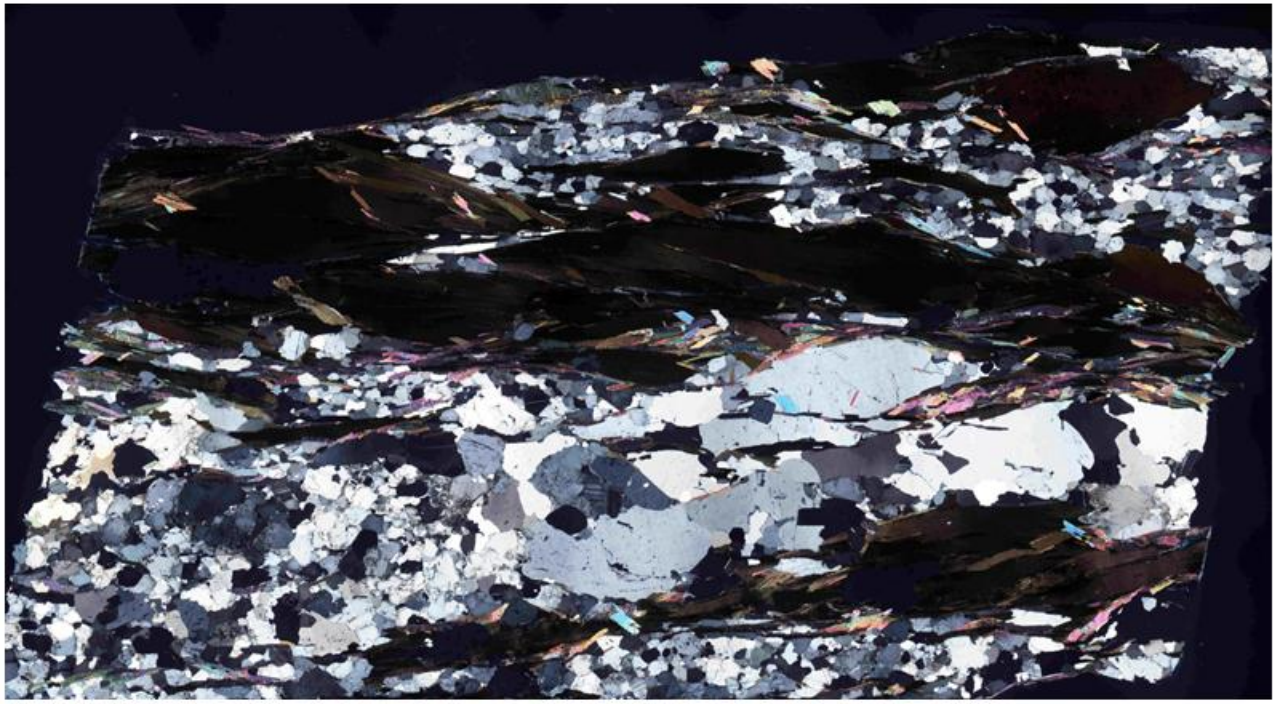

Thin Section	09-01 (141)
Rock Name	Mica Schist
Grain Size	<1mm to >3mm
Texture	Foliated / granoblastic bands

Mayor Mineralogy	% present	Size(mm) Min.	Max.	Av.	Color	Habit & Cleavage	Comments
Quartz	25	0.5	2	0.5	Colorless	Anhedral crystals	recrystallized, various grains have serrated contacts.
Muscovite	20	0.5	1	0.5	Colorless		Low relief, lack of color
Biotite	25	0.5	5	2	Pleochroic		Brown in PP, high occurrence in this slide. Grouped in big lens.
Plagioclase (albite)	20	0.5	0.5	0.5	Lack of color	Euhedral crystals, twinning in some grains	Dirty weathered quartz looking, White with bare eyes
Minor Mineralogy	**% present**	**Size(mm) Min.**	**Max.**	**Av.**	**Color**	**Habit & Cleavage**	**Comments**
acc. Min	5	0.1	0.1	0.1	Opaque		Scattered, probably metallic minerals such magnetite
Hornblende	5	0.5	1	0.5	Greenish	Flakes, similar to biotite or muscovite.Single Cleavage	

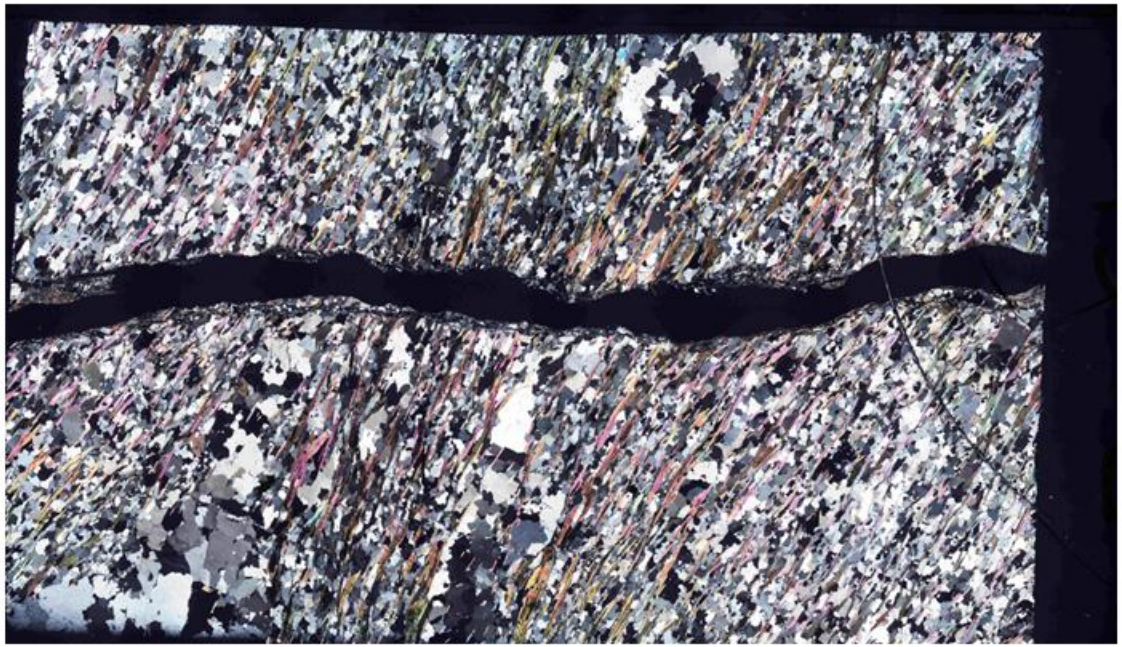

Thin Section	09-01 (174.7)
Rock Name	. Mica Schist
Grain Size	<1mm
Texture	Foliated/ granoblastic quartz bands

Mayor Mineralogy	% present	Size(mm) Min.	Max.	Av.	Color	Habit & Cleavage	Comments
Quartz	25	0.5	2	0.5	Colorless	Anhedral crystals	recrystallized, serrated contacts
Muscovite	20	0.5	1	0.5	Colorless		Low relief, lack of color
Biotite	20	0.5	5	2	Pleochroic		Brown in PP
Feldspar	20	0.1	1.5	1	Colorless	Altered giving it a grainy or grayish appearance	Dirty weathered quartz looking
Minor Mineralogy	% present	Size(mm) Min.	Max.	Av.	Color	Habit & Cleavage	Comments
acc. Min	5	0.1	0.1	0.1	Opaque		Scattered, probably metallic minerals such magnetite
Garnet	5	0.1	0.1	0.1	Colorless	Irregularly fractured	Scattered, not very common.
Hornblende	5	0.5	1	0.5	Greenish	Flakes, similar to biotite or muscovite.Single Cleavage	

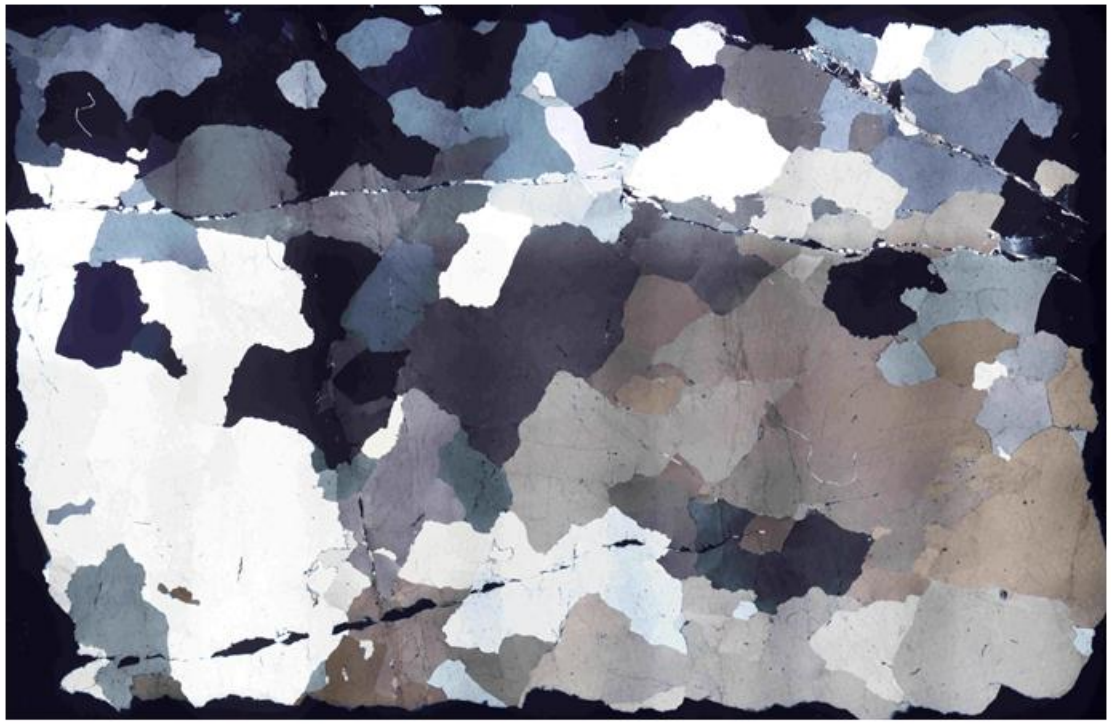

Thin Section	09-01 (216)
Rock Name	Mica Schist
Grain Size	<2mm to >4mm
Texture	Highly strain grains

Mayor Mineralogy	% present	Size(mm) Min.	Max.	Av.	Color	Habit & Cleavage	Comments
Quartz	100	0.1	4	2	Colorless	Anhedral crystals	Undulose extinction separated by subgrains band domains, recrystallizing, serrated contacts

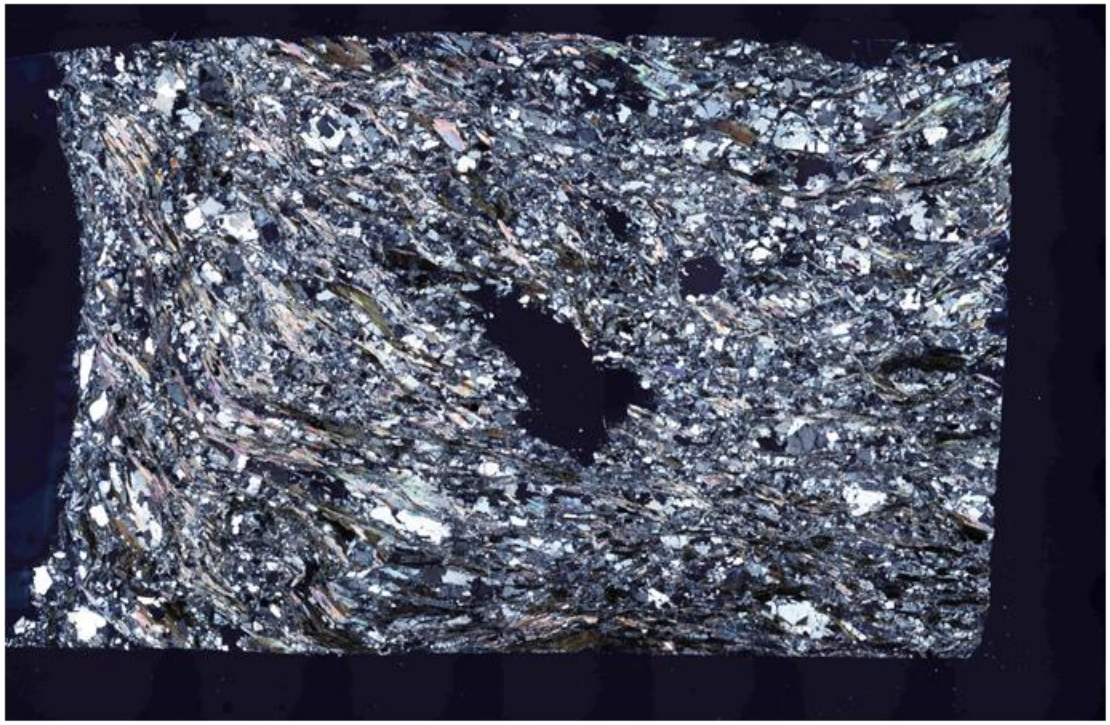

Thin Section	09-01 (222.8)
Rock Name	Mica Schist
Grain Size	<1mm
Texture	Foliated

Mayor Mineralogy	% present	Size(mm) Min.	Max.	Av.	Color	Habit & Cleavage	Comments
Quartz	30	0.5	2	0.5	Colorless	Anhedral crystals	recrystallized, serrated contacts. Undulose extiction
Muscovite	20	0.5	1	0.5	Colorless		Low relief, lack of color
Biotite	20	0.5	5	2	Pleochroic		Brown in PP
Feldspar	20	0.1	1.5	1	Colorless	Altered giving it a grainy or grayish appearance	Dirty weathered quartz looking
Minor Mineralogy	**% present**	**Size(mm) Min.**	**Max.**	**Av.**	**Color**	**Habit & Cleavage**	**Comments**
acc. Min	5	0.1	0.1	0.1	Opaque		Scattered, probably metallic minerals such magnetite
Hornblende	5	0.5	1	0.5	Greenish	Flakes, similar to biotite or muscovite.Single Cleavage	

Thin Section	09-01 (255)
Rock Name	Mica Schist
Grain Size	<1mm
Texture	Foliated

Mayor Mineralogy	% present	Size(mm) Min.	Max.	Av.	Color	Habit & Cleavage	Comments
Quartz	30	0.5	2	0.5	Colorless	Anhedral crystals	recrystallized, serrated contacts
Muscovite	20	0.5	1	0.5	Colorless		Low relief, lack of color
Biotite	20	0.5	5	2	Pleochroic		Brown in PP
Plagioclase (albite)	25	0.5	0.5	0.5	Lack of color	Euhedral crystals, twinning in some grains	Dirty weathered quartz looking, White with bare eyes
Minor Mineralogy	% present	Size(mm) Min.	Max.	Av.	Color	Habit & Cleavage	Comments
acc. Min	5	0.1	0.1	0.1	Opaque		Scattered, probably metallic minerals such magnetite

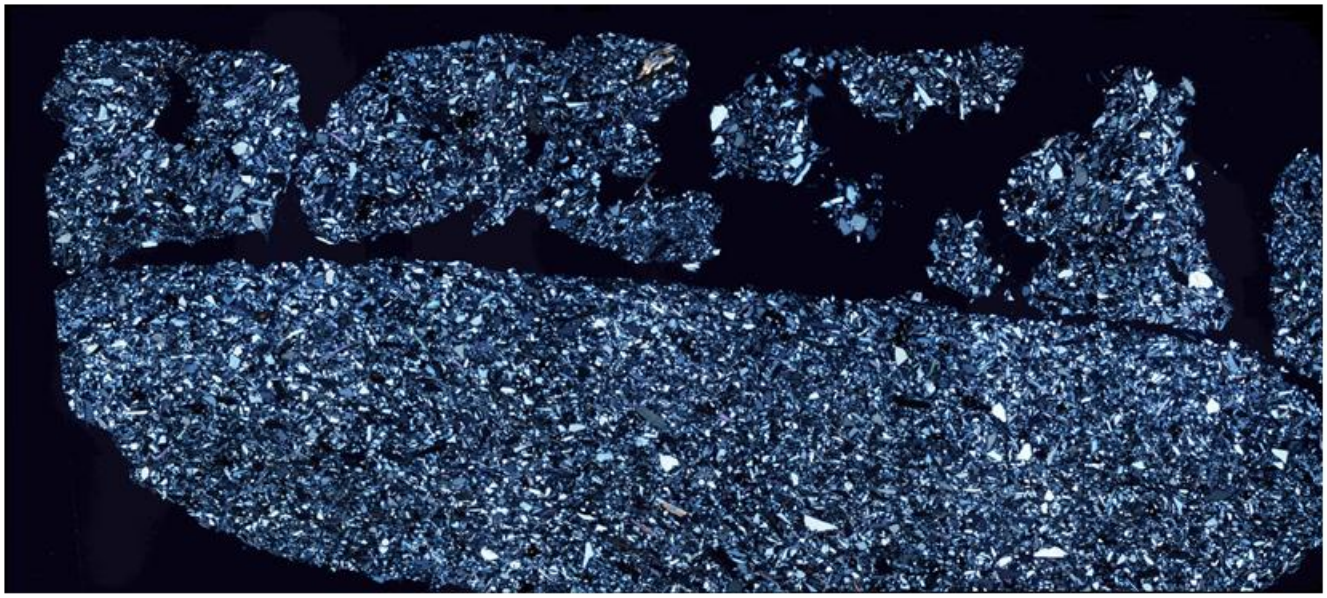

Thin Section	09-01 (Breccia zone)
Rock Name	Mica Schist
Grain Size	<1mm
Texture	Breccia/sand

Mayor Mineralogy	% present	Size(mm) Min.	Max.	Av.	Color	Habit & Cleavage	Comments
Quartz	30	0.05	1.5	0.1	Colorless	Anhedral crystals	Undulose extiction
Muscovite	20	0.05	1	0.5	Colorless		Low relief, lack of color
Biotite	20	0.05	1	0.5	Pleochroic		Brown in PP
Feldspar	20	0.05	0.5	0.1	Colorless	Altered giving it a grainy or grayish appearance	Dirty weathered quartz looking

Minor Mineralogy	% present	Size(mm) Min.	Max.	Av.	Color	Habit & Cleavage	Comments
acc. Min	5	0.05	0.1	0.1	Opaque		Scattered, probably metallic minerals such magnetite
Hornblende	5	0.5	0.5	0.5	Greenish	Flakes, similar to biotite or muscovite.Single Cleavage	

C) Digital Geological Map

Wetumpka Geologic Map

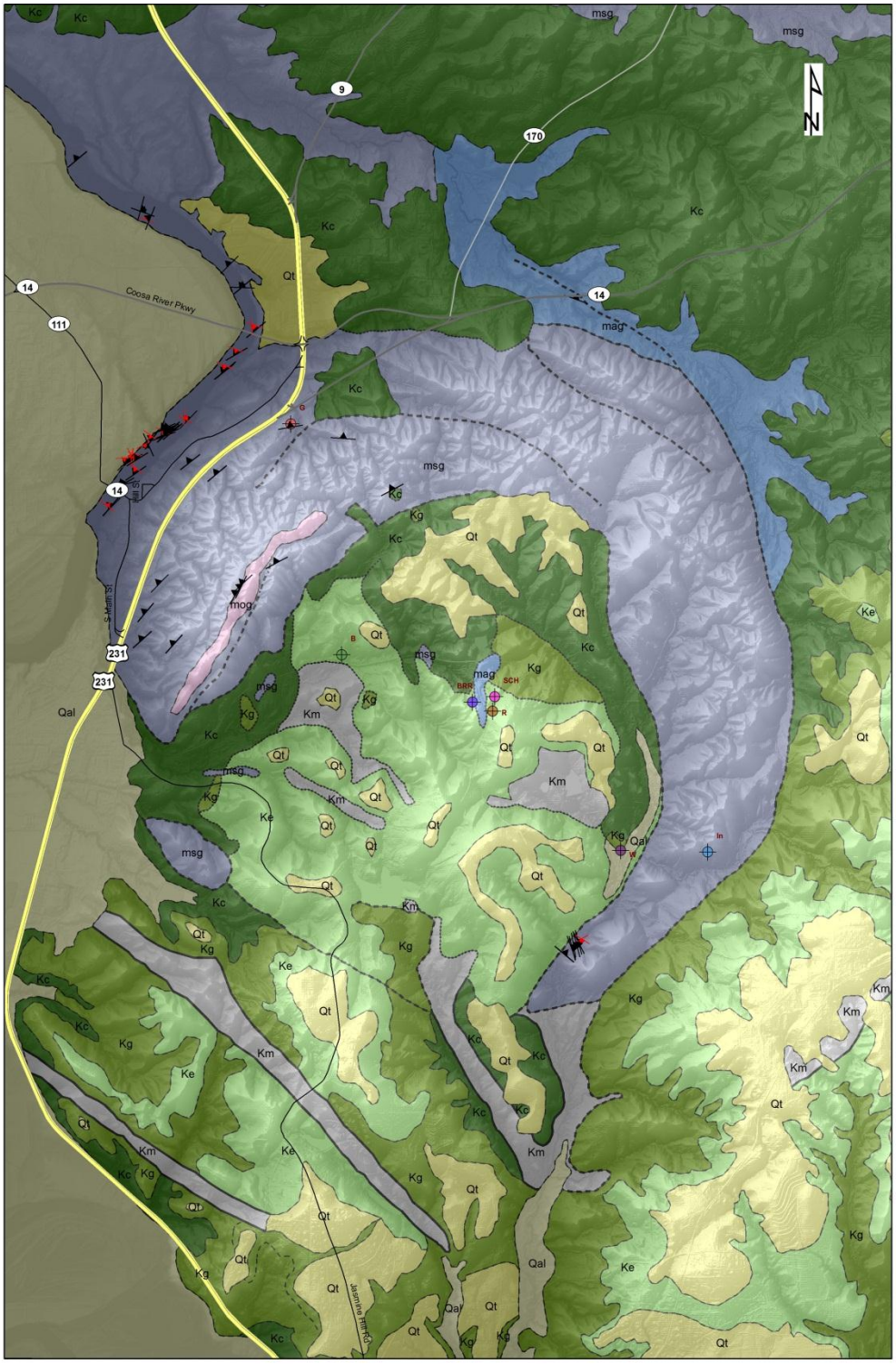

Wetumpka Geologic Map

Legend

USA Major Roads

Road Classification

- Freeway or Other Major Road
- Major Road Less Important than a Freeway
- Other Major Road
- Secondary Road
- Local Connecting Road
- Important Local Road

Schistosity & Fractures

Label

- F1
- F2
- Sch

Research_wells

Name

- Baillif
- Buck Ridge road
- Gardner
- Inscoe
- Reeves
- Schroeder
- Wadsworth

Elmore County DEM

Value **780ft**

118ft

- Probable fault
- Inferred fault
- Fault
- Inferred contact

Unit Name

Unit Definition, Acronym

- Quaternary Alluvial, Qal
- Quaternary Terraces, Qt
- Mooreville chalk, Km
- Eutaw Formation, Ke
- Gordo Formation; Tuscaloosa Group, Kg
- Coker Formation; Tuscaloosa Group, Kc
- Metaargillite and metagraywacke, msg
- Metaorthoquarzite and graphite quartz schist, mog
- Potassium feldspar augen gneiss, mag